

# **Mass spectrometry based analyses of posttranslational protein modification in bacterial and viral (co)-infection**

**Inauguraldissertation**

zur

Erlangung des akademischen Grades eines

Doktors der Naturwissenschaften

(Dr. rer. nat.)

der

Mathematisch-Naturwissenschaftlichen Fakultät

der

Universität Greifswald

vorgelegt von

Thomas Sura

geboren am 22.05.1990

in Rüdersdorf

Greifswald, den 16.02.2023

Dekan: Prof. Dr. Gerald Kerth

1. Gutachter: Prof. Dr. Dörte Becher

2. Gutachter: Prof. Dr. Andreas Pich

Tag der Promotion: 19.06.2023



## Table of contents

<b>Summary</b> .....	<b>1</b>
<b>Abbreviations</b> .....	<b>3</b>
<b>1 Introduction</b> .....	<b>5</b>
1.1 Bacterial and viral (co)-infection in the respiratory tract and the oral cavity .....	6
1.2 The ubiquitin proteasome system .....	8
1.3 Involvement of ubiquitin in immunity.....	11
1.4 UPS is hijacked by pathogens.....	12
1.5 Tools to investigate ubiquitination.....	13
1.6 Protein citrullination by the Porphyromonas peptidylarginine deiminase.....	16
1.7 Identification of citrullinated peptides by mass spectrometry .....	16
1.8 Aim of the thesis .....	18
<b>2 Methodology</b> .....	<b>19</b>
2.1 Bacterial and viral strains.....	19
2.2 Experimental approach and sample processing (Manuscript II & III) .....	19
<b>3 Results and Discussion</b> .....	<b>22</b>
3.1 Citrullination of host proteins as part of a pathogens immune evasion strategy (Manuscript I) .....	22
3.2 Establishing a protocol for the analysis of UPS components and polyubiquitinated proteins.....	24
3.2.1 Increasing proteomic depth by sample processing and measurement procedures ....	24
3.2.2 Enrichment of polyubiquitinated proteins.....	25
3.3 Bacterial and viral co-infection in 16HBE cells (Manuscript II).....	27
3.3.1 Adaptation of the proteome.....	27
3.3.2 Alterations in polyubiquitination of proteins .....	29
3.4 Proteome and ubiquitinome upon bacterial and viral co-infection in A549 cells (Manuscript III).....	31
<b>4 Concluding remarks and outlook</b> .....	<b>34</b>
<b>5 References</b> .....	<b>35</b>



**Manuscript I .....51**  
**Manuscript II.....67**  
**Manuscript III .....77**  
**Appendix .....90**  
Published peer-reviewed manuscripts included in this thesis.....90  
Published peer-reviewed manuscripts not included in this thesis.....90  
Conference contributions .....93

### Summary

Posttranslational modifications are involved in the regulation of virtually all cellular processes, including immune response, nevertheless, they are also targets manipulated by invading pathogens. The first investigated example is protein citrullination which is an important posttranslational modification that acts on a multitude of processes like supervision of cell pluripotency and rheumatoid arthritis. Citrullination of targeted arginine residues is performed by the Peptidylarginine deiminase. Within the first published manuscript, being part of this thesis, it was possible to show the use of this posttranslational modification by the human pathogen *Porphyromonas gingivalis* to facilitate innate immune evasion at three distinct level. *P. gingivalis* was demonstrated to citrullinate proteins by Porphyromonas peptidylarginine deiminase resulting in diminished phagocytosis and subsequent killing by neutrophils. Furthermore, it was shown that citrullination of histone H3 enables *P. gingivalis* to survive in neutrophil extracellular traps and incapacitate the lysozyme-derived peptide LP9.

The second investigated posttranslational modification is ubiquitination and its role in respiratory tract infections. Ubiquitination is the covalent attachment of a small protein that consisting of only 76 amino acids to the  $\epsilon$ -amino group of lysine residues to posttranslational modify proteins. Acute infections of the lower respiratory tract such as viral and bacterial co-infections are among the most prevalent reasons of fatal casualties worldwide. Therefore, the interactions between host and pathogens resulting in the impairment of the hosts immune response and immune evasion of the pathogens, need to be elucidated. To get new insights in the infection driven changes in protein polyubiquitination and alterations in the abundance of ubiquitin E3 ligases involved in ubiquitination, cellular proteomes were monitored in detail by high resolution mass spectrometry. Therefore, the epithelial cell lines 16HBE14o- (Manuscript II) and A549 (Manuscript III) were co-infected with influenza A virus H1N1 and *Streptococcus pyogenes* or *Staphylococcus aureus* or with influenza A virus H1N1 and *Streptococcus pneumoniae*, respectively. Here, it could be shown in 16HBE14o- cells that co-infection of epithelial cells is not characterized by decreased cell survival and that observable effects on the proteome and ubiquitinome are mostly additive rather than synergistic. *S. pyogenes* infection affected the mitochondrial function, cell-cell adhesion, endocytosis and actin organization. Viral infection affected mRNA processing and Rho signaling. Viral and bacterial co-infection was detected to affect processes that were already affected by both of the corresponding single infections. No further pathways were strongly affected by the co-infection. A similar result has been observed in A549 cells co-infected IAV

and *S. pneumoniae*. Overrepresented gene ontology terms depict the sum of those observed in the viral and bacterial single infection. Moreover, no significant change in cell survival upon co-infection compared to single bacterial infection was noticed for A549 cells either. This led to the suggestion that co-infection of investigated epithelial cells under examined conditions possesses additive rather than synergistic effect and thus, may not worsen the outcome of the infection within the studied conditions. Infections in other systems, may provide varying results and thus should be examined in future studies.

## Abbreviations

16HBE	16HBE14o- cell line
A549	Type II alveolar epithelial cell line A549
ATP	Adenosine triphosphate
Da	Dalton
DAVID	Database for Annotation, Visualization and Integrated Discovery
DUB	Deubiquitinating enzyme
E1	Ubiquitin activating enzyme
E2	Ubiquitin transferring enzyme
E3	Ubiquitin ligating enzyme
GO	Gene Ontology
GTPase	Guanosine triphosphate hydrolyzing enzyme
H <sub>2</sub> O <sub>2</sub>	Hydrogen peroxide
IAV	Influenza A virus
IFN	Interferon
K-GG	Lysine residue modified with a di-glycine remnant at the ε-amine group
LC-MS/MS	Liquid chromatography with tandem mass spectrometry
MAPK	Mitogen-activated protein kinase
mRNA	Messenger ribonucleic acid
MS	Mass spectrometry
NET	Neutrophil extracellular trap
NF-κB	Nuclear factor kappa-light-chain-enhancer of activated B cells
<i>P. gingivalis</i>	<i>Porphyromonas gingivalis</i>
PAD	Peptidylarginine deiminase
PPAD	Porphyromonas peptidylarginine deiminase
PRR	Pattern recognition receptor
RNA	Ribonucleic acid
rRNA	Ribosomal ribonucleic acid
<i>S. aureus</i>	<i>Staphylococcus aureus</i>

<i>S. pneumoniae</i>	<i>Streptococcus pneumoniae</i>
<i>S. pyogenes</i>	<i>Streptococcus pyogenes</i>
S-Trap	Suspension trap
TNF	Tumor necrosis factor
TUBE	Tandem ubiquitin binding entities
UPS	Ubiquitin proteasome system

## 1 Introduction

The human organism serves as an ecological habitat for numerous microbial species colonizing the human body which easily exceed the number of human cells (Sender et al., 2016). The composition of the microbial community differs depending on the investigated site (Ding and Schloss, 2014; Dekaboruah et al., 2020). Symbiotic microbial communities are related to health and are postulated to be beneficial for the host by preventing disease (Dagli et al., 2016; Mishra et al., 2021). Disturbance or dysbiosis of the microbial community is related to disease and enables potential pathogenic colonizers to unlock their pathogenic potential (Dickson et al., 2016; Mishra et al., 2021; Hou et al., 2022). This thesis is confined to the oral cavity, predominantly the periodontal pocket, and the lower respiratory tract.

A disbalance of the microbiota in the deepened gingival sulcus can be induced by the presence of so called keystone pathogens and result in severe periodontitis (Hajishengallis et al., 2012). Pathogens such as *Porphyromonas gingivalis* are able to modulate the immune response which can result in severe inflammation that destructs the surrounding tissue (Hajishengallis et al., 2012; How et al., 2016). Furthermore, oral pathogens can be aspirated, and thus, lead to infections of the respiratory tract (Saini et al., 2010; Moghadam et al., 2017). Infection with influenza A virus enables the dissemination of potential pathogens present as colonizers of the upper respiratory tract to the lower respiratory tract (Ruuskanen and Järvinen, 2014; Self et al., 2017). Among these colonizers are *Staphylococcus aureus*, *Streptococcus pneumoniae* and *Streptococcus pyogenes*, which are in focus of the investigations of this thesis (Brouwer et al., 2016; Sillanpää et al., 2017; Weiser et al., 2018). Respiratory tract infections represent one of the predominant causes of death occurring worldwide (Roth et al., 2018). Epithelial cells represent a physical barrier and are as well as neutrophils among the first cells to respond to pathogens (Vareille et al., 2011; Hiemstra et al., 2015; Leiding, 2017; Jenne et al., 2018; LeMessurier et al., 2020). Recognition of pathogens and subsequent immune activation requires tight regulation of protein activity achieved by posttranslational modification of contributing proteins.

## 1.1 Bacterial and viral (co)-infection in the respiratory tract and the oral cavity

The microbial community in the oral cavity, especially the biofilm in the periodontal pocket, is responsible to prevent colonization of pathogenic bacteria and maintains a balance between the biofilm and the host immune system (Sedghi et al., 2021). Certain pathogens, like those belonging to the red group, are known to have the ability to change the composition of the microbial community (Hajishengallis et al., 2011; Hajishengallis and Lamont, 2012). Among these pathogens is *Porphyromonas gingivalis*. According to the keystone hypothesis, *P. gingivalis* changes the microbial community and initiates dysbiosis. *P. gingivalis* can make up to 7% of the biomass of these manipulated microbial communities (Leys et al., 1999; Hajishengallis et al., 2012). As a result, the balance between the immune response and the oral community is disturbed (How et al., 2016). This initiates increased infiltration by neutrophils and inflammatory processes, and eventually leads to chronic inflammation of the surrounding tissue, teeth loss and degradation of alveolar bone (How et al., 2016; Patini et al., 2018). *P. gingivalis* possesses a multitude of virulence factors, such as lipopolysaccharide, gingipains, a peptidylarginine deiminase effectively enabling immune evasion (Zheng et al., 2021; Nuñez-Belmar et al., 2022). One of the key features in immune evasion of *P. gingivalis* is its ability to posttranslational modify arginine residues of targeted proteins (Bielecka et al., 2014). Within the first published manuscript of this thesis we focused on the connection between the posttranslational modification of arginine to citrulline as a tool in pathogenic immune evasion.

In 1933 Smith, Andrewes and Laidlaw isolated a filterable virus from throat-washings, which was identified to be the causative agent of the human influenza disease (Smith et al., 1933). Already two years ago, Shope identified a filterable virus to cause swine influenza in pigs (Lewis and Shope, 1931; Shope, 1931a, 1931b). Influenza A viruses are negative-sense, single-stranded, segmented RNA viruses and provoke influenza illness in numerous mammalian and avian species. Immunity towards IAV is conferred by antibodies against two glycoproteins covering the surface of the virus particle: hemagglutinin and neuraminidase. Mutations in these proteins enable the infection of individuals even if they have cured from preceding influenza disease.

There are two forms of influenza outbreaks: local epidemic outbreaks and pandemic outbreaks. Usually epidemics are annual events with viruses that originate from mutations of former virus variants, the so-called antigenic drift. Epidemics take place in the humid and cold winter months of the year. In contrast to epidemics, pandemics are caused by virus variants

that have acquired a hemagglutinin or neuraminidase unknown to the hosts immune system from other reservoirs like swine, duck or chicken. This change of hemagglutinin or neuraminidase is therefore called antigenic shift. As the majority of the population has never seen this virus variant there is no immunological protection. It was already shown in 1933 that multiple species can be infected with the same viral strain. Smith and colleagues could show that ferrets are susceptible to human and swine influenza virus and that ferrets first infected with swine influenza virus develop immunity towards human influenza virus (Smith et al., 1933).

The first influenza A pandemic has been reported as early as in the 16<sup>th</sup> century (Potter C. W., 2001; Taubenberger and Morens, 2009). Data are more robust from 18<sup>th</sup> century and later. Pandemics occur every 10-50 years (Potter C. W., 2001; Taubenberger and Morens, 2009). Death rates of 0.5% and 2% of the infected population are reported (Potter C. W., 2001). In the last decades it has been shown that the majority of fatal cases during the Spanish flu and other influenza pandemics was not solely caused by the viral infection alone but rather by bacterial superinfection of influenza infected individuals (Taubenberger and Morens, 2006; Morris et al., 2017). Bacterial superinfection or co-infection in influenza A infected patients is connected to numerous bacterial pathogens, but the main causative agents are *Streptococcus pneumoniae*, *Staphylococcus aureus* and *Streptococcus pyogenes* (Aliberti and Kaye, 2013; Chertow and Memoli, 2013; Klein et al., 2016; Morris et al., 2017; Troeger et al., 2019). Here, viral and bacterial co-infection experiments have been performed using these pathogens. Nowadays, it is commonly accepted that IAV infections can result in the dissemination of bacteria to the lower respiratory tract, and thus enable viral and bacterial co-infection (Ruuskanen and Järvinen, 2014; Self et al., 2017). Co-infection of bacteria and filterable viruses was already shown and discussed in 1931 by Shope when infecting pigs with swine influenza virus and *Hemophilus influenzae suis* (Shope, 1931b). As a result of the performed experiments Shope came up with the hypothesis that both pathogens act together, because infections with only one pathogen resulted only in mild illness. Accordingly, co-infection of virus and bacteria is linked to greater mortality compared to single infections (Palacios et al., 2009; Chertow and Memoli, 2013; Morris et al., 2017). Secondary bacterial infection in influenza A virus infected individuals is not restricted to pandemic influenza strains and also occurs with seasonal epidemic strains (Brundage, 2006; Chertow and Memoli, 2013; Martin-Loeches et al., 2017). However, for the studies presented as part of this thesis, the 2009 pandemic H1N1 strain was chosen to study co-infection in human lung epithelial cells.



In the lung, epithelial cells act as an important line of defense and are involved in pathogen sensing and initiation of the host immune response (Vareille et al., 2011; Hiemstra et al., 2015). Influenza A virus infection can cause disruption of the epithelial barrier by induction of apoptosis, impaired immune response and cleavage of epithelial cell sialic acids causing increased bacterial adhesion, dissemination and reduced killing (Chertow and Memoli, 2013; Siemens et al., 2017). In addition, bacterial proteases can cleave viral hemagglutinin, and thus enable multiple cycles of viral infection (Chertow and Memoli, 2013).

Co-infection is generally related with increased pathogenesis and worse outcomes due to a potential (lethal) synergism of both pathogens (Oliva and Terrier, 2021; Bartley et al., 2022). Consequently, bacterial and viral co-infection of the respiratory tract cause severe economic burden and is related to higher costs of treatment than viral infections alone (Oliva and Terrier, 2021). Therefore, better treatment and vaccination strategies are required. Consequently, it is indispensable to understand cellular processes that drive infection. One cellular machinery that is involved in nearly every cellular process of eukaryotes, and that was shown to be misused by various viral and bacterial pathogens is the ubiquitin proteasome system. Many studies investigated ubiquitination from infection experiments with focus on specific proteins or pathways. Nevertheless, there is a lack of studies examining global variations in protein ubiquitination upon viral and bacterial co-infection. For that reason, an emphasis was placed on changes in polyubiquitination of proteins at a global scale.

## **1.2 The ubiquitin proteasome system**

The ever growing field of research on the ubiquitin proteasome system started already more than 40 years ago when Aaron Ciechanover, Avram Hershko and Irwin Rose detected and described an ATP dependent cytosolic protein degradation mechanism related to a polypeptide which later was named ubiquitin (Hershko et al., 1979; Ciechanover et al., 1980; Hershko et al., 1980). In 2004 their fundamental work was acknowledged with the Nobel Prize in Chemistry. During the last decades the involvement of ubiquitin in major cellular processes of eukaryotic cells has become commonly accepted. Ubiquitination is a reversible posttranslational protein modification involved in cell cycle control, protein degradation, antigen processing, transcription control, immunity, and many more cellular processes (Komander and Rape, 2012; Akutsu et al., 2016). The process of ubiquitin protein ligation is driven by a cascade of three different proteins E1, E2 and E3, first purified and identified by Hershko and coworkers in 1983 (Hershko et al., 1983). In Figure 1 the proposed model of

protein ubiquitin ligation is displayed. In a first step a ubiquitin-activating enzyme (E1) activates ubiquitin in an ATP-dependent manner. Then the ubiquitin is transferred to a cysteine residue localized in the active site of a ubiquitin conjugating enzyme (E2). Hereafter, ubiquitin is conjugated to specific substrates recognized by ubiquitin ligases (E3). E3 ligases convey substrate specific protein ubiquitin ligation. Comparative genome analysis enabled the detection of up to 1.000 putative E3 ligases (Li et al., 2008). In addition, nine E1 coding genes and 37 E2 coding genes were identified in the human genome (Michelle et al., 2009; Schulman and Harper, 2009). During the process of protein ubiquitin ligation, the C-terminal glycine residue of ubiquitin, a protein composed of 76 amino acids, is covalently linked (isopeptide bond) to the  $\epsilon$ -amine group of a lysine residue within the substrate protein.

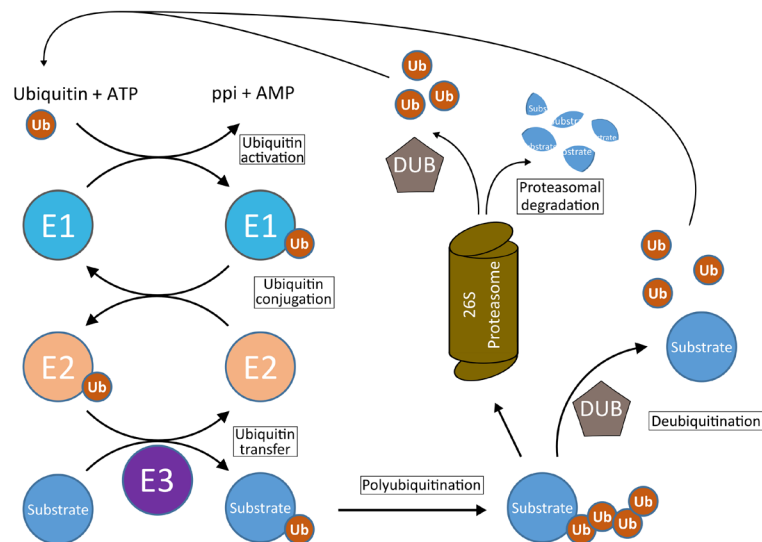


**Figure 1 The ubiquitin proteasome system.**

Ubiquitination is a multistep process that involves different proteins to work in a cascade like mechanism. In a first step an E1 enzyme (E1) activates ubiquitin which will be transferred to an E2 enzyme (E2). Hereafter, ubiquitin is conjugated to specific substrates, recognized by ubiquitin ligases (E3). Deubiquitinating enzymes (DUB) trim ubiquitin chains from the target protein before it is unfolded and degraded by the proteasome. Moreover, DUB can remove ubiquitin from target proteins and deliver free ubiquitin to the system.

Ubiquitin itself harbors eight potential sites (M1, K6, K11, K27, K29, K33, K48, K63) that can be used for additional ubiquitin ligation cycles resulting in the formation of polyubiquitin chains. These chains can either consist of a single or multiple linkage types, and are therefore further grouped into different categories (Figure 2).

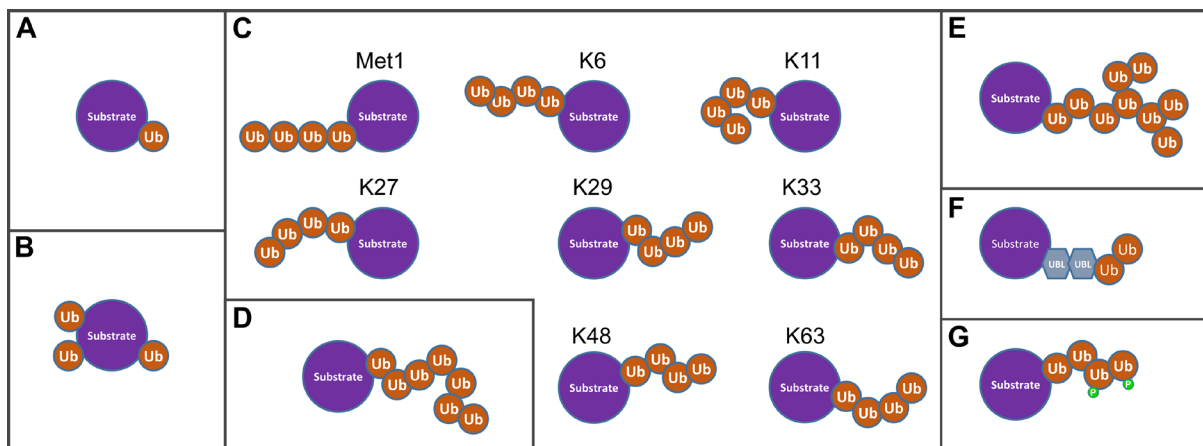


**Figure 2 Different types of ubiquitination on substrate proteins**

Depending on the number of ubiquitin molecules and how different ubiquitin molecules are covalently linked, ubiquitination can be divided into several groups. Proteins can be modified with a single ubiquitin on a single site for mono-ubiquitination (A) or at multiple sites for multi mono-ubiquitination (B). Polyubiquitin chains can be categorized by the topology. Chains composed of only one linkage type are homogenous chains (C) and chains composed of multiple linkage types are heterogeneous chains (D). Ubiquitin chains can also occur as branched chains (E) or as hybrid chains (F) with ubiquitin like modifiers in the same chain. Moreover, ubiquitin chains can be a substrate for further posttranslational modification (G) like phosphorylation or acetylation.

Deubiquitinating enzymes (DUB) represent another important class of proteins for the function of ubiquitin signaling (Figure 1). These proteins have important roles in ubiquitin signaling, like counteracting E2 or E3 enzymes, removing ubiquitin chains from the target protein before it is unfolded and degraded by the proteasome, generation of free ubiquitin or trimming ubiquitin chains (He et al., 2016).

The outcome of the ubiquitination or polyubiquitination of the substrate proteins depends on the type of ubiquitin chain attached. It is commonly accepted that K48 linked polyubiquitin chains most frequently result in degradation of the target protein by the 26S proteasome, whereas K63 polyubiquitin chains are involved in lysosomal degradation processes (Komander and Rape, 2012; Erpapazoglou et al., 2014; Kwon and Ciechanover, 2017). The functions of the different types of ubiquitination have been extensively discussed in the literature, and thus, will not be discussed further within this thesis (Komander and Rape, 2012; Akutsu et al., 2016; Tracz and Bialek, 2021)

### 1.3 Involvement of ubiquitin in immunity

Besides various cellular mechanisms modified and regulated by the UPS, ubiquitination and deubiquitination is also important for a sufficient immune response (Zinngrebe et al., 2014). The *in vitro* infection set up using epithelial cells is limited to the innate immune response of the cultured epithelial mono layer. Therefore, the ubiquitination dependent regulation of innate immunity other than those present in lung epithelial cells and adaptive immunity will not be discussed within this thesis. Here, the focus is on pathways which are part of the innate immune response related to pathogen recognition in epithelial cells. However, only selected recognition pathways and the involvement of UPS proteins will be reviewed.

Recognition of IAV infection is mediated by several pattern recognition receptors (PRR), like RIG-1, TLR3 and 7 and NLRP3 (Tripathi et al., 2015). In epithelial cells recognition is predominantly mediated through RIG-1 and TLR3 (Pichlmair et al., 2006; Le Goffic et al., 2007). Upon detection of viral structures, the cytosolic PRR RIG-1, involved in sensing viral RNA, is K63 ubiquitinated by the ubiquitin E3-ligases TRIM25 and RNF135 inducing oligomerization of RIG-1, and thus the binding of MAVS (Takeuchi and Akira, 2010; Jiang et al., 2012). Besides, the recruitment of additional proteins, binding of the E3-Ligase TRAF3 allows for IRF3 dependent interferon (IFN) synthesis (Michallet et al., 2008), whereas binding of TRAF6 together with TRAF2 and TRAF5 enables activation of IRF3 and NF- $\kappa$ B (Liu et al., 2013). Another E3-ligase, RNF125, is involved in silencing of RIG-1 signaling by mediating proteasomal degradation of RIG-1 and MAVS by K48 polyubiquitination (Arimoto et al., 2007). Moreover, the E3-ligase LUBAC was shown to lead to reduced RIG-1 signaling (Belgnaoui et al., 2012). Also DUBs can facilitate alterations in RIG-1 signaling. For example, the DUB USP21 removes K63 ubiquitin chains from RIG-1 reducing its activity (Fan et al., 2014), whereas OTUB1 was demonstrated to protect RIG-1 from K48 mediated degradation (Jahan et al., 2020). Besides OTUB1 and USP21, the DUB A20 is able to inhibit the RIG-1 mediated IFN response (Catrysse et al., 2014). Ubiquitination mediated regulation of endosomal TLR3 also depends on the E3-ligase recruited to the TLR3-TRIF complex. K63 ubiquitination of attached RIP1 by TRAF6 and PELI-1 results in NF- $\kappa$ B activation (Chang et al., 2009), while TRAF3 recruitment and its subsequent K63 ubiquitination results in IRF3 mediated IFN production (Häcker et al., 2006; Oganessian et al., 2006).

Recognition of bacteria by epithelial cells is accomplished via several mechanisms. Within this thesis epithelial cells were challenged with the Gram-positive pathogens *S. aureus*,

*S. pneumoniae*, and *S. pyogenes*. Therefore, recognition of Gram-positive pathogens is emphasized within this chapter of the thesis. Bacterial peptidoglycan is recognized by the NOD-like receptor (NLR) nucleotide-binding oligomerization domain 2 (NOD2) (Girardin et al., 2003). Moreover, many Gram-positive pathogens are recognized by TLR2. *S. aureus* interacts with the TNF- $\alpha$  receptor which activates TNF signaling (Krivan et al., 1988; Gómez et al., 2004). Sufficient NOD2 signaling and subsequent NF- $\kappa$ B activation relies on the recruitment of the E3-ligases cIAP1/2 facilitating K63 ubiquitination of RIP2 (Hasegawa et al., 2008; Damgaard et al., 2012). The DUB A20 has a dual role in downregulation of NF- $\kappa$ B activity by removing K63 polyubiquitination from RIP2 (Wertz et al., 2004). Moreover, A20 was shown to target RIP2 for proteasomal degradation by polyubiquitination with K48 linked chains (Wertz et al., 2004; Hasegawa et al., 2008). Downregulation of TLR2 signaling is achieved in a similar fashion. TLR2 is K48 ubiquitinated at lysine K754 by the E3-ligase PPP1R11, and thus degraded by the proteasome (Mckelvey et al., 2016).

#### **1.4 UPS is hijacked by pathogens**

Immune signaling pathways are highly dependent on ubiquitination and deubiquitination events to mediate proper signaling and pathogen clearance. Consequently, pathogens have developed mechanisms to hijack and manipulate the host UPS to achieve immune evasion and proper infection.

The life cycle of IAV is associated with ubiquitin at many stages like viral entry into the host cell and unpacking from the late endosome (Rudnicka and Yamauchi, 2016). Furthermore, activity of viral polymerase is increased by ubiquitination (Kirui et al., 2016). A strong relationship between IAV propagation and the UPS can be assumed from studies demonstrating that inhibition of the proteasome impairs viral replication (Widjaja et al., 2010; Xia et al., 2015). Viral HA was shown to inhibit the cellular interferon response by mediating the degradation of the interferon receptor IFNR1 (Xia et al., 2015). The main mediator of immune evasion by alteration of the UPS is the viral protein NS1 (Lamotte and Tafforeau, 2021). NS1 inhibits RIG-1 signaling by binding TRIM25, and thus disables the attachment of K63 ubiquitin chains to RIG-1 (Gack et al., 2009). In addition, NS1 is able to target the DUBs A20 and OTUB1 by increasing expression and probably mediating degradation, respectively (Feng et al., 2017; Jahan et al., 2020). Another viral protein, PB1, counteracts the ZAPL mediated proteasomal degradation of viral PB2 and PA (Liu et al., 2015).

Less literature focusing on host UPS in *S. aureus*, *S. pyogenes* and *S. pneumoniae* infection exists. A virulence factor of streptococci is the secreted, membrane associated cysteine protease Streptococcal pyrogenic exotoxin B (SpeB) (Shelburne et al., 2005). Barnett and colleagues demonstrated the ability of SpeB to degrade ubiquitin-LC3 adaptor proteins NDP52, p62 and NBR1 enabling streptococci to evade selective autophagy and efficient cytosolic replication (Barnett et al., 2013; Nakagawa, 2013). Cytosolic pneumococci are able to evade clearance by selective autophagy, as well. In contrast to streptococci, pneumococci use a different mechanism. Secreted pneumococcal CbpC binds Atg-14, and thus, enables autophagic degradation of Atg-14 and suppresses xenophagy at the same time (Shizukuishi et al., 2020). *S. aureus* utilizes a different strategy to evade degradation by selective autophagy than *S. pyogenes* or *S. pneumoniae*. Staphylococci activate MAPK14 which allows the phosphorylation of ATG5, inhibiting the fusion of lysosomes and autophagosomes (Neumann et al., 2016).

### 1.5 Tools to investigate ubiquitination

Proteins of the UPS are involved in immune regulation, cancer progression, and are particularly important in neurodegenerative diseases (Celebi et al., 2020). Also, the UPS is considered as a therapeutic target in cancer therapy (Fujita et al., 2019) and for targeted degradation of proteins, otherwise not druggable (Faust et al., 2021; Békés et al., 2022). Therefore, understanding the functions and mechanisms of ubiquitination is of great importance. Mass spectrometry (MS) based proteomics has become the method of choice for the identification and quantification of changes in ubiquitination in single proteins or at a global scale. The MS based identification of ubiquitination sites depends on a diglycine remnant at the  $\epsilon$ -amine group of the modified lysine residue left after tryptic digest of the ubiquitinated protein. The Lys- $\epsilon$ -GG (K-GG) remnant is identified due to a characteristic mass shift of 114.0429 Da detected by MS. The generation of these peptides and the subsequent identification is depicted in Figure 3.

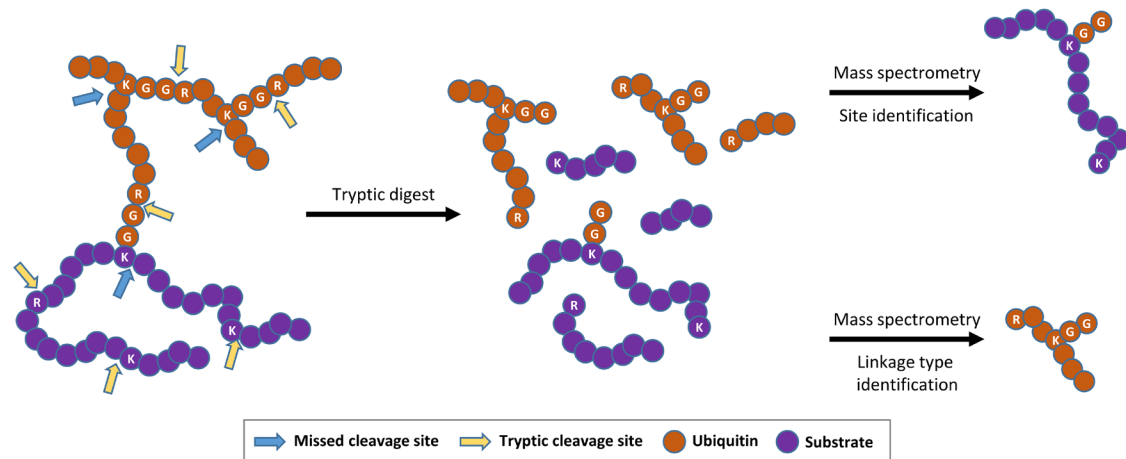


**Figure 3 MS based identification of ubiquitination sites**

Tryptic digestion of ubiquitinated proteins results in peptides that carry a characteristic Lys- $\epsilon$ -GG remnant motif at the ubiquitination site. This remnant induces a characteristic mass shift of 114.0429 Da detectable by MS.

Even though, ubiquitination is involved in many cellular processes, the fraction of proteins modified is rather low and therefore, quantification on a large scale remains challenging. To overcome the limitations of low abundance and to achieve reasonable coverage, enrichment of modified proteins or peptides prior MS analysis is inevitable (Steger et al., 2022a).

Enrichment of peptides is based on the enrichment of peptides harboring the K-GG remnant after tryptic digest of ubiquitinated proteins by monoclonal antibodies and enables identification and accurate quantification of ubiquitination sites (Xu et al., 2010; Kim et al., 2011; Rose et al., 2016). Nonetheless, the peptide-based enrichment has some drawbacks. Tryptic peptides of proteins posttranslational modified with ISG15 or NEDD8 harbor the same K-GG remnant and are therefore enriched, as well. Moreover, for application of K-GG remnant enrichment large amounts, up to 20 mg, of starting material are required. The latter limitation has been overcome recently by Rose and colleagues by combination of K-GG remnant enrichment and sample multiplexing with TMT10plex allowing to utilize only 1 mg of peptide per sample (Rose et al., 2016). Recently, Steger and co-workers used the K-GG enrichment strategy in combination with data independent acquisition for identification and quantification of up to 70,000 ubiquitinated peptides in a single MS run (Steger et al., 2021).

Selective enrichment of ubiquitinated proteins can be achieved by application of linkage specific antibodies, tandem ubiquitin binding entities (TUBEs) (Hjerpe et al., 2009) or by expression of epitope tagged ubiquitin within cells (Peng et al., 2003). TUBEs enable the pan-selective or chain-selective enrichment of polyubiquitinated proteins under non-denaturing

conditions. Therefore, TUBE based enrichment suffers from co-isolation of ubiquitin binding proteins and proteins interacting with the ubiquitinated substrate. Apart from TUBEs, enrichment of ubiquitinated proteins by expression of affinity tagged ubiquitin, allows cell lysis in denaturing conditions, and therefore avoids co-purification of non-covalently linked proteins. However, expression of exogenous ubiquitin can interfere with physiological UPS activity. In contrast to K-GG remnant enrichment, protein based methods do not inherently allow for ubiquitin site identification due to the high number of non-modified peptides generated by the tryptic digest (Steger et al., 2022b). Nevertheless, when compared to K-GG antibodies, TUBEs are less expensive, require fewer amounts of input material, and overall sample processing is less complex.



## 1.6 Protein citrullination by the *Porphyromonas* peptidylarginine deiminase

Citrullination of proteins is another important posttranslational modification that acts on a multitude of processes within the human organism like supervision of cell pluripotency, sepsis and rheumatoid arthritis (Vossenaar et al., 2003; Christophorou et al., 2014; Darrah and Andrade, 2018; Reizine et al., 2022). Peptidylarginine deiminases (PAD) are able to posttranslational modify arginine residues to citrulline (Figure 4) (Vossenaar et al., 2003). The modification of arginine to citrulline is accompanied by a loss in positive charge, and thus, can affect the proteins binding capabilities or folding.

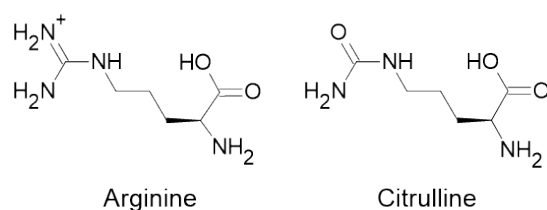


**Figure 4 Structure of arginine and citrulline**

Differences in the structure of arginine and the non-standard amino acid citrulline. Created with ACD/ChemSketch (Freeware) 2022.1.0.

The human oral pathogen *Porphyromonas gingivalis* possesses the ability to posttranslational modify host and self-proteins by expression of *Porphyromonas* peptidylarginine deiminase (PPAD) (McGraw et al., 1999; Wegner et al., 2010). PPAD was observed to be conserved among *Porphyromonas* strains (Gabarrini et al., 2015). In addition, PPAD contributes to the virulence of *P. gingivalis*, as PPAD was shown to citrullinate arginine residues on the human antimicrobial peptide LP9 diminishing LP9 derived bacterial killing (Stobernack et al., 2018). Moreover, the citrullination of histone H3 by PPAD enables *P. gingivalis* to escape from neutrophil extracellular traps (NETs) (Stobernack et al., 2018). Likewise, PPAD disturbs complement signaling by citrullination of C5a (Bielecka et al., 2014). Consequently, citrullination of host proteins by PPAD aids *P. gingivalis* to evade the host immune defense.

## 1.7 Identification of citrullinated peptides by mass spectrometry

Analysis of protein ubiquitination may be performed upon enrichment of ubiquitinated proteins or K-GG remnant peptides. The use of iodoacetamide as a alkylating agent should be avoided as it mimics 114.0429 Da mass shift of the K-GG remnant by modifying free lysin  $\epsilon$ -amine groups (Nielsen et al., 2008). In contrast, the analysis of protein citrullination by mass

spectrometry is not affected by the alkylating agent and relies on the identification of the 0.984016 Da mass shift resulting from the amino acids side chain modification (Figure 4). The low mass shift leads to misidentification and false positive hits by search engines used to identify citrullinated spectra (Lee et al., 2018). Moreover, the loss of positive charge of the arginine side chain results in a missed tryptic cleavage site. Recently, different strategies ranging from protein modification by citrulline reactive groups to improvements in MS data acquisition and data analysis have been developed to improve the reliable identification of citrullinated peptides by mass spectrometry (Clancy et al., 2016; Maurais et al., 2021; Shi et al., 2022).

## 1.8 Aim of the thesis

Posttranslational modification of proteins are involved in a wide variety of cellular processes. This thesis emphasizes especially posttranslational citrullination and ubiquitination of proteins in the context of bacterial and viral (co)-infections. Citrullination is linked to a variety of diseases like the autoimmune disease rheumatoid arthritis, Alzheimer and diabetes. *P. gingivalis* is the only known bacterial pathogen that is able to citrullinate host proteins. Mass spectrometry was applied to investigate the connection between citrullination of proteins and the ensuing immune evasion of this oral pathogen.

Another posttranslational modification playing a crucial role in conducting the cellular response towards pathogens is ubiquitination. Thus, it is not particularly surprising that viral as well as bacterial pathogens have developed strategies to misuse and manipulate the hosts ubiquitin proteasome system. Therefore, the aim of this thesis was to scrutinize potential effects of common respiratory pathogens on the abundance of components of the ubiquitin proteasome system, and furthermore, to observe the effect of the selected pathogens on protein polyubiquitination. Moreover, mass spectrometry-based proteomics was applied to discover potential synergistic or additive effects between viral and bacterial pathogens in a co-infection model using different human lung epithelial cell lines. Data obtained within this study could serve as the basis for further investigations.

## 2 Methodology

In the following chapter the main methods used in the study and the experimental approaches are briefly described. Detailed information on the used methods can be found in the corresponding manuscripts. The methodology section primarily focuses on the applied methods used to investigate infection driven changes in the proteome and ubiquitinome of lung epithelial cells.

### 2.1 Bacterial and viral strains

All viral and bacterial strains that were used to study (co)-infection in neutrophil and lung epithelial cells are listed below (Table 1). Culture conditions are described in detail in the corresponding manuscripts.

**Table 1 List of viral and bacterial strains used in the study**

Manuscript	Strain	Reference
Manuscript I	<i>P. gingivalis</i> W83	
	<i>P. gingivalis</i> W83 $\Delta$ PPAD	(Wegner et al., 2010)
Manuscript II	<i>S. aureus</i> LUG2012	(Shambat et al., 2015)
	<i>S. pyogenes</i> 5448	(Siemens et al., 2016)
	IAV A/Bavaria/74/2009 (H1N1)	
Manuscript III	<i>S. pneumoniae</i> D39 $\Delta$ <i>cps</i>	(Saleh et al., 2013)
	IAV A/Bavaria/74/2009 (H1N1)	

### 2.2 Experimental approach and sample processing (Manuscript II & III)

During infections lung epithelial cells display a physical barrier and play a role in the first defense against the infecting pathogens (Vareille et al., 2011; LeMessurier et al., 2020). To elaborate on the lung epithelial cell response towards pathogens, we performed viral as well as bacterial single infections and co-infections in the bronchial epithelial cell line 16HBE14o- (16HBE) (Cozens et al., 1994) [Manuscript II], and in the type II alveolar epithelial cell line A549 (Giard et al., 1973) [Manuscript III]. The cells were infected and sampled according to the scheme displayed in Figure 5. The manuscripts II and III intended to explore

the alterations in the proteome of the epithelial cells as a response towards the infections. In addition, as pathogens are known to act on the hosts UPS, the examination of protein polyubiquitination was emphasized in both manuscripts, but with different enrichment strategies for polyubiquitinated proteins.

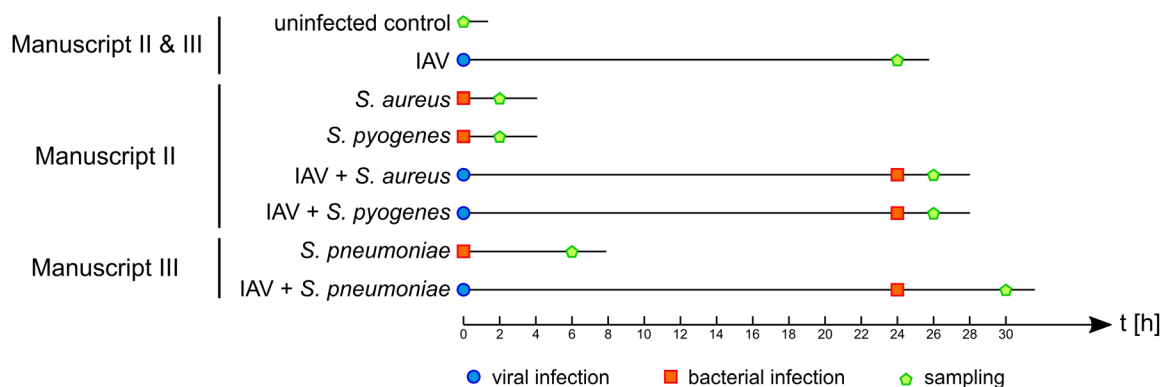


**Figure 5 Infection duration and sample time scheme**

For the infection experiments performed in Manuscript I and II the scheme above was applied for viral and bacterial single infections as well as viral and bacterial co-infection in A549 (**Manuscript III**) and 16HBE cells (**Manuscript II**). Viral infection was conducted for 24 h in both cell lines. 16HBE cells were infected with either *S. pyogenes* 5448 or *S. aureus* LUG2012 for 2 h, whereas A549 cells were infected with *S. pneumoniae* D39Δcps for 6 h. In co-infection experiments, epithelial cells were infected with IAV for 24 h followed by the bacterial infection.

Mass spectrometry (MS) has become a powerful tool for the analysis of large proteomes. Thus, MS enables the identification and relative quantification of thousands of proteins within a single measurement. Although certain posttranslational modifications like protein ubiquitination are involved in the regulation of many cellular processes, they are low abundant therefore, the application of enrichment strategies is required for a comprehensive analysis. To elaborate alterations in the proteome in Manuscript II and III cell lysate of sampled cells were digested with trypsin on suspension traps (S-Trap). The generated tryptic peptides were fractionated by basic pH reversed phase chromatography which was performed with in house packed C18 spin columns. Manuscript II further aimed to analyze alterations in the global polyubiquitination landscape of infected 16HBE cells. Consequently, pan-selective TUBEs were utilized to enrich for polyubiquitinated proteins. Further sample processing was performed as described for the proteome samples. In manuscript III the selective analysis of K48 and K63 polyubiquitin chains was emphasized. After selective TUBE based enrichment of desired chain types, proteins were digested on S-Traps. All generated samples were analyzed

by LC-MS/MS on a Q Exactive mass spectrometer operated in data dependent acquisition mode. Resulting MS .raw files were searched and quantified with the MaxQuant (Cox and Mann, 2008; Tyanova et al., 2016a) software and search results were processed with the Perseus (Tyanova et al., 2016b) software suit. Functional analysis was performed with the DAVID (Da Huang et al., 2009; Sherman et al., 2022) and Reactome (Gillespie et al., 2022) web tool.

### 3 Results and Discussion

#### 3.1 Citrullination of host proteins as part of a pathogens immune evasion strategy (Manuscript I)

The periodontal pocket harbors a unique niche with a steady state between the microbial community, present as a biofilm, and the host immune response (Sedghi et al., 2021). The emergence of keystone pathogens like *Porphyromonas gingivalis* initiates an imbalance of this homeostasis (Hajishengallis et al., 2012). This causes increased inflammation and infiltration of immune cells into surrounding tissue and eventually loss of teeth and reduction of the alveolar bone (How et al., 2016; Patini et al., 2018). Apart from the ability to secrete proteases (Gingipains), *P. gingivalis* possess the ability to posttranslational modify proteins by the secreted Porphyromonas peptidylarginine deiminase (McGraw et al., 1999; Wegner et al., 2010). With the first study published as part of this thesis it could be demonstrated that *P. gingivalis* has the ability to evade the host innate immune response by posttranslational citrullination of host and self-proteins.

The citrullination of the arginine specific proteases RgpA and RgpB secreted by *P. gingivalis* potentially increases their stability and provides protection from proteolytic self-degradation (Curtis et al., 1999; Potempa et al., 2003; Stobernack et al., 2016; Stobernack et al., 2018). In addition, the presence of secreted PPAD protects a PPAD deficient mutant from opsonization and phagocytic uptake by neutrophils (Stobernack et al., 2018). Mass spectrometry revealed that neutrophils contain a lower amount of proteins related to phagocytosis when infected with PPAD proficient compared to PPAD deficient *P. gingivalis*. Further experiments and mass spectrometric measurements have shown that PPAD citrullinates histone H3 at the arginine residue R73 (Stobernack et al., 2018). Histone H3 is involved in the formation and bactericidal effect of neutrophil extracellular traps (NETs). The citrullination of histone H3 reduces the net charge of the proteins and therefore may lower its ability to disrupt the bacterial cell membrane. Reduction in the bactericidal activity of histone H3 was also shown upon citrullination by human PAD4 (Tanner et al., 2021). Nonetheless, histone H3 citrullination by PAD4 is essential for NET antibacterial activity and the formation of NETs (Li et al., 2010). Moreover, it was demonstrated that PPAD deficient bacteria induce stronger NET release as more intact neutrophil nuclei were detected upon infection with PPAD proficient bacteria. Even though *P. gingivalis* W83 and its PPAD deficient mutant are not susceptible to be killed by the lysozyme-derived peptide LP9 we could show PPAD dependent

citrullination by mass spectrometry. Reduction in LP9 bactericidal activity was demonstrated by exposing *Bacillus subtilis* to PPAD treated and untreated LP9. Finally, a *Galleria mellonella* model showed reduced virulence of PPAD deficient bacteria as *G. mellonella* was more sensitive to PPAD proficient bacteria.

Overall, this study demonstrates that citrullination of proteins by PPAD enables *P. gingivalis* to evade the host innate immune system at three different levels. Consequently, providing evidence for an back then unknown bacterial immune evasion factor.



## 3.2 Establishing a protocol for the analysis of UPS components and polyubiquitinated proteins

### 3.2.1 Increasing proteomic depth by sample processing and measurement procedures

Ubiquitin E3-ligases are important in immune regulatory processes by influencing the inflammation status of the cell. Moreover, E3-ligases are also involved in the clearance process of intracellular pathogens. Therefore, analysis of E3-ligases and other UPS proteins with emphasis on their abundance is necessary to understand host pathogen interactions. Thus, the number of quantified E3-ligases in an experiment should be as large as possible. For that reason, we tested different sample preparation approaches to maximize the number of quantified E3-ligases. Applying suspension trapping combined with basic reversed phase fractionation of tryptic peptides was superior to other methods tested and resulted in the largest number of quantified E3-ligases (Figure 6A). Simultaneously, this method required less MS runtime than other methods tested (Figure 6A) and enabled the quantification of most E3-ligases (Figure 6B). So, analysis of the proteome to identify changes in UPS protein abundance was carried out by suspension trapping and basic reversed phase fractionation of tryptic peptides.

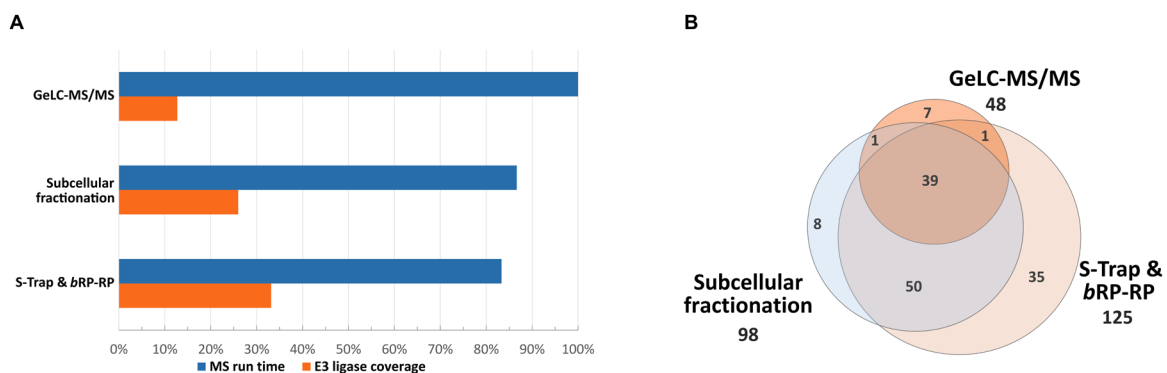


**Figure 6 Comparison of MS runtime and number of quantified E3 ligases**

Comparison of GeLC-MS/MS, subcellular fractionation by differential centrifugation and suspension trapping (S-Trap) with basic reversed phase fractionation of tryptic peptides. S-Trap and bRP-RP based sample processing led to the highest number of quantified E3-ligases, and required least MS runtime (A). Comparative overlap of quantified E3-ligases of the applied sample processing methods (B).

### 3.2.2 Enrichment of polyubiquitinated proteins

Enrichment of ubiquitinated proteins or K-GG remnant peptides is inevitable to access the ubiquitinome and determine changes on the level of ubiquitination sites (Steger et al., 2022b). Due to the high amount of input material required to enrich for K-GG peptides, the ubiquitinome was accessed by enrichment of polyubiquitinated proteins. Pan-selective enrichment of polyubiquitinated proteins was conducted with TUBE2 coupled to magnetic beads since they were tested to enabled the reproducible quantification of ubiquitinated proteins combined with a straightforward workflow. Preliminary experiments revealed inferior performance of TUBE2 coupled to agarose beads or GST affinity tags when tested against magnetic TUBEs. Therefore, TUBE2 coupled to magnetic beads was applied for pan-selective enrichment of polyubiquitinated proteins.

Besides pan selective enrichment, certain TUBEs enable chain selective enrichment, as well. The selectivity of different TUBEs was tested to ensure selective enrichment of polyubiquitinated proteins modified with the ubiquitin chain of interest. Surprisingly, the attachment of different tags dramatically influences the selectivity of certain TUBEs (Figure 7). Selective enrichment of K48 polyubiquitinated proteins was achieved by use of K48 TUBEs coupled to magnetic beads. In contrast, K63 TUBEs coupled to magnetic beads failed to selectively enrich for K63 polyubiquitinated proteins. Increasing the protein to TUBE ratio improved the selectivity (Figure 7). Still, the majority of proteins enriched by K63 magnetic TUBEs was also enriched by K48 magnetic TUBEs to the same extend. Affinity tagged TUBEs for enrichment of K63 polyubiquitinated proteins were more selective than magnetic K63 TUBEs. Again, an increased protein to TUBE ratio further enhanced the selectivity.

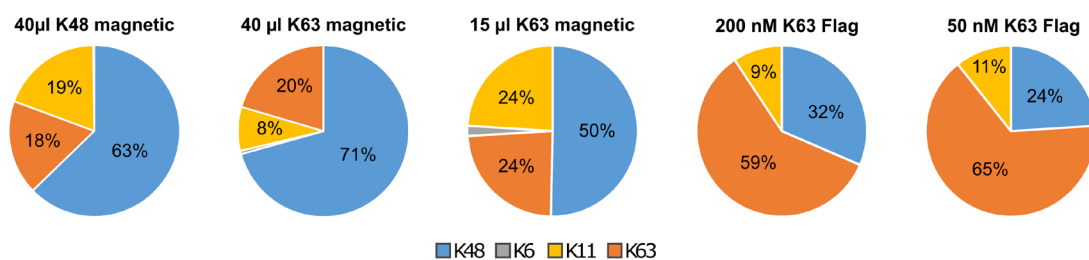


**Figure 7 Chain selectivity of tested TUBEs**

Selectivity of TUBEs was calculated from the MS1 based quantification of K-GG remnant peptides of ubiquitin. K48 magnetic TUBEs were used for selective enrichment of K48 ubiquitin chains and K63 Flag TUBEs at a concentration of 50 nM were used to selectively enrich for K63 polyubiquitinated proteins from cell lysates containing 500 µg of total protein.

The results of selective enrichment strategies depend on the cell line or tissue investigated as the linkage type distribution of ubiquitin chains within the sample may vary (Heunis et al., 2020). Moreover, proteins can be modified by several ubiquitin chains or branched chains possessing multiple chains, and thus present different linkage types. Therefore, selectivity of selected TUBEs should be tested when applied to a different type of sample.

### 3.3 Bacterial and viral co-infection in 16HBE cells (Manuscript II)

Lung epithelial cells represent a physical barrier within the hosts first line of defense counteracting potential pathogens. To investigate the cellular response of epithelial cells challenged with different pathogens, emphasizing the ubiquitinome and UPS protein abundance, 16HBE cells were infected with IAV, *S. aureus* LUG2012, *S. pyogenes* 5448, or co-infected with IAV and *S. aureus* LUG2012 or *S. pyogenes* 5448. Here, the focus is set on infections with either IAV, *S. pyogenes* 5448 and the corresponding co-infection. Life dead staining of 16HBE cells 24 hours post infection (hpi) with IAV revealed continuous growth rather than attenuated or decreased cell counts. Still, viral replication was proven to occur in the experimental setup (Surabhi et al., 2021). In contrast to IAV infections, *S. pyogenes* 5448 infections caused a rapid decrease of viable cells already at 2 hpi. Upon viral and bacterial co-infection no additional decrease in viable cell counts was detected. To elaborate on the cellular pathways and proteins changing their abundance upon infections, the 16HBE cell proteome was investigated by shotgun proteomics. This study provides the first report on the global changes in protein polyubiquitination upon IAV and *S. pyogenes* 5448 co-infection.

#### 3.3.1 Adaptation of the proteome

Label free quantification of the epithelial cell proteome enabled the detection of 63, 400, and 428 differentially abundant proteins upon infection with IAV, *S. pyogenes*, and the corresponding co-infection, respectively (Figure 8). Moreover, the number of differentially abundant proteins correlates with the results obtained from viable cell counts. Still, only a minor fraction of differentially abundant proteins was shared between the single infections. Also, the co-infection did show a greater similarity with the bacterial single infection than with the viral infection. This is reflected by the overlap of altered proteins and represented pathways resulting from annotation enrichment. Infection with *S. pyogenes* 5448 greatly affected the abundance of proteins related to mitochondria. This observation is potentially explained by an induction of apoptosis and an increase in mitochondrial dysfunction (Suen et al., 2008; Mai et al., 2017). Both, Tom22 and Tom40 were found with increased abundance upon *S. pyogenes* infection leading to the suggestion of a potential role in intracellular streptococcal propagation as it was demonstrated for *Chlamydia* (Derré et al., 2007). Changes in the abundance of proteins related to mitochondrial processes and besides, proteins connected to *cell-cell adhesion* and Rab-GTPases were detected with decreased abundance upon *S. pyogenes* 5448 infection. *S. pyogenes* invades host cells by endocytosis and the early endosomes recruit Rab5 (Sakurai

et al., 2010) which was found to be decreased in abundance upon bacterial infection. Moreover, other proteins involved in endocytosis and endosomal trafficking were reduced in abundance, as well. Streptococcal toxins like Streptococcal pyrogenic exotoxin B (SpeB), streptolysin S (SLS) and streptolysin O (SLO) participate in the streptococcal escape from the endosome, the induction of mitochondrial dysfunction and cell death by elevated mitochondrial ROS level (Aikawa et al., 2010; Tsatsaronis et al., 2014; Tsao et al., 2019). Besides Rab5, Rab11, also involved in repair of membrane damage induced by pore forming toxins, was also detected with reduced abundance upon infection (Los et al., 2011). The mechanism inducing the reduction in abundance of these proteins remains unknown but is potentially beneficial for intracellular streptococcal propagation.

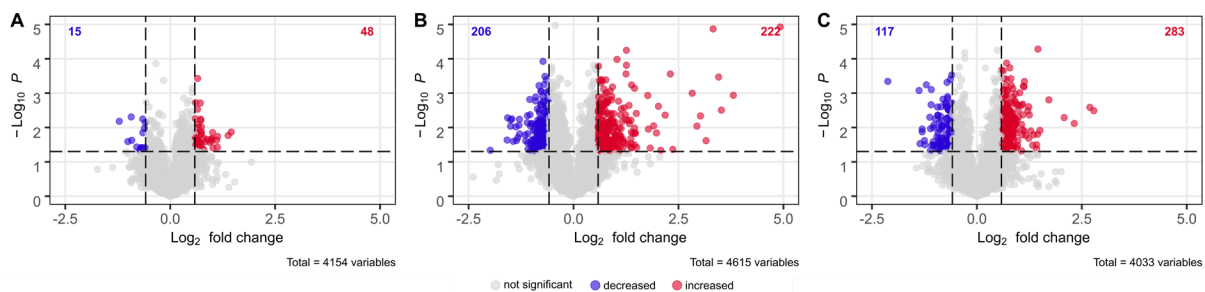


**Figure 8 Differential expression analysis of proteome samples**

Results of the differential expression analysis of proteome samples comparing the uninfected control with the respective infection (**A**--H1N1 infection; **B**--co-infection; **C**--*S. pyogenes* 5448 infection) displayed as volcano plots ( $-\log_{10} p$ -value vs.  $\log_2$  expression level). Proteins were considered as differentially abundant with a  $p$ -value  $< 0.05$  and a fold change  $> 1.5$  (students  $t$ -test). Only proteins with quantitative values in all biological replicates ( $n=3$ ) of both compared groups were tested.

Bacterial and viral co-infection mostly mirrors the patterns of the corresponding single infections leading to the assumption that the co-infection is characterized by additive, rather than synergistic effects of the infecting pathogens. This is supported by the obtained results from cell viability analysis.

### 3.3.2 Alterations in polyubiquitination of proteins

Ubiquitin serves as an important posttranslational modification being involved in protein homeostasis, signaling, protein function and localization and many other important cellular processes. Thus, the ubiquitinome was analyzed by enrichment of polyubiquitinated proteins using TUBEs. Both, viral and bacterial pathogens are described to interfere with the hosts UPS (Maculins et al., 2016; Rudnicka and Yamauchi, 2016). Therefore, it was expected that the number of proteins, detected with differential abundance in ubiquitinome samples is greater than or at least similar to numbers in proteome samples. Indeed, upon IAV infection 498 proteins (127 decreased and 371 increased) were found to be differentially abundant in their polyubiquitination incidence. Bacterial single and co-infection resembled similar numbers of differentially abundant proteins in ubiquitinome and proteome. Analogous to single infections, the shared fraction of proteins with altered abundance, and of the GO terms enriched from those proteins is rather small. But, the GO terms enriched from proteins with altered abundance in *S. pyogenes* 5448 infections is highly similar between the proteome and the ubiquitinome which leads to the assumption that the changes in the ubiquitinome are mainly driven by changes in overall protein abundance. Proteins with differential ubiquitination incidence in IAV infections are mainly related to the GO terms mRNA processing and splicing, cell-cell adhesion, and Rho-GTPases. The GO terms overrepresented from proteins of increased (Figure 9A) and decreased (Figure 9B) abundance in polyubiquitination analysis upon IAV and *S. pyogenes* 5448 co-infection resemble the terms overrepresented by differentially abundant proteins in single infections. Moreover, the results of polyubiquitin analysis do not support a synergistic effect of the infecting pathogens. This is in contrast to studies performed in mice which were able to detect a synergistic effect between pathogens in co-infection (Okamoto et al., 2003; Small et al., 2010; Jia et al., 2018). However, those studies have mainly been performed applying co-infection of IAV and *S. aureus*. Still, it could be shown in this study that IAV induces numerous changes in the incidence of polyubiquitination in 16HBE cells. Co-infection resulted in loss of some overrepresented terms identified from differentially abundant proteins in single infections. This is potentially due to counteracting regulations when the cells are infected with both pathogens.

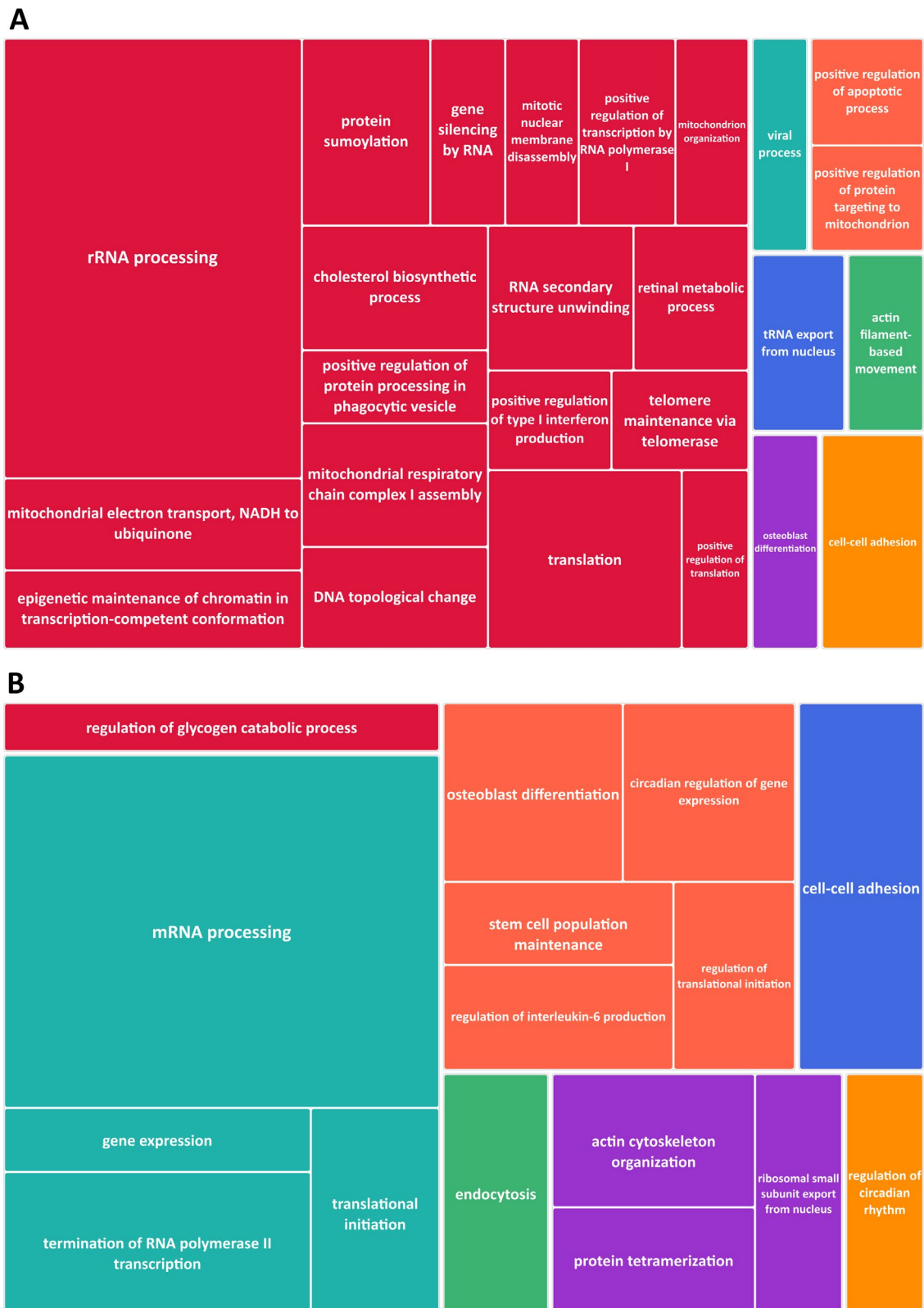


**Figure 9 GO annotation enrichment results**

Treemap representing the overrepresented *gene ontology-biological process* terms enriched from proteins of increased (A) and decreased (B) abundance in polyubiquitination analysis upon IAV and *S. pyogenes* 5448 co-infection. The size of the cell correlates with the enrichment *p*-value of the presented term and the color of the cells is based on a clustering algorithm that relies on semantic similarity measures. The treemaps were created with Revigo (Supek et al., 2011).

### **3.4 Proteome and ubiquitinome upon bacterial and viral co-infection in A549 cells (Manuscript III)**

In addition to professional immune cells, alveolar type II epithelial cells are postulated to be defenders of the alveolar space (Fehrenbach, 2001). A549 cells, a tumor derived alveolar type II epithelial cell line enable the investigation of the cellular response of alveolar epithelial cells towards viral and bacterial co-infection. Thus, A549 cells were either infected with IAV, *S. pneumoniae* D39 $\Delta$ *cps*, or the corresponding co-infection. The most frequent polyubiquitin chains in the lung are K48 chains followed by K63 chains (Heunis et al., 2020). Therefore, enrichment of polyubiquitinated proteins was not conducted by application of pan selective TUBEs but with K48 and K63 chain selective TUBEs.

In A549 cells, like in 16HBE cells, IAV infection does not impede cell proliferation. Moreover, bacterial infection and co-infection had a similar effect on A549 cell survival. Thus, the co-infection showed no deteriorating effect on the outcome of the infection. However, the highest number of proteins detected with differential abundance was upon viral and bacterial co-infection.

Viral infection featured an antiviral state of the A549 cell. This was characterized by RIG-I and MAVS mediated type I interferon induction. Upon infection DDX60, required for RIG-I signaling, was increased 25 times. Furthermore, induction of the JAK-STAT cascade, assumed from increased abundance of the interacting transcription factor IRF9, and interferon  $\gamma$  signaling were activated. Thus, protein abundance of interferon stimulated genes increased upon viral infection. Interferon stimulation can act on the abundance of UPS proteins (Seifert et al., 2010). Altered abundance was observed for nine E3-ligases and one E2 enzyme. Also, increased abundance was detected for the ISG15 and its E3 ligases HERC5 and TRIM25 as well as for its E2 transferring enzyme UBE2L6 (Mathieu et al., 2021). Additionally, an increase in abundance was detected for OAS1-3 which are involved in RNase L mediated degradation of viral RNA (Shim et al., 2017). RNase L itself was only quantified with low abundance in a single replicate of the viral and two replicates of the co-infection but not in the bacterial infection or the uninfected control. Surprisingly, less proteins were detected with altered abundance in K48 and K63 polyubiquitin enriched samples which is in contrast to previous data obtained from viral infections in 16HBE cells, where the highest number of altered proteins was detected from polyubiquitin enriched samples (Sura et al., 2021). The difference in the obtained data might be due to altered sample processing and experimental parameters.



Still, K48 polyubiquitinated proteins with increased abundance reflect the anti-viral state of the cells by overrepresentation of the GO terms *defense response to virus*, *type I interferon signaling*, and others. Moreover, proteins with alterations in K63 polyubiquitination enrich for GO terms representing mRNA processing.

*S. pneumoniae* D39 $\Delta$ *cps* infection had the greatest impact on K48 polyubiquitination and only minor effects on K63 polyubiquitination and the proteome. Thus, alterations in the proteome were related to redox processes, potentially caused by H<sub>2</sub>O<sub>2</sub> generated by pneumococci, and alteration in K63 polyubiquitination to the permeabilization of the mitochondrial outer membrane. The most prominent increase in protein abundance was detected for COX-2, induced in a p38 MAPK and NF $\kappa$ B dependent fashion (N'Guessan et al., 2006; Szymanski et al., 2012). Alterations detected in K48 polyubiquitination enable the elucidation of host responses to pneumococcal infection not detectable in the proteome. GO enrichment analysis revealed involvement of K48 polyubiquitination in Arp2/3 mediated actin organization and multiple other terms related to actin and cytoskeletal organization. Moreover, Rho-GTPase signaling was affected by differential K48 and K63 polyubiquitination. This might indicate a potential role of K48 polyubiquitination in the process of pneumococcal endocytosis and phagocytosis as the Rho-GTPases and Arp2/3 complex participate in the clathrin mediated pneumococcal uptake (Sirotkin, 2011; Sumida and Yamada, 2015; Jin et al., 2021). The involvement of pneumolysin, a cholesterol-dependent pneumococcal cytolysin shown to act on actin and GTPases (Hupp et al., 2013), in the alteration of K48 polyubiquitination remains a subject of future studies. Furthermore, a reduction in K48 polyubiquitination was detected for proteins involved in mRNA and rRNA processing.

Although the highest number of differentially abundant proteins was detected after viral and bacterial co-infection in all data sets, and enhanced alteration of abundance compared to the single infections of few proteins was detected, no synergistic effect of the infecting pathogens was observed. The additional increase in protein abundance of immunoproteasome subunits and therefore, a potential shift in the resulting antigenic peptides generated for MHC I presentation is of great interest for future studies. Here, like described before in 16HBE cells, only additive effects of the contributing pathogens were identified (Sura et al., 2021). This is especially apparent as overrepresented GO terms from proteins with differential protein abundance or differential polyubiquitination upon co-infection (Figure 10) resembled the overrepresented GO term from both of the single infections.



**Figure 10**

Treemap representing the overrepresented *gene ontology-biological process* terms enriched from differentially abundant proteins in the proteome (**A**), K48 polyubiquitin enrichment (**B**) and K63 polyubiquitin enrichment (**C**) upon IAV and *S. pneumoniae* D39Δ*cps* co-infection. The size of the cell correlates with the enrichment *p*-value of the presented term and the color of the cells is based on a clustering algorithm that relies on semantic similarity measures. The treemaps were created with Revigo (Supek et al., 2011).

Moreover, the GO terms found to be overrepresented by differentially abundant proteins detected after co-infection in proteome, K48 enriched and K63 enriched samples (Figure 10ABC) can be assumed as a result of the hypothesized additive effects. Together, this led to the conclusion that viral and bacterial co-infection is not a synergistic but an additive process, at least in the applied setup.

## 4 Concluding remarks and outlook

Within this thesis it was demonstrated that bacterial and viral co-infections under the tested conditions had no synergistic effects and did not exacerbate the outcome of the infection. Major effects on the ubiquitinome were observed in viral infections. Future analyses of different ubiquitin linkages and their alterations upon infection in different cell types, especially when coupled with ubiquitination site quantification, could provide additional knowledge on host-pathogen interaction, and possibly uncover novel therapeutic strategies. Moreover, the presented work has demonstrated that bacterial pathogens are able to utilize posttranslational protein modification to evade the human innate immune response. Here, we analyzed ubiquitination and citrullination, but the variety of posttranslational modification provides enormous potential for further investigations of pathogen induced modifications of host proteins, thus, may providing future treatment strategies.

## 5 References

- Aikawa, C., Nozawa, T., Maruyama, F., Tsumoto, K., Hamada, S., and Nakagawa, I. (2010). Reactive oxygen species induced by *Streptococcus pyogenes* invasion trigger apoptotic cell death in infected epithelial cells. *Cell Microbiol* 12, 814–830. doi: 10.1111/j.1462-5822.2010.01435.x
- Akutsu, M., Dikic, I., and Bremm, A. (2016). Ubiquitin chain diversity at a glance. *J Cell Sci* 129, 875–880. doi: 10.1242/jcs.183954
- Aliberti, S., and Kaye, K. S. (2013). The changing microbiologic epidemiology of community-acquired pneumonia. *Postgraduate Medicine* 125, 31–42. doi: 10.3810/pgm.2013.11.2710
- Arimoto, K., Takahashi, H., Hishiki, T., Konishi, H., Fujita, T., and Shimotohno, K. (2007). Negative regulation of the RIG-I signaling by the ubiquitin ligase RNF125. *Proc Natl Acad Sci U S A* 104, 7500–7505. doi: 10.1073/pnas.0611551104
- Barnett, T. C., Liebl, D., Seymour, L. M., Gillen, C. M., Lim, J. Y., Larock, C. N., et al. (2013). The globally disseminated MIT1 clone of group A *Streptococcus* evades autophagy for intracellular replication. *Cell Host Microbe* 14, 675–682. doi: 10.1016/j.chom.2013.11.003
- Bartley, P. S., Deshpande, A., Yu, P.-C., Klompas, M., Haessler, S. D., Imrey, P. B., et al. (2022). Bacterial coinfection in influenza pneumonia: Rates, pathogens, and outcomes. *Infect Control Hosp Epidemiol* 43, 212–217. doi: 10.1017/ice.2021.96
- Békés, M., Langley, D. R., and Crews, C. M. (2022). PROTAC targeted protein degraders: the past is prologue. *Nat Rev Drug Discov* 21, 181–200. doi: 10.1038/s41573-021-00371-6
- Belgnaoui, S. M., Paz, S., Samuel, S., Goulet, M.-L., Sun, Q., Kikkert, M., et al. (2012). Linear ubiquitination of NEMO negatively regulates the interferon antiviral response through disruption of the MAVS-TRAF3 complex. *Cell Host Microbe* 12, 211–222. doi: 10.1016/j.chom.2012.06.009
- Bielecka, E., Scavenius, C., Kantyka, T., Jusko, M., Mizgalska, D., Szmigielski, B., et al. (2014). Peptidyl arginine deiminase from *Porphyromonas gingivalis* abolishes anaphylatoxin C5a activity. *J Biol Chem* 289, 32481–32487. doi: 10.1074/jbc.C114.617142
- Brouwer, S., Barnett, T. C., Rivera-Hernandez, T., Rohde, M., and Walker, M. J. (2016). *Streptococcus pyogenes* adhesion and colonization. *FEBS Lett* 590, 3739–3757. doi: 10.1002/1873-3468.12254

- 
- Brundage, J. F. (2006). Interactions between influenza and bacterial respiratory pathogens: implications for pandemic preparedness. *The Lancet Infectious Diseases* 6, 303–312. doi: 10.1016/S1473-3099(06)70466-2
- Catrysse, L., Vereecke, L., Beyaert, R., and van Loo, G. (2014). A20 in inflammation and autoimmunity. *Trends in Immunology* 35, 22–31. doi: 10.1016/j.it.2013.10.005
- Celebi, G., Kesim, H., Ozer, E., and Kutlu, O. (2020). The effect of dysfunctional ubiquitin enzymes in the pathogenesis of most common diseases. *Int J Mol Sci* 21. doi: 10.3390/ijms21176335
- Chang, M., Jin, W., and Sun, S.-C. (2009). Peli1 facilitates TRIF-dependent Toll-like receptor signaling and proinflammatory cytokine production. *Nature immunology* 10, 1089–1095. doi: 10.1038/ni.1777
- Chertow, D. S., and Memoli, M. J. (2013). Bacterial coinfection in influenza: a grand rounds review. *JAMA* 309, 275–282. doi: 10.1001/jama.2012.194139
- Christophorou, M. A., Castelo-Branco, G., Halley-Stott, R. P., Oliveira, C. S., Loos, R., Radzishchanskaya, A., et al. (2014). Citrullination regulates pluripotency and histone H1 binding to chromatin. *Nature* 507, 104–108. doi: 10.1038/nature12942
- Ciechanover, A., Elias, S., Heller, H., Ferber, S., and Hershko, A. (1980). Characterization of the heat-stable polypeptide of the ATP-dependent proteolytic system from reticulocytes. *J Biol Chem* 255, 7525–7528.
- Clancy, K. W., Weerapana, E., and Thompson, P. R. (2016). Detection and identification of protein citrullination in complex biological systems. *Curr Opin Chem Biol* 30, 1–6. doi: 10.1016/j.cbpa.2015.10.014
- Cox, J., and Mann, M. (2008). MaxQuant enables high peptide identification rates, individualized p.p.b.-range mass accuracies and proteome-wide protein quantification. *Nat Biotechnol* 26, 1367–1372. doi: 10.1038/nbt.1511
- Cozens, A. L., Yezzi, M. J., Kunzelmann, K., Ohrui, T., Chin, L., Eng, K., et al. (1994). CFTR expression and chloride secretion in polarized immortal human bronchial epithelial cells. *Am J Respir Cell Mol Biol* 10, 38–47. doi: 10.1165/ajrcmb.10.1.7507342
- Curtis, M. A., Thickett, A., Slaney, J. M., Rangarajan, M., Aduse-Opoku, J., Shepherd, P., et al. (1999). Variable carbohydrate modifications to the catalytic chains of the RgpA and RgpB proteases of *Porphyromonas gingivalis* W50. *Infect Immun* 67, 3816–3823. doi: 10.1128/IAI.67.8.3816-3823.1999
-

- Da Huang, W., Sherman, B. T., and Lempicki, R. A. (2009). Systematic and integrative analysis of large gene lists using DAVID bioinformatics resources. *Nat Protoc* 4, 44–57. doi: 10.1038/nprot.2008.211
- Dagli, N., Dagli, R., Darwish, S., and Baroudi, K. (2016). Oral microbial shift: Factors affecting the microbiome and prevention of oral disease. *J Contemp Dent Pract* 17, 90–96. doi: 10.5005/jp-journals-10024-1808
- Damgaard, R. B., Nachbur, U., Yabal, M., Wong, W. W.-L., Fiil, B. K., Kastirr, M., et al. (2012). The ubiquitin ligase XIAP recruits LUBAC for NOD2 signaling in inflammation and innate immunity. *Mol Cell* 46, 746–758. doi: 10.1016/j.molcel.2012.04.014
- Darrah, E., and Andrade, F. (2018). Rheumatoid arthritis and citrullination. *Curr Opin Rheumatol* 30, 72–78. doi: 10.1097/BOR.0000000000000452
- Dekaboruah, E., Suryavanshi, M. V., Chettri, D., and Verma, A. K. (2020). Human microbiome: an academic update on human body site specific surveillance and its possible role. *Arch Microbiol* 202, 2147–2167. doi: 10.1007/s00203-020-01931-x
- Derré, I., Pypaert, M., Dautry-Varsat, A., and Agaisse, H. (2007). RNAi screen in *Drosophila* cells reveals the involvement of the Tom complex in Chlamydia infection. *PLoS Pathog* 3, 1446–1458. doi: 10.1371/journal.ppat.0030155
- Dickson, R. P., Erb-Downward, J. R., Martinez, F. J., and Huffnagle, G. B. (2016). The microbiome and the respiratory tract. *Annu Rev Physiol* 78, 481–504. doi: 10.1146/annurev-physiol-021115-105238
- Ding, T., and Schloss, P. D. (2014). Dynamics and associations of microbial community types across the human body. *Nature* 509, 357–360. doi: 10.1038/nature13178
- Erpapazoglou, Z., Walker, O., and Haguenaer-Tsapis, R. (2014). Versatile roles of k63-linked ubiquitin chains in trafficking. *Cells* 3, 1027–1088. doi: 10.3390/cells3041027
- Fan, Y., Mao, R., Yu, Y., Liu, S., Shi, Z., Cheng, J., et al. (2014). USP21 negatively regulates antiviral response by acting as a RIG-I deubiquitinase. *J Exp Med* 211, 313–328. doi: 10.1084/jem.20122844
- Faust, T. B., Donovan, K. A., Yue, H., Chamberlain, P. P., and Fischer, E. S. (2021). Small-molecule approaches to targeted protein degradation. *Annu. Rev. Cancer Biol.* 5, 181–201. doi: 10.1146/annurev-cancerbio-051420-114114
- Fehrenbach, H. (2001). Alveolar epithelial type II cell: defender of the alveolus revisited. *Respir Res* 2, 33–46. doi: 10.1186/rr36
- Feng, W., Sun, X., Shi, N., Zhang, M., Guan, Z., and Duan, M. (2017). Influenza A virus NS1 protein induced A20 contributes to viral replication by suppressing interferon-induced

- antiviral response. *Biochem Biophys Res Commun* 482, 1107–1113. doi: 10.1016/j.bbrc.2016.11.166
- Fujita, Y., Tinoco, R., Li, Y., Senft, D., and Ronai, Z. A. (2019). Ubiquitin ligases in cancer immunotherapy - balancing antitumor and autoimmunity. *Trends Mol Med* 25, 428–443. doi: 10.1016/j.molmed.2019.02.002
- Gabarrini, G., Smit, M. de, Westra, J., Brouwer, E., Vissink, A., Zhou, K., et al. (2015). The peptidylarginine deiminase gene is a conserved feature of *Porphyromonas gingivalis*. *Sci Rep* 5, 13936. doi: 10.1038/srep13936
- Gack, M. U., Albrecht, R. A., Urano, T., Inn, K.-S., Huang, I.-C., Carnero, E., et al. (2009). Influenza A virus NS1 targets the ubiquitin ligase TRIM25 to evade recognition by the host viral RNA sensor RIG-I. *Cell Host Microbe* 5, 439–449. doi: 10.1016/j.chom.2009.04.006
- Giard, D. J., Aaronson, S. A., Todaro, G. J., Arnstein, P., Kersey, J. H., Dosik, H., et al. (1973). In vitro cultivation of human tumors: establishment of cell lines derived from a series of solid tumors. *J Natl Cancer Inst* 51, 1417–1423. doi: 10.1093/jnci/51.5.1417
- Gillespie, M., Jassal, B., Stephan, R., Milacic, M., Rothfels, K., Senff-Ribeiro, A., et al. (2022). The reactome pathway knowledgebase 2022. *Nucleic Acids Res* 50, D687–D692. doi: 10.1093/nar/gkab1028
- Girardin, S. E., Boneca, I. G., Viala, J., Chamailard, M., Labigne, A., Thomas, G., et al. (2003). Nod2 is a general sensor of peptidoglycan through muramyl dipeptide (MDP) detection. *J Biol Chem* 278, 8869–8872. doi: 10.1074/jbc.C200651200
- Gómez, M. I., Lee, A., Reddy, B., Muir, A., Soong, G., Pitt, A., et al. (2004). *Staphylococcus aureus* protein A induces airway epithelial inflammatory responses by activating TNFR1. *Nat Med* 10, 842–848. doi: 10.1038/nm1079
- Häcker, H., Redecke, V., Blagoev, B., Kratchmarova, I., Hsu, L.-C., Wang, G. G., et al. (2006). Specificity in Toll-like receptor signalling through distinct effector functions of TRAF3 and TRAF6. *Nature* 439, 204–207. doi: 10.1038/nature04369
- Hajishengallis, G., Darveau, R. P., and Curtis, M. A. (2012). The keystone-pathogen hypothesis. *Nat Rev Microbiol* 10, 717–725. doi: 10.1038/nrmicro2873
- Hajishengallis, G., and Lamont, R. J. (2012). Beyond the red complex and into more complexity: the polymicrobial synergy and dysbiosis (PSD) model of periodontal disease etiology. *Mol Oral Microbiol* 27, 409–419. doi: 10.1111/j.2041-1014.2012.00663.x
- Hajishengallis, G., Liang, S., Payne, M. A., Hashim, A., Jotwani, R., Eskan, M. A., et al. (2011). Low-abundance biofilm species orchestrates inflammatory periodontal disease

- through the commensal microbiota and complement. *Cell Host Microbe* 10, 497–506. doi: 10.1016/j.chom.2011.10.006
- Hasegawa, M., Fujimoto, Y., Lucas, P. C., Nakano, H., Fukase, K., Núñez, G., et al. (2008). A critical role of RICK/RIP2 polyubiquitination in Nod-induced NF-kappaB activation. *EMBO J* 27, 373–383. doi: 10.1038/sj.emboj.7601962
- He, M., Zhou, Z., Shah, A. A., Zou, H., Tao, J., Chen, Q., et al. (2016). The emerging role of deubiquitinating enzymes in genomic integrity, diseases, and therapeutics. *Cell Biosci* 6, 62. doi: 10.1186/s13578-016-0127-1
- Hershko, A., Ciechanover, A., Heller, H., Haas, A. L., and Rose, I. A. (1980). Proposed role of ATP in protein breakdown: conjugation of protein with multiple chains of the polypeptide of ATP-dependent proteolysis. *Proc Natl Acad Sci U S A* 77, 1783–1786. doi: 10.1073/pnas.77.4.1783
- Hershko, A., Ciechanover, A., and Rose, I. A. (1979). Resolution of the ATP-dependent proteolytic system from reticulocytes: a component that interacts with ATP. *Proc Natl Acad Sci U S A* 76, 3107–3110. doi: 10.1073/pnas.76.7.3107
- Hershko, A., Heller, H., Elias, S., and Ciechanover, A. (1983). Components of ubiquitin-protein ligase system. Resolution, affinity purification, and role in protein breakdown. *J Biol Chem* 258, 8206–8214.
- Heunis, T., Lamoliatte, F., Marín-Rubio, J. L., Dannoura, A., and Trost, M. (2020). Technical report: Targeted proteomic analysis reveals enrichment of atypical ubiquitin chains in contractile murine tissues. *Journal of Proteomics* 229, 103963. doi: 10.1016/j.jprot.2020.103963
- Hiemstra, P. S., McCray, P. B., and Bals, R. (2015). The innate immune function of airway epithelial cells in inflammatory lung disease. *Eur Respir J* 45, 1150–1162. doi: 10.1183/09031936.00141514
- Hjerpe, R., Aillet, F., Lopitz-Otsoa, F., Lang, V., England, P., and Rodriguez, M. S. (2009). Efficient protection and isolation of ubiquitylated proteins using tandem ubiquitin-binding entities. *EMBO Rep* 10, 1250–1258. doi: 10.1038/embor.2009.192
- Hou, K., Wu, Z.-X., Chen, X.-Y., Wang, J.-Q., Zhang, D., Xiao, C., et al. (2022). Microbiota in health and diseases. *Signal Transduct Target Ther* 7, 135. doi: 10.1038/s41392-022-00974-4
- How, K. Y., Song, K. P., and Chan, K. G. (2016). *Porphyromonas gingivalis*: An Overview of Periodontopathic Pathogen below the Gum Line. *Front Microbiol* 7, 53. doi: 10.3389/fmicb.2016.00053



- 
- Hupp, S., Förtsch, C., Wippel, C., Ma, J., Mitchell, T. J., and Iliev, A. I. (2013). Direct transmembrane interaction between actin and the pore-competent, cholesterol-dependent cytolysin pneumolysin. *J Mol Biol* 425, 636–646. doi: 10.1016/j.jmb.2012.11.034
- Jahan, A. S., Biquand, E., Muñoz-Moreno, R., Le Quang, A., Mok, C. K.-P., Wong, H. H., et al. (2020). OTUB1 is a key regulator of RIG-I-dependent immune signaling and is targeted for proteasomal degradation by influenza A NS1. *Cell Rep* 30, 1570-1584.e6. doi: 10.1016/j.celrep.2020.01.015
- Jenne, C. N., Liao, S., and Singh, B. (2018). Neutrophils: multitasking first responders of immunity and tissue homeostasis. *Cell Tissue Res* 371, 395–397. doi: 10.1007/s00441-018-2802-5
- Jia, L., Zhao, J., Yang, C., Liang, Y., Long, P., Liu, X., et al. (2018). Severe pneumonia caused by coinfection with influenza virus followed by methicillin-resistant *Staphylococcus aureus* induces higher mortality in mice. *Front. Immunol.* 9, 3189. doi: 10.3389/fimmu.2018.03189
- Jiang, X., Kinch, L. N., Brautigam, C. A., Chen, X., Du, F., Grishin, N. V., et al. (2012). Ubiquitin-induced oligomerization of the RNA sensors RIG-I and MDA5 activates antiviral innate immune response. *Immunity* 36, 959–973. doi: 10.1016/j.immuni.2012.03.022
- Jin, M., Shirazinejad, C., Wang, B., Yan, A., Schöneberg, J., Upadhyayula, S., et al. (2021). Asymmetric Arp2/3-mediated actin assembly facilitates clathrin-mediated endocytosis at stalled sites in genome-edited human stem cells. *Preprint at bioRxiv*. doi: 10.1101/2021.07.16.452693
- Kim, W., Bennett, E. J., Huttlin, E. L., Guo, A., Li, J., Possemato, A., et al. (2011). Systematic and quantitative assessment of the ubiquitin-modified proteome. *Mol Cell* 44, 325–340. doi: 10.1016/j.molcel.2011.08.025
- Kirui, J., Mondal, A., and Mehle, A. (2016). Ubiquitination upregulates influenza virus polymerase function. *J Virol* 90, 10906–10914. doi: 10.1128/JVI.01829-16
- Klein, E. Y., Monteforte, B., Gupta, A., Jiang, W., May, L., Hsieh, Y.-H., et al. (2016). The frequency of influenza and bacterial coinfection: a systematic review and meta-analysis. *Influenza Other Respir Viruses* 10, 394–403. doi: 10.1111/irv.12398
- Komander, D., and Rape, M. (2012). The ubiquitin code. *Annu Rev Biochem* 81, 203–229. doi: 10.1146/annurev-biochem-060310-170328
-

- Krivan, H. C., Roberts, D. D., and Ginsburg, V. (1988). Many pulmonary pathogenic bacteria bind specifically to the carbohydrate sequence GalNAc beta 1-4Gal found in some glycolipids. *Proc Natl Acad Sci U S A* 85, 6157–6161. doi: 10.1073/pnas.85.16.6157
- Kwon, Y. T., and Ciechanover, A. (2017). The ubiquitin code in the ubiquitin-proteasome system and autophagy. *Trends Biochem Sci* 42, 873–886. doi: 10.1016/j.tibs.2017.09.002
- Lamotte, L.-A., and Tafforeau, L. (2021). How influenza A virus NS1 deals with the ubiquitin system to evade innate immunity. *Viruses* 13. doi: 10.3390/v13112309
- Le Goffic, R., Pothlichet, J., Vitour, D., Fujita, T., Meurs, E., Chignard, M., et al. (2007). Cutting edge: influenza A virus activates TLR3-dependent inflammatory and RIG-I-dependent antiviral responses in human lung epithelial cells. *J Immunol* 178, 3368–3372. doi: 10.4049/jimmunol.178.6.3368
- Lee, C.-Y., Wang, D., Wilhelm, M., Zolg, D. P., Schmidt, T., Schnatbaum, K., et al. (2018). Mining the human tissue proteome for protein citrullination. *Mol Cell Proteomics* 17, 1378–1391. doi: 10.1074/mcp.RA118.000696
- Leiding, J. W. (2017). Neutrophil evolution and their diseases in humans. *Front. Immunol.* 8, 1009. doi: 10.3389/fimmu.2017.01009
- LeMessurier, K. S., Tiwary, M., Morin, N. P., and Samarasinghe, A. E. (2020). Respiratory barrier as a safeguard and regulator of defense against influenza A virus and *Streptococcus pneumoniae*. *Front Immunol* 11, 3. doi: 10.3389/fimmu.2020.00003
- Lewis, P. A., and Shope, R. E. (1931). Swine influenza: II. a hemophilic bacillus from the respiratory tract of infected swine. *J Exp Med* 54, 361–371. doi: 10.1084/jem.54.3.361
- Leys, E. J., Smith, J. H., Lyons, S. R., and Griffen, A. L. (1999). Identification of *Porphyromonas gingivalis* strains by heteroduplex analysis and detection of multiple strains. *Journal of Clinical Microbiology* 37, 3906–3911. doi: 10.1128/JCM.37.12.3906-3911.1999
- Li, P., Li, M., Lindberg, M. R., Kennett, M. J., Xiong, N., and Wang, Y. (2010). PAD4 is essential for antibacterial innate immunity mediated by neutrophil extracellular traps. *J Exp Med* 207, 1853–1862. doi: 10.1084/jem.20100239
- Li, W., Bengtson, M. H., Ulbrich, A., Matsuda, A., Reddy, V. A., Orth, A., et al. (2008). Genome-wide and functional annotation of human E3 ubiquitin ligases identifies MULAN, a mitochondrial E3 that regulates the organelle's dynamics and signaling. *PLoS One* 3, e1487. doi: 10.1371/journal.pone.0001487

- 
- Liu, C.-H., Zhou, L., Chen, G., and Krug, R. M. (2015). Battle between influenza A virus and a newly identified antiviral activity of the PARP-containing ZAPL protein. *Proc Natl Acad Sci U S A* 112, 14048–14053. doi: 10.1073/pnas.1509745112
- Liu, S., Chen, J., Cai, X., Wu, J., Chen, X., Wu, Y.-T., et al. (2013). MAVS recruits multiple ubiquitin E3 ligases to activate antiviral signaling cascades. *eLife* 2, e00785. doi: 10.7554/eLife.00785
- Los, F. C. O., Kao, C.-Y., Smitham, J., McDonald, K. L., Ha, C., Peixoto, C. A., et al. (2011). RAB-5- and RAB-11-dependent vesicle-trafficking pathways are required for plasma membrane repair after attack by bacterial pore-forming toxin. *Cell Host Microbe* 9, 147–157. doi: 10.1016/j.chom.2011.01.005
- Maculins, T., Fiskin, E., Bhogaraju, S., and Dikic, I. (2016). Bacteria-host relationship: ubiquitin ligases as weapons of invasion. *Cell Res* 26, 499–510. doi: 10.1038/cr.2016.30
- Mai, N., Chrzanowska-Lightowlers, Z. M. A., and Lightowlers, R. N. (2017). The process of mammalian mitochondrial protein synthesis. *Cell Tissue Res* 367, 5–20. doi: 10.1007/s00441-016-2456-0
- Martin-Loeches, I., van Someren Gréve, F., and Schultz, M. J. (2017). Bacterial pneumonia as an influenza complication. *Curr Opin Infect Dis* 30, 201–207. doi: 10.1097/QCO.0000000000000347
- Mathieu, N. A., Papparisto, E., Barr, S. D., and Spratt, D. E. (2021). HERC5 and the ISGylation pathway: Critical modulators of the antiviral immune response. *Viruses* 13. doi: 10.3390/v13061102
- Maurais, A. J., Salinger, A. J., Tobin, M., Shaffer, S. A., Weerapana, E., and Thompson, P. R. (2021). A streamlined data analysis pipeline for the identification of sites of citrullination. *Biochemistry* 60, 2902–2914. doi: 10.1021/acs.biochem.1c00369
- McGraw, W. T., Potempa, J., Farley, D., and Travis, J. (1999). Purification, characterization, and sequence analysis of a potential virulence factor from *Porphyromonas gingivalis*, peptidylarginine deiminase. *Infect Immun* 67, 3248–3256. doi: 10.1128/IAI.67.7.3248-3256.1999
- Mckelvey, A. C., Lear, T. B., Dunn, S. R., Evankovich, J., Londino, J. D., Bednash, J. S., et al. (2016). RING finger E3 ligase PPP1R11 regulates TLR2 signaling and innate immunity. *eLife Sciences Publications, Ltd.*
- Michallet, M.-C., Meylan, E., Ermolaeva, M. A., Vazquez, J., Rebsamen, M., Curran, J., et al. (2008). TRADD protein is an essential component of the RIG-like helicase antiviral pathway. *Immunity* 28, 651–661. doi: 10.1016/j.immuni.2008.03.013
-

- Michelle, C., Vourc'h, P., Mignon, L., and Andres, C. R. (2009). What was the set of ubiquitin and ubiquitin-like conjugating enzymes in the eukaryote common ancestor? *J Mol Evol* 68, 616–628. doi: 10.1007/s00239-009-9225-6
- Mishra, K., Bukavina, L., and Ghannoum, M. (2021). Symbiosis and dysbiosis of the human mycobiome. *Front Microbiol* 12, 636131. doi: 10.3389/fmicb.2021.636131
- Moghadam, S. A., Shirzaiy, M., and Risbaf, S. (2017). The associations between periodontitis and respiratory disease. *J Nepal Health Res Counc* 15, 1–6. doi: 10.3126/jnhrc.v15i1.18023
- Morris, D. E., Cleary, D. W., and Clarke, S. C. (2017). Secondary bacterial infections associated with influenza pandemics. *Front Microbiol* 8, 1041. doi: 10.3389/fmicb.2017.01041
- Nakagawa, I. (2013). *Streptococcus pyogenes* escapes from autophagy. *Cell Host Microbe* 14, 604–606. doi: 10.1016/j.chom.2013.11.012
- Neumann, Y., Bruns, S. A., Rohde, M., Prajsnar, T. K., Foster, S. J., and Schmitz, I. (2016). Intracellular *Staphylococcus aureus* eludes selective autophagy by activating a host cell kinase. *Autophagy* 12, 2069–2084. doi: 10.1080/15548627.2016.1226732
- N'Guessan, P. D., Hippenstiel, S., Etouem, M. O., Zahlten, J., Beermann, W., Lindner, D., et al. (2006). *Streptococcus pneumoniae* induced p38 MAPK- and NF-kappaB-dependent COX-2 expression in human lung epithelium. *Am J Physiol Lung Cell Mol Physiol* 290, L1131-8. doi: 10.1152/ajplung.00383.2005
- Nielsen, M. L., Vermeulen, M., Bonaldi, T., Cox, J., Moroder, L., and Mann, M. (2008). Iodoacetamide-induced artifact mimics ubiquitination in mass spectrometry. *Nat Methods* 5, 459–460. doi: 10.1038/nmeth0608-459
- Núñez-Belmar, J., Morales-Olavarria, M., Vicencio, E., Vernal, R., Cárdenas, J. P., and Cortez, C. (2022). Contribution of -omics technologies in the study of *Porphyromonas gingivalis* during periodontitis pathogenesis: A minireview. *Int J Mol Sci* 24. doi: 10.3390/ijms24010620
- Oganesyan, G., Saha, S. K., Guo, B., He, J. Q., Shahangian, A., Zarnegar, B., et al. (2006). Critical role of TRAF3 in the Toll-like receptor-dependent and -independent antiviral response. *Nature* 439, 208–211. doi: 10.1038/nature04374
- Okamoto, S., Kawabata, S., Nakagawa, I., Okuno, Y., Goto, T., Sano, K., et al. (2003). Influenza A virus-infected hosts boost an invasive type of *Streptococcus pyogenes* infection in mice. *J Virol* 77, 4104–4112. doi: 10.1128/jvi.77.7.4104-4112.2003

- 
- Oliva, J., and Terrier, O. (2021). Viral and bacterial co-infections in the lungs: dangerous liaisons. *Viruses* 13. doi: 10.3390/v13091725
- Palacios, G., Hornig, M., Cisterna, D., Savji, N., Bussetti, A. V., Kapoor, V., et al. (2009). *Streptococcus pneumoniae* coinfection is correlated with the severity of H1N1 pandemic influenza. *PLOS ONE* 4, e8540. doi: 10.1371/journal.pone.0008540
- Patini, R., Staderini, E., Lajolo, C., Lopetuso, L., Mohammed, H., Rimondini, L., et al. (2018). Relationship between oral microbiota and periodontal disease: a systematic review. *Eur Rev Med Pharmacol Sci* 22, 5775–5788. doi: 10.26355/eurrev\_201809\_15903
- Peng, J., Schwartz, D., Elias, J. E., Thoreen, C. C., Cheng, D., Marsischky, G., et al. (2003). A proteomics approach to understanding protein ubiquitination. *Nat Biotechnol* 21, 921–926. doi: 10.1038/nbt849
- Pichlmair, A., Schulz, O., Tan, C. P., Näslund, T. I., Liljeström, P., Weber, F., et al. (2006). RIG-I-mediated antiviral responses to single-stranded RNA bearing 5'-phosphates. *Science* 314, 997–1001. doi: 10.1126/science.1132998
- Potempa, J., Sroka, A., Imamura, T., and Travis, J. (2003). Gingipains, the major cysteine proteinases and virulence factors of *Porphyromonas gingivalis*: structure, function and assembly of multidomain protein complexes. *Curr Protein Pept Sci* 4, 397–407. doi: 10.2174/1389203033487036
- Potter C. W. (2001). A history of influenza. *Journal of Applied Microbiology* 91, 572–579.
- Reizine, F., Grégoire, M., Lesouhaitier, M., Coirier, V., Gauthier, J., Delaloy, C., et al. (2022). Beneficial effects of citrulline enteral administration on sepsis-induced T cell mitochondrial dysfunction. *Proc Natl Acad Sci U S A* 119. doi: 10.1073/pnas.2115139119
- Rose, C. M., Isasa, M., Ordureau, A., Prado, M. A., Beausoleil, S. A., Jedrychowski, M. P., et al. (2016). Highly multiplexed quantitative mass spectrometry analysis of ubiquitylomes. *Cell Syst* 3, 395–403.e4. doi: 10.1016/j.cels.2016.08.009
- Roth, G. A., Abate, D., Abate, K. H., Abay, S. M., Abbafati, C., Abbasi, N., et al. (2018). Global, regional, and national age-sex-specific mortality for 282 causes of death in 195 countries and territories, 1980–2017: a systematic analysis for the Global Burden of Disease Study 2017. *The Lancet* 392, 1736–1788. doi: 10.1016/S0140-6736(18)32203-7
- Rudnicka, A., and Yamauchi, Y. (2016). Ubiquitin in influenza virus entry and innate immunity. *Viruses* 8, 293. doi: 10.3390/v8100293
- Ruuskanen, O., and Järvinen, A. (2014). What is the real role of respiratory viruses in severe community-acquired pneumonia? *Clinical Infectious Diseases* 59, 71–73. doi: 10.1093/cid/ciu242
-

- Saini, R., Saini, S., and Sharma, S. (2010). Periodontitis: A risk factor to respiratory diseases. *Lung India* 27, 189. doi: 10.4103/0970-2113.68313
- Sakurai, A., Maruyama, F., Funao, J., Nozawa, T., Aikawa, C., Okahashi, N., et al. (2010). Specific behavior of intracellular *Streptococcus pyogenes* that has undergone autophagic degradation is associated with bacterial streptolysin O and host small G proteins Rab5 and Rab7. *J Biol Chem* 285, 22666–22675. doi: 10.1074/jbc.M109.100131
- Saleh, M., Bartual, S. G., Abdullah, M. R., Jensch, I., Asmat, T. M., Petruschka, L., et al. (2013). Molecular architecture of *Streptococcus pneumoniae* surface thioredoxin-fold lipoproteins crucial for extracellular oxidative stress resistance and maintenance of virulence. *EMBO Mol Med* 5, 1852–1870. doi: 10.1002/emmm.201202435
- Schulman, B. A., and Harper, J. W. (2009). Ubiquitin-like protein activation by E1 enzymes: the apex for downstream signalling pathways. *Nat Rev Mol Cell Biol* 10, 319–331. doi: 10.1038/nrm2673
- Sedghi, L., DiMassa, V., Harrington, A., Lynch, S. V., and Kapila, Y. L. (2021). The oral microbiome: Role of key organisms and complex networks in oral health and disease. *Periodontol 2000* 87, 107–131. doi: 10.1111/prd.12393
- Seifert, U., Bialy, L. P., Ebstein, F., Bech-Otschir, D., Voigt, A., Schröter, F., et al. (2010). Immunoproteasomes preserve protein homeostasis upon interferon-induced oxidative stress. *Cell* 142, 613–624. doi: 10.1016/j.cell.2010.07.036
- Self, W. H., Balk, R. A., Grijalva, C. G., Williams, D. J., Zhu, Y., Anderson, E. J., et al. (2017). Procalcitonin as a marker of etiology in adults hospitalized with community-acquired pneumonia. *Clinical Infectious Diseases* 65, 183–190. doi: 10.1093/cid/cix317
- Sender, R., Fuchs, S., and Milo, R. (2016). Revised Estimates for the Number of Human and Bacteria Cells in the Body. *PLoS Biol* 14, e1002533. doi: 10.1371/journal.pbio.1002533
- Shambat, S. M., Chen, P., Nguyen Hoang, A. T., Bergsten, H., Vandenesch, F., Siemens, N., et al. (2015). Modelling staphylococcal pneumonia in a human 3D lung tissue model system delineates toxin-mediated pathology. *Dis Model Mech* 8, 1413–1425. doi: 10.1242/dmm.021923
- Shelburne, S. A., Granville, C., Tokuyama, M., Sitkiewicz, I., Patel, P., and Musser, J. M. (2005). Growth characteristics of and virulence factor production by group A *Streptococcus* during cultivation in human saliva. *Infect Immun* 73, 4723–4731. doi: 10.1128/IAI.73.8.4723-4731.2005

- 
- Sherman, B. T., Hao, M., Qiu, J., Jiao, X., Baseler, M. W., Lane, H. C., et al. (2022). DAVID: a web server for functional enrichment analysis and functional annotation of gene lists (2021 update). *Nucleic Acids Res* 50, W216-21. doi: 10.1093/nar/gkac194
- Shi, Y., Li, Z., Wang, B., Shi, X., Ye, H., Delafield, D. G., et al. (2022). Enabling Global Analysis of Protein Citrullination via Biotin Thiol Tag-Assisted Mass Spectrometry. *Anal Chem* 94, 17895–17903. doi: 10.1021/acs.analchem.2c03844
- Shim, J. M., Kim, J., Tenson, T., Min, J.-Y., and Kainov, D. E. (2017). Influenza virus infection, interferon response, viral counter-response, and apoptosis. *Viruses* 9. doi: 10.3390/v9080223
- Shizukuishi, S., Ogawa, M., Matsunaga, S., Tomokiyo, M., Ikebe, T., Fushinobu, S., et al. (2020). *Streptococcus pneumoniae* hijacks host autophagy by deploying CbpC as a decoy for Atg14 depletion. *EMBO Rep* 21, e49232. doi: 10.15252/embr.201949232
- Shope, R. E. (1931a). Swine influenza : I. experimental transmission and pathology. *J Exp Med* 54, 349–359. doi: 10.1084/jem.54.3.349
- Shope, R. E. (1931b). Swine influenza : III. filtration experiments and etiology. *J Exp Med* 54, 373–385. doi: 10.1084/jem.54.3.373
- Siemens, N., Chakrakodi, B., Shambat, S. M., Morgan, M., Bergsten, H., Hyldegaard, O., et al. (2016). Biofilm in group A streptococcal necrotizing soft tissue infections. *JCI Insight* 1, e87882. doi: 10.1172/jci.insight.87882
- Siemens, N., Oehmcke-Hecht, S., Mettenleiter, T. C., Kreikemeyer, B., Valentin-Weigand, P., and Hammerschmidt, S. (2017). Port d'entrée for respiratory infections - does the influenza A virus pave the way for bacteria? *Front Microbiol* 8, 2602. doi: 10.3389/fmicb.2017.02602
- Sillanpää, S., Kramna, L., Oikarinen, S., Sipilä, M., Rautiainen, M., Aittoniemi, J., et al. (2017). Next-Generation Sequencing Combined with Specific PCR Assays To Determine the Bacterial 16S rRNA Gene Profiles of Middle Ear Fluid Collected from Children with Acute Otitis Media. *mSphere* 2. doi: 10.1128/mSphere.00006-17
- Sirotkin, V. (2011). Cell biology: actin keeps endocytosis on a short leash. *Curr Biol* 21, R552-4. doi: 10.1016/j.cub.2011.06.029
- Small, C.-L., Shaler, C. R., McCormick, S., Jeyanathan, M., Damjanovic, D., Brown, E. G., et al. (2010). Influenza infection leads to increased susceptibility to subsequent bacterial superinfection by impairing NK cell responses in the lung. *J Immunol* 184, 2048–2056. doi: 10.4049/jimmunol.0902772
-

- Smith, W., Andrewes, C. H., and Laidlaw, P. P. (1933). A virus obtained from influenza patients. *The Lancet* 222, 66–68. doi: 10.1016/S0140-6736(00)78541-2
- Steger, M., Demichev, V., Backman, M., Ohmayer, U., Ihmor, P., Müller, S., et al. (2021). Time-resolved in vivo ubiquitinome profiling by DIA-MS reveals USP7 targets on a proteome-wide scale. *Nat Commun* 12, 5399. doi: 10.1038/s41467-021-25454-1
- Steger, M., Karayel, Ö., and Demichev, V. (2022a). Ubiquitinomics: history, methods and applications in basic research and drug discovery. *Proteomics*, e2200074. doi: 10.1002/pmic.202200074
- Steger, M., Karayel, Ö., and Demichev, V. (2022b). Ubiquitinomics: history, methods and applications in basic research and drug discovery. *Proteomics*, e2200074. doi: 10.1002/pmic.202200074
- Stobernack, T., Du Teil Espina, M., Mulder, L. M., Palma Medina, L. M., Piebenga, D. R., Gabarrini, G., et al. (2018). A secreted bacterial peptidylarginine deiminase can neutralize human innate immune defenses. *mBio* 9. doi: 10.1128/mBio.01704-18
- Stobernack, T., Glasner, C., Junker, S., Gabarrini, G., Smit, M. de, Jong, A. de, et al. (2016). Extracellular proteome and citrullinome of the oral pathogen *Porphyromonas gingivalis*. *J Proteome Res* 15, 4532–4543. doi: 10.1021/acs.jproteome.6b00634
- Suen, D.-F., Norris, K. L., and Youle, R. J. (2008). Mitochondrial dynamics and apoptosis. *Genes Dev* 22, 1577–1590. doi: 10.1101/gad.1658508
- Sumida, G. M., and Yamada, S. (2015). Rho GTPases and the downstream effectors actin-related protein 2/3 (Arp2/3) complex and myosin II induce membrane fusion at self-contacts. *J Biol Chem* 290, 3238–3247. doi: 10.1074/jbc.M114.612168
- Supek, F., Bošnjak, M., Škunca, N., and Šmuc, T. (2011). REVIGO summarizes and visualizes long lists of gene ontology terms. *PLoS One* 6, e21800. doi: 10.1371/journal.pone.0021800
- Sura, T., Surabhi, S., Maaß, S., Hammerschmidt, S., Siemens, N., and Becher, D. (2021). The global proteome and ubiquitinome of bacterial and viral co-infected bronchial epithelial cells. *Journal of Proteomics* 250, 104387. doi: 10.1016/j.jprot.2021.104387
- Surabhi, S., Jachmann, L. H., Lalk, M., Hammerschmidt, S., Methling, K., and Siemens, N. (2021). Bronchial epithelial cells accumulate citrate intracellularly in response to pneumococcal hydrogen peroxide. *ACS Infect Dis* 7, 2971–2978. doi: 10.1021/acsinfecdis.1c00372



- 
- Szymanski, K. V., Toennies, M., Becher, A., Fatykhova, D., N'Guessan, P. D., Gutbier, B., et al. (2012). *Streptococcus pneumoniae*-induced regulation of cyclooxygenase-2 in human lung tissue. *Eur Respir J* 40, 1458–1467. doi: 10.1183/09031936.00186911
- Takeuchi, O., and Akira, S. (2010). Pattern recognition receptors and inflammation. *Cell* 140, 805–820. doi: 10.1016/j.cell.2010.01.022
- Tanner, L., Bhongir, R. K. V., Karlsson, C. A. Q., Le, S., Ljungberg, J. K., Andersson, P., et al. (2021). Citrullination of extracellular histone H3.1 reduces antibacterial activity and exacerbates its proteolytic degradation. *J Cyst Fibros* 20, 346–355. doi: 10.1016/j.jcf.2020.07.010
- Taubenberger, J. K., and Morens, D. M. (2006). 1918 Influenza: the mother of all pandemics. *Emerg Infect Dis* 12, 15–22. doi: 10.3201/eid1201.050979
- Taubenberger, J. K., and Morens, D. M. (2009). Pandemic influenza--including a risk assessment of H5N1. *Rev Sci Tech* 28, 187–202. doi: 10.20506/rst.28.1.1879
- Tracz, M., and Bialek, W. (2021). Beyond K48 and K63: non-canonical protein ubiquitination. *Cell Mol Biol Lett* 26, 1. doi: 10.1186/s11658-020-00245-6
- Tripathi, S., White, M. R., and Hartshorn, K. L. (2015). The amazing innate immune response to influenza A virus infection. *Innate Immun* 21, 73–98. doi: 10.1177/1753425913508992
- Troeger, C. E., Blacker, B. F., Khalil, I. A., Zimsen, S. R. M., Albertson, S. B., Abate, D., et al. (2019). Mortality, morbidity, and hospitalisations due to influenza lower respiratory tract infections, 2017: an analysis for the Global Burden of Disease Study 2017. *The Lancet Respiratory Medicine* 7, 69–89. doi: 10.1016/S2213-2600(18)30496-X
- Tsao, N., Kuo, C.-F., Cheng, M.-H., Lin, W.-C., Lin, C.-F., and Lin, Y.-S. (2019). Streptolysin S induces mitochondrial damage and macrophage death through inhibiting degradation of glycogen synthase kinase-3 $\beta$  in *Streptococcus pyogenes* infection. *Sci Rep* 9, 5371. doi: 10.1038/s41598-019-41853-3
- Tsatsaronis, J. A., Walker, M. J., and Sanderson-Smith, M. L. (2014). Host responses to group a streptococcus: cell death and inflammation. *PLoS Pathog* 10, e1004266. doi: 10.1371/journal.ppat.1004266
- Tyanova, S., Temu, T., and Cox, J. (2016a). The MaxQuant computational platform for mass spectrometry-based shotgun proteomics. *Nat Protoc* 11, 2301–2319. doi: 10.1038/nprot.2016.136
-

- Tyanova, S., Temu, T., Sinitcyn, P., Carlson, A., Hein, M. Y., Geiger, T., et al. (2016b). The Perseus computational platform for comprehensive analysis of (prote)omics data. *Nat Methods* 13, 731–740. doi: 10.1038/nmeth.3901
- Vareille, M., Kieninger, E., Edwards, M. R., and Regamey, N. (2011). The airway epithelium: soldier in the fight against respiratory viruses. *Clin Microbiol Rev* 24, 210–229. doi: 10.1128/CMR.00014-10
- Vossenaar, E. R., Zendman, A. J. W., van Venrooij, W. J., and Pruijn, G. J. M. (2003). PAD, a growing family of citrullinating enzymes: genes, features and involvement in disease. *Bioessays* 25, 1106–1118. doi: 10.1002/bies.10357
- Wegner, N., Lundberg, K., Kinloch, A., Fisher, B., Malmström, V., Feldmann, M., et al. (2010). Autoimmunity to specific citrullinated proteins gives the first clues to the etiology of rheumatoid arthritis. *Immunol Rev* 233, 34–54. doi: 10.1111/j.0105-2896.2009.00850.x
- Weiser, J. N., Ferreira, D. M., and Paton, J. C. (2018). *Streptococcus pneumoniae*: transmission, colonization and invasion. *Nat Rev Microbiol* 16, 355–367. doi: 10.1038/s41579-018-0001-8
- Wertz, I. E., O'Rourke, K. M., Zhou, H., Eby, M., Aravind, L., Seshagiri, S., et al. (2004). De-ubiquitination and ubiquitin ligase domains of A20 downregulate NF-kappaB signalling. *Nature* 430, 694–699. doi: 10.1038/nature02794
- Widjaja, I., Vries, E. de, Tscherne, D. M., García-Sastre, A., Rottier, P. J. M., and Haan, C. A. M. de (2010). Inhibition of the ubiquitin-proteasome system affects influenza A virus infection at a postfusion step. *J Virol* 84, 9625–9631. doi: 10.1128/JVI.01048-10
- Xia, C., Vijayan, M., Pritzl, C. J., Fuchs, S. Y., McDermott, A. B., and Hahm, B. (2015). Hemagglutinin of influenza A virus antagonizes type I interferon (IFN) responses by inducing degradation of type I IFN receptor 1. *J Virol* 90, 2403–2417. doi: 10.1128/JVI.02749-15
- Xu, G., Paige, J. S., and Jaffrey, S. R. (2010). Global analysis of lysine ubiquitination by ubiquitin remnant immunoaffinity profiling. *Nat Biotechnol* 28, 868–873. doi: 10.1038/nbt.1654
- Zheng, S., Yu, S., Fan, X., Zhang, Y., Sun, Y., Lin, L., et al. (2021). *Porphyromonas gingivalis* survival skills: Immune evasion. *J Periodontal Res* 56, 1007–1018. doi: 10.1111/jre.12915
- Zinngrebe, J., Montinaro, A., Peltzer, N., and Walczak, H. (2014). Ubiquitin in the immune system. *EMBO Rep* 15, 28–45. doi: 10.1002/embr.201338025



## Manuscript I

### A Secreted Bacterial Peptidylarginine Deiminase Can Neutralize Human Innate Immune Defenses

Stobernack T, du Teil Espina M, Mulder LM, Palma Medina LM, Piebenga DR, Gabarrini G, Zhao X, Janssen KMJ, Hulzebos J, Brouwer E, Sura T, Becher D, van Winkelhoff AJ, Götz F, Otto A, Westra J, van Dijl JM

Published in *mBIO* 2018,  
DOI: 10.1128/mBio.01704-18

Author contributions: T. Stobernack, M. du Teil Espina, A. Otto, J. Westra, and J. M. van Dijl conceived and designed the experiments. T. Stobernack, M. du Teil Espina, L. M. Mulder, L. M. Palma Medina, D. R. Piebenga, G. Gabarrini, X. Zhao, K. M. J. Janssen, J. Hulzebos, T. Sura, and A. Otto performed the experiments and analyzed the data. D. Becher, F. Götz, and J. Westra contributed reagents. E. Brouwer applied for medical ethics approval and recruited volunteers. A. J. van Winkelhoff, J. Westra, and J. M. van Dijl supervised the project. T. Stobernack, M. du Teil Espina, and J. M. van Dijl wrote the manuscript.

---

Thomas Sura

---

Prof. Dr. Dörte Becher



## A Secreted Bacterial Peptidylarginine Deiminase Can Neutralize Human Innate Immune Defenses

Tim Stobernack,<sup>a</sup> Marines du Teil Espina,<sup>a</sup> Lianne M. Mulder,<sup>a</sup> Laura M. Palma Medina,<sup>a</sup> Dillon R. Piebenga,<sup>a</sup> Giorgio Gabarrini,<sup>a,b</sup> Xin Zhao,<sup>a</sup> Koen M. J. Janssen,<sup>c</sup> Jarnick Hulzebos,<sup>d</sup> Elisabeth Brouwer,<sup>d</sup> Thomas Sura,<sup>e</sup> Dörte Becher,<sup>e</sup> Arie Jan van Winkelhoff,<sup>a,b</sup> Friedrich Götz,<sup>f</sup> Andreas Otto,<sup>e</sup> Johanna Westra,<sup>d</sup> Jan Maarten van Dijl<sup>a</sup>

<sup>a</sup>Department of Medical Microbiology, University of Groningen, University Medical Center Groningen, Groningen, The Netherlands

<sup>b</sup>Department of Periodontology, University of Groningen, University Medical Center Groningen, Center for Dentistry and Oral Hygiene, Groningen, The Netherlands

<sup>c</sup>Department of Oral and Maxillofacial Surgery, University of Groningen, University Medical Center Groningen, Groningen, The Netherlands

<sup>d</sup>Department of Rheumatology and Clinical Immunology, University of Groningen, University Medical Center Groningen, Groningen, The Netherlands

<sup>e</sup>Institute for Microbiology, Ernst-Moritz-Armdt-University Greifswald, Greifswald, Germany

<sup>f</sup>Microbial Genetics, Interfaculty Institute of Microbiology and Infection Medicine and Infection Medicine (IMT), University of Tübingen, Tübingen, Germany

**ABSTRACT** The keystone oral pathogen *Porphyromonas gingivalis* is associated with severe periodontitis. Intriguingly, this bacterium is known to secrete large amounts of an enzyme that converts peptidylarginine into citrulline residues. The present study was aimed at identifying possible functions of this citrullinating enzyme, named *Porphyromonas* peptidylarginine deiminase (PPAD), in the periodontal environment. The results show that PPAD is detectable in the gingiva of patients with periodontitis, and that it literally neutralizes human innate immune defenses at three distinct levels, namely bacterial phagocytosis, capture in neutrophil extracellular traps (NETs), and killing by the lysozyme-derived cationic antimicrobial peptide LP9. As shown by mass spectrometry, exposure of neutrophils to PPAD-proficient bacteria reduces the levels of neutrophil proteins involved in phagocytosis and the bactericidal histone H2. Further, PPAD is shown to citrullinate the histone H3, thereby facilitating the bacterial escape from NETs. Last, PPAD is shown to citrullinate LP9, thereby restricting its antimicrobial activity. The importance of PPAD for immune evasion is corroborated in the infection model *Galleria mellonella*, which only possesses an innate immune system. Together, the present observations show that PPAD-catalyzed protein citrullination defuses innate immune responses in the oral cavity, and that the citrullinating enzyme of *P. gingivalis* represents a new type of bacterial immune evasion factor.

**IMPORTANCE** Bacterial pathogens do not only succeed in breaking the barriers that protect humans from infection, but they also manage to evade insults from the human immune system. The importance of the present study resides in the fact that protein citrullination is shown to represent a new bacterial mechanism for immune evasion. In particular, the oral pathogen *P. gingivalis* employs this mechanism to defuse innate immune responses by secreting a protein-citrullinating enzyme. Of note, this finding impacts not only the global health problem of periodontitis, but it also extends to the prevalent autoimmune disease rheumatoid arthritis, which has been strongly associated with periodontitis, PPAD activity, and loss of tolerance against citrullinated proteins, such as the histone H3.

**KEYWORDS** *Porphyromonas gingivalis*, citrullination, immune evasion, neutrophils, protein modification

Received 31 August 2018 Accepted 17 September 2018 Published 30 October 2018

**Citation** Stobernack T, du Teil Espina M, Mulder LM, Palma Medina LM, Piebenga DR, Gabarrini G, Zhao X, Janssen KMJ, Hulzebos J, Brouwer E, Sura T, Becher D, van Winkelhoff AJ, Götz F, Otto A, Westra J, van Dijl JM. 2018. A secreted bacterial peptidylarginine deiminase can neutralize human innate immune defenses. *mBio* 9:e01704-18. <https://doi.org/10.1128/mBio.01704-18>.

**Editor** Rino Rappuoli, GSK Vaccines

**Copyright** © 2018 Stobernack et al. This is an open-access article distributed under the terms of the [Creative Commons Attribution 4.0 International license](https://creativecommons.org/licenses/by/4.0/).

Address correspondence to Jan Maarten van Dijl, [j.m.van.dijl01@umcg.nl](mailto:j.m.van.dijl01@umcg.nl).

T.S. and M.D.T.E. contributed equally.

Periodontitis affects around 10% to 15% of the adult population, making it one of the most prevalent diseases worldwide (1). It is characterized by chronic inflammation of the tissues supporting the teeth and is associated with a dysbiotic oral microbiome found primarily in the form of biofilms in the periodontal pocket (Fig. 1a). These conditions trigger an increased tissue infiltration by immune cells, mainly neutrophils, which play a pivotal role in maintaining periodontal health by employing diverse and potent bactericidal mechanisms (2, 3). Successful periodontal pathogens, however, have evolved sophisticated strategies to avoid or subvert neutrophil killing and to thrive in an inflamed environment. In particular, the Gram-negative anaerobe *Porphyromonas gingivalis*, which is considered a major etiological agent of periodontitis, possesses the ability to dysregulate the homeostasis between oral biofilms and innate immunity (2, 3). The bacterium secretes large amounts of a unique enzyme, the *P. gingivalis* peptidylarginine deiminase (PPAD), which catalyzes the citrullination of both bacterial and host proteins (4–8). This posttranslational protein modification involves the deimination of positively charged arginine residues into neutral citrulline residues. Intriguingly, *P. gingivalis* has not only been implicated in periodontitis but also in the prevalent autoimmune disease rheumatoid arthritis, which is strongly associated with periodontitis, PPAD activity, and a loss of tolerance against citrullinated proteins, such as the histone H3 (2, 9–11). Nonetheless, the biological and clinical relevance of PPAD for dysbiosis in the oral cavity had so far remained enigmatic. The question raised in our present study was whether this citrullinating enzyme may literally neutralize human innate immune defenses in the periodontal environment, thereby serving as a secreted bacterial immune evasion factor.

## RESULTS AND DISCUSSION

**PPAD impairs bacterial binding and internalization by neutrophils.** To verify the relevance of PPAD production in inflamed periodontal tissue, we performed immunohistochemistry using a previously developed PPAD-specific antibody. As shown in Fig. 1b, this allowed us to detect the presence of PPAD in gingival tissues of periodontitis patients for the first time. This observation enticed us to further investigate the interaction of *P. gingivalis* with key host immune cells. In particular, we aimed this investigation at dissecting potentially pleiotropic functions of PPAD in the evasion of neutrophil-specific innate immunity by *P. gingivalis* W83, previously characterized as one of the most virulent *Porphyromonas* strains (12). Challenge with human neutrophils showed that strain W83 is bound and internalized by these neutrophils (Fig. 2a and b). Notably, the association and internalization levels observed for a genetically engineered PPAD-deficient *P. gingivalis* mutant were 2- to 3-fold higher than in the parental W83 strain (Fig. 2b). This is partly related to a higher percentage of the neutrophils binding and internalizing PPAD-deficient *P. gingivalis* (Fig. S1a). The addition of PPAD-containing culture supernatant allowed the PPAD-deficient mutant to evade neutrophil association and internalization, and significant evasion of neutrophil internalization was even observed upon the addition of purified recombinant PPAD (Fig. 2c and d). This shows that PPAD helps *P. gingivalis* evade destruction by neutrophils, which is a prerequisite to survive the high neutrophil influx in inflamed gingival tissue of periodontitis patients.

We have recently shown that PPAD is secreted in two different forms, either in a soluble state or bound to excreted outer membrane vesicles (OMVs) (7, 8). As shown with the recombinant protein, soluble PPAD can limit neutrophil internalization, and the same effect was observed upon addition of purified PPAD-containing OMVs to the PPAD-deficient *P. gingivalis* (Fig. 2d; see also Fig. S1b and c in the supplemental material). Moreover, these OMVs even inhibited binding of the PPAD mutant bacteria by neutrophils (Fig. 2c). Together, these observations imply that both forms of secreted PPAD, soluble and OMV bound, can serve to protect *P. gingivalis* against containment and elimination by human neutrophils. Further, the data suggest that OMV-bound PPAD could be primarily used by *P. gingivalis* to evade neutrophil binding, while the soluble PPAD might be more effective against internalization. However, it is important

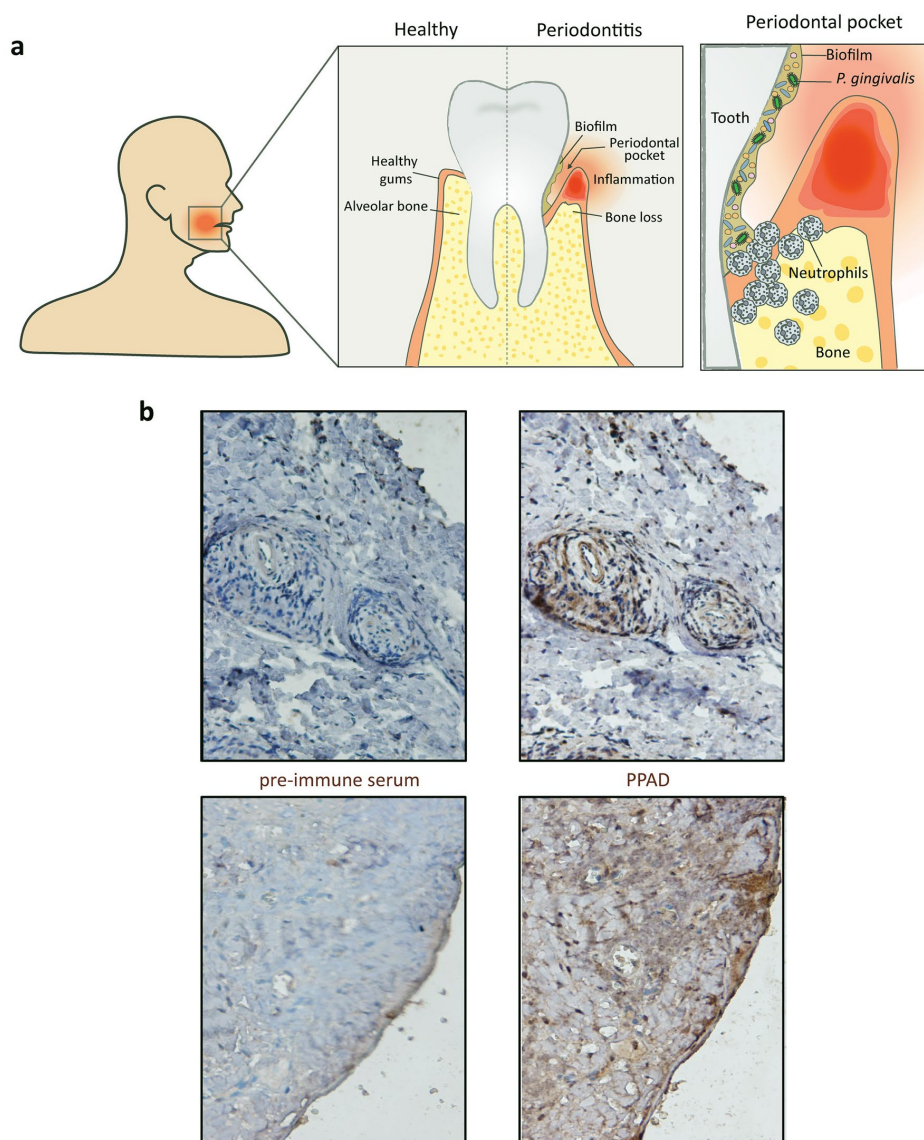


**FIG 1** Detection of PPAD in gingival tissue of a periodontitis patient. (a) Hallmarks of periodontitis, with schematic representation of biofilm formation and neutrophil recruitment in the periodontal pocket. Note that the periodontal biofilm is polymicrobial, where *P. gingivalis* is represented in green and other microorganisms in orange and blue. (b) PPAD detection by immunohistochemistry in gingival tissues of a periodontitis patient using a PPAD-specific antibody. Control staining of the same gingival tissues was performed with the respective rabbit preimmune serum. PPAD staining is observed in gingival tissue primarily around blood vessels (upper images) or at the epithelium (lower images).

to bear in mind that the recombinant PPAD isolated from *Lactococcus lactis*, though soluble and enzymatically active, may lack particular as-yet-unidentified posttranslational modifications that are present in the soluble PPAD produced by *P. gingivalis*. Such modifications could impact, for example, the enzyme's substrate specificity and specific activity. This awaits further experimental verification by purification of soluble

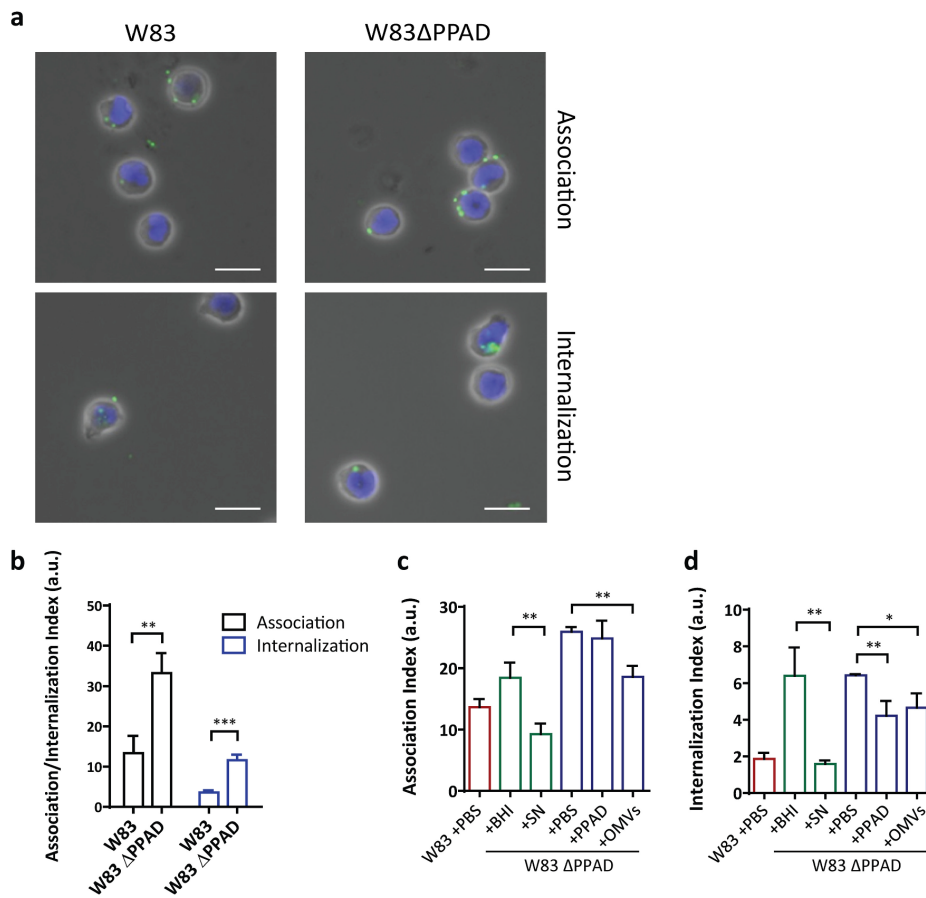


**FIG 2** PPAD impairs bacterial binding and internalization by neutrophils. (a and b) *P. gingivalis* W83 ΔPPAD is bound and internalized by neutrophils at a higher rate than wild-type *P. gingivalis* W83. Microscopic visualization of neutrophils with bound or internalized *P. gingivalis* (a) (scale bars = 10 μm), and the respective association and internalization indices as determined by flow cytometry (b). (c and d) Rescue of bacterial binding and internalization by neutrophils upon addition of 2.5 μg recombinant PPAD (indicated as PPAD), 16 μg PPAD-containing W83 outer membrane vesicles (OMVs), or 100 μl PPAD-containing W83 culture supernatant (SN). Association and internalization indices determined by flow cytometry are shown. (b) Data are means of three biologically independent samples (neutrophils from three donors), where each infection experiment was carried out four times. (c and d) Data are means of four replicates of one biological sample (one neutrophil donor). \*,  $P < 0.05$ ; \*\*,  $P < 0.01$ ; \*\*\*,  $P < 0.001$ ; two-tailed unpaired Student's *t* tests. Data are presented as mean values ± standard deviation (SD). a.u., arbitrary units.

PPAD from the *P. gingivalis* W83 growth medium and subsequent functional and structural characterization.

How could PPAD mediate neutrophil evasion? An attractive hypothesis is that this involves the so-called gingipains of *P. gingivalis*, a group of highly proteolytic enzymes, including the arginine-specific enzymes RgpA and RgpB (13, 14). We recently reported that these gingipains are subject to citrullination by PPAD (6). Further, Maekawa et al. have previously shown that RgpA and RgpB induce Toll-like receptor 2 (TLR2)-C5aR cross talk, ultimately leading to the inhibition of actin polymerization and consequent inhibition of phagocytosis (44). We therefore assessed the RgpA and RgpB levels by Western blotting. As shown in Fig. 3a and S1d, the neutrophils are exposed to lower levels of RgpA and RgpB in the absence of PPAD. Moreover, the overall proteolytic activity in the growth medium of PPAD-deficient *P. gingivalis* is significantly reduced, as shown by a lowered rate of histone H3 protein degradation by PPAD-deficient W83



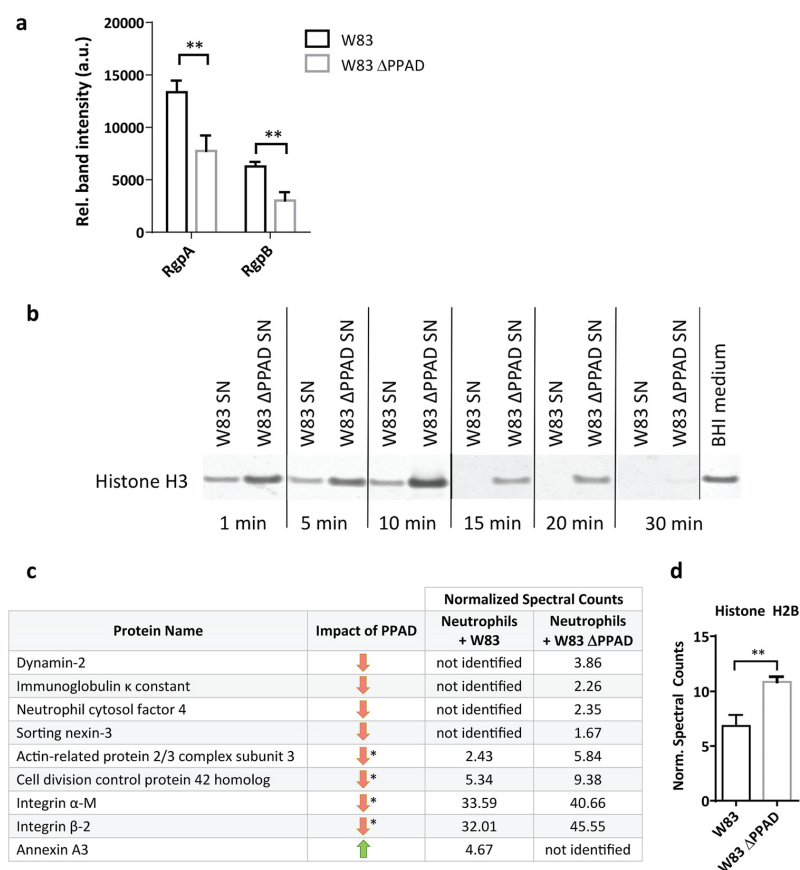


**FIG 3** PPAD stabilizes gingipains and modulates the levels of phagocytosis-related proteins. (a) Relative (Rel.) levels of gingipains (RgpA/RgpB) in infected neutrophils. (b) Time course of histone H3 degradation by *P. gingivalis* proteases in the presence or absence of PPAD, as determined by Western blotting (SN, culture supernatant). (c and d) Quantification of significant changes in the amounts of phagocytosis-related proteins (c) and the antimicrobial histone H2B (d) in infected neutrophils, as approximated by mass spectrometry. (a, c, and d) Data are means of three replicates of one neutrophil donor. \*\*,  $P < 0.01$ , two-tailed unpaired Student's *t* tests. Data are presented as mean values  $\pm$  SD. \*,  $P < 0.05$ , Fisher's exact test. Green and red arrows indicate up- or downregulation of  $>10\%$  of the respective protein in W83-infected neutrophils. Norm., normalized.

compared to that by the PPAD-proficient strain (Fig. 3b). Overall, in accordance with the model of Maekawa and colleagues (44), lower levels of RgpA and RgpB at the neutrophil surface, as observed for neutrophils infected with PPAD-deficient bacteria, will lead to less suppression of phagocytosis and therefore enhanced internalization of these bacteria, as shown in Fig. 2b. The underlying mechanism by which the presence of PPAD results in increased levels and activity of RgpA and RgpB is likely to be their previously documented citrullination by PPAD (6), which could confer protection against possible (self-)cleavage at arginine residues.

Furthermore, to verify the possibility that phagocytosis in neutrophils is decreased due to lower actin polymerization in the presence of PPAD-proficient bacteria, we applied a mass spectrometry-based approach. Indeed, the results show that the levels of the actin assembly-related proteins dynamain-2 (15), actin-related protein 2/3 (16), and the cell division control protein 42 (17) are decreased when neutrophils are challenged by wild-type *P. gingivalis* (Fig. 3c). This is consistent with a role of gingipain citrullination in the inhibition of actin polymerization and evasion of phagocytosis.

However, our mass spectrometry analyses provide more clues as to how *P. gingivalis* corrupts the neutrophil. For example, the immunoglobulin  $\kappa$  constant protein is not detectable in neutrophils infected with wild-type *P. gingivalis*, while this protein is identified in neutrophils infected with the PPAD mutant (Fig. 3c). This implies a role of PPAD in inhibiting opsonization of the bacteria, as immunoglobulins are important in opsonization, which is the first step of phagocytosis. Altogether, a challenge with wild-type *P. gingivalis* leads to altered levels of 17 phagocytosis-related proteins compared to the PPAD mutant (Table S1). In particular, the levels of the integrins  $\alpha$ -M and  $\beta$ -2, involved in actin polymerization (18), are reduced (Fig. 3c). These integrins play also crucial roles in cell signaling, neutrophil adhesion to endothelial cells, and granule exocytosis for releasing bactericidal toxins into the intracellular milieu (19). In fact, once a bacterial prey is internalized by neutrophils, several granule and cytosolic proteins facilitate its efficient destruction. Among these, the neutrophil cytosolic factor 4 (NCF4/p40phox) is involved in the oxidative burst that serves to kill internalized bacteria (20). Indeed, the NCF4 levels are also substantially lower when neutrophils are challenged with wild-type *P. gingivalis* than with PPAD-deficient bacteria (Fig. 3c). Last, the bactericidal histone H2B (21) is present in smaller amounts when neutrophils are exposed to PPAD-proficient *P. gingivalis* (Fig. 3d). Altogether, these findings show that *P. gingivalis* needs PPAD to escape internalization and subsequent elimination by neutrophils. Further, our results correlate the increased phagocytosis in the absence of PPAD to reduced levels of gingipains and a restricted impact of PPAD-deficient *P. gingivalis* on neutrophil proteins needed for phagocytosis.

**PPAD citrullinates histone H3 and helps evade NETs.** Neutrophils can also capture bacteria with neutrophil extracellular traps (NETs), which are web-like structures mainly consisting of decondensed chromatin and bactericidal proteins (22, 23). Recent studies have shown that NETs are abundantly produced in periodontitis (24, 25). During the process of NET activation and release (known as NETosis), DNA-bound histones are citrullinated by the human peptidylarginine deiminases, leading to a change in charge and decondensation of the DNA (26). Of note, histones are known to have different roles in NET formation. On the one hand, the positive charge of histones is needed for their bactericidal effects. On the other hand, Li and colleagues have shown that citrullination of histone H3 by the human peptidylarginine deiminase 4 (PAD4) is essential for bacterial killing in NETs (27). The process of NETosis can be artificially induced by the addition of phorbol myristate acetate (PMA), as shown in Fig. 4a and b (see also Fig. S2). We exposed PPAD-proficient and PPAD-deficient *P. gingivalis* to neutrophils undergoing NETosis and observed higher NETosis in both infection situations than in the uninfected PMA-activated neutrophils. However, a greater number of intact neutrophil nuclei were noticed for PPAD-proficient bacteria than for the PPAD-deficient bacteria (Fig. 4c and d). This indicates that PPAD activity can impair the bacteria-induced NETosis. Consistent with this view, higher numbers of PPAD-deficient bacteria were observed to be trapped in NETs (Fig. 4c and d) and eliminated upon capture (Fig. 4e). The exact mechanisms by which PPAD could interfere with NET formation are currently unknown and should be a topic of future investigations. A possible explanation could be that the higher levels of secreted protease activity produced by the PPAD-proficient bacteria have a negative impact on the NET formation, for example, by degrading certain human proteins needed for DNA decondensation.

Histones are critical actors in capture and killing of bacteria in the NETs, and arginine-rich histones especially directly disrupt the bacterial cell membrane by virtue of their positive charge (21). We therefore inspected histone H3 citrullination in neutrophils undergoing NETosis, which revealed a strong PPAD-dependent citrullination of this antibacterial agent (Fig. 4c and d). This result was subsequently validated by incubating purified histone H3 with the recombinant PPAD, which led to histone H3 citrullination, as shown by Western blotting and mass spectrometry (Fig. 5a and b and S3a and b). Compared to the purified human peptidylarginine deiminase 2 (PAD2),

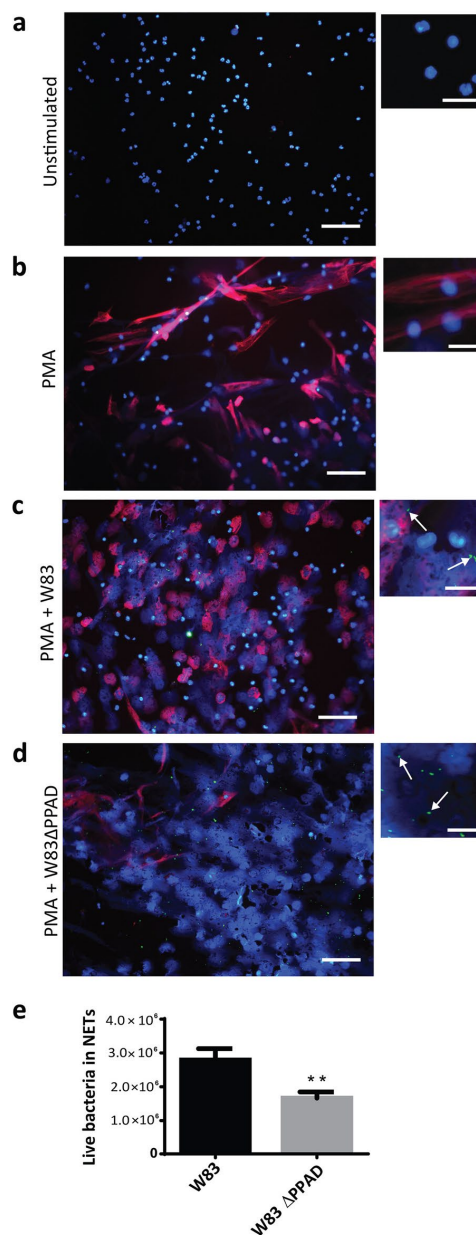


**FIG 4** PPAD impacts on histone H3 citrullination and allows *P. gingivalis* to evade and survive capture in neutrophil extracellular traps (NETs). (a to d) Representative fluorescence microscopy images of NETosis and citrullinated histone H3 levels in the presence of *P. gingivalis*. PMA was applied at a concentration of 20 nM to induce NETosis. DNA was stained with DAPI (blue), *P. gingivalis* was labeled with FITC (green), and citrullinated histone H3 (citH3; red) was visualized with a specific antibody (scale bars, 200  $\mu$ m in regular images and 50  $\mu$ m in enlarged images). (e) Quantification of live bacteria present in isolated NETs.

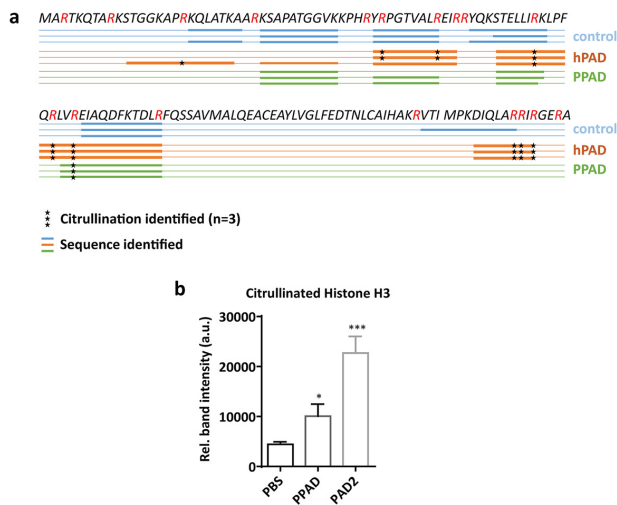


**FIG 5** PPAD citrullinates histone H3. *In vitro* citrullination of histone H3. Citrullination by human PAD2 was used as a positive control. (a) Schematic representation of citrullinated arginine residues in histone H3 upon incubation with PPAD or PAD2, as determined by mass spectrometry. (b) Western blot analysis of citrullinated histone H3. Quantification of band intensity in three independent experiments is shown. \*,  $P < 0.05$ ; \*\*\*,  $P < 0.001$ , two-tailed unpaired Student's *t* tests. Data are presented as mean values  $\pm$  SD.

PPAD showed a somewhat lower citrullinating activity on purified histone H3 that correlated with the citrullination of only one arginine residue (Arg73), whereas human PAD2 was capable of citrullinating up to nine different arginine residues in histone H3 (Fig. 5a). Even so, in terms of citrullination of the NET-associated histone H3, the impact of PPAD was much higher than that of any other human PAD released by neutrophils undergoing NETosis (Fig. 4b and d). These findings are fully consistent with the previously published observation that citrullinated histone H3 is abundantly detectable in inflamed periodontal tissue (28). Thus, *P. gingivalis* is capable of neutralizing a major NET-associated histone implicated in bacterial elimination in the periodontium, where PPAD is clearly detectable (Fig. 1b).

**PPAD citrullinates human lysozyme-derived peptide LP9, neutralizing its antibacterial activity.** The bacterial cell wall-degrading enzyme lysozyme is an important contributor to human innate immunity. This enzyme, abundantly present in our saliva, is also produced by neutrophils (29, 30). It acts in two different modes, the first that the full-size protein has muramidase activity that degrades peptidoglycan, leading to bacterial lysis. In addition, degradation products of lysozyme act as cationic antimicrobial peptides (CAMPs), as was shown for the LP9 peptide (<sub>107</sub>RAWVAWRNR<sub>115</sub>) (31). LP9 introduces pores into the bacterial cell membrane by electrostatic interaction, leading to bacterial death. Presumably, this relates to LP9's three arginine residues. We therefore tested whether PPAD can neutralize LP9 by citrullination, thereby abrogating its bactericidal activity toward LP9-susceptible bacteria. This is indeed the case, as mass spectrometry showed that PPAD can convert all three arginines of LP9 to citrulline (Fig. 6a). Concomitantly, citrullination reduced the bactericidal activity of LP9, as demonstrated with the LP9-susceptible indicator *Bacillus subtilis* (Fig. 6b). This shows that PPAD can even neutralize CAMPs, which belong to our most effective defenses against bacterial pathogens. Notably, PPAD-proficient and PPAD-deficient *P. gingivalis* strains are not susceptible to LP9 (Fig. S4). This shows that PPAD is not the only factor that protects *P. gingivalis* against LP9 activity. In fact, this finding is in agreement with the previous observation that gingipains play an important role in the deactivation of CAMPs by proteolytic degradation (32, 33).

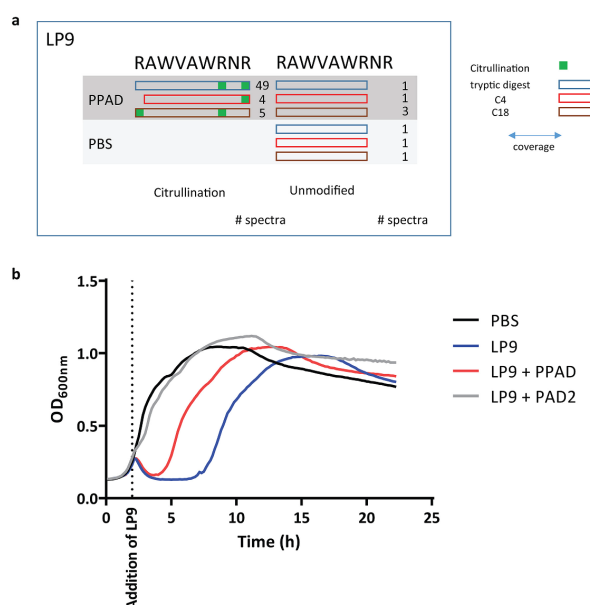


**FIG 6** PPAD citrullinates human lysozyme-derived peptide LP9, neutralizing its antibacterial activity. (a) Arginine residues in the LP9 peptide (RAWVAWRNR) are citrullinated by PPAD, as determined by mass spectrometry. Blue, red, and brown rectangles mark the outcomes from three distinct analytical approaches, tryptic digest,  $C_4$  exclusion filtration, and  $C_{18}$  inclusion filtration, respectively. (b) Citrullination of LP9 by PPAD or PAD2 impairs the antibacterial activity of LP9. Citrullinated LP9 exhibits significantly reduced growth inhibition of the indicator bacterium *B. subtilis*. Results are representative of three independent experiments, with three technical replicates per experiment. OD<sub>600nm</sub>, optical density at 600 nm.

**PPAD is a critical virulence factor of *P. gingivalis*.** While the above-mentioned studies show that PPAD targets innate immunity at three different levels, an important question that remained to be addressed was whether it contributes *in vivo* to the virulence of *P. gingivalis*. This was investigated using larvae of the wax moth *Galleria mellonella*, because this infection model only possesses an innate immune system. Hemocytes, the main innate immune cells of *G. mellonella*, closely resemble human neutrophils, since they employ the same defense mechanisms, in particular, phagocytosis and NETosis (34). As shown in Fig. 7, *G. mellonella* larvae are less susceptible to injected PPAD-deficient *P. gingivalis* than to the wild-type bacteria, whereas heat-killed *P. gingivalis* bacteria do not affect larval viability. This observation is fully in line with the here-proposed role of PPAD as an immune evasion factor.

**Conclusion.** Altogether, our present findings show for the first time that the virulence factor PPAD of the oral pathogen *P. gingivalis* defuses antibacterial neutrophil insults at three distinct levels, namely, phagocytosis, NETosis, and CAMP activity. This identifies PPAD as a major agent in the evasion of human innate immunity, a view that is supported by studies from Potempa and coworkers showing PPAD-dependent citrullination of the complement system (35). Importantly, an essential role of PPAD in immune evasion explains why this enzyme is invariably produced by all of the over 100 clinical isolates of *P. gingivalis* investigated to date (8, 36).

## MATERIALS AND METHODS

**Immunohistochemistry.** Immunohistochemical staining of PPAD was performed as described before (28). Briefly, human paraffin-embedded gingival tissues were collected from *P. gingivalis*-colonized periodontitis patients at the dentistry department of the University Medical Center Groningen. Deparaffinization of 5- $\mu$ m sections was performed by several xylene, ethanol, and water washes. Endogenous peroxidase activity was inhibited by the addition of hydrogen peroxide in methanol, followed by

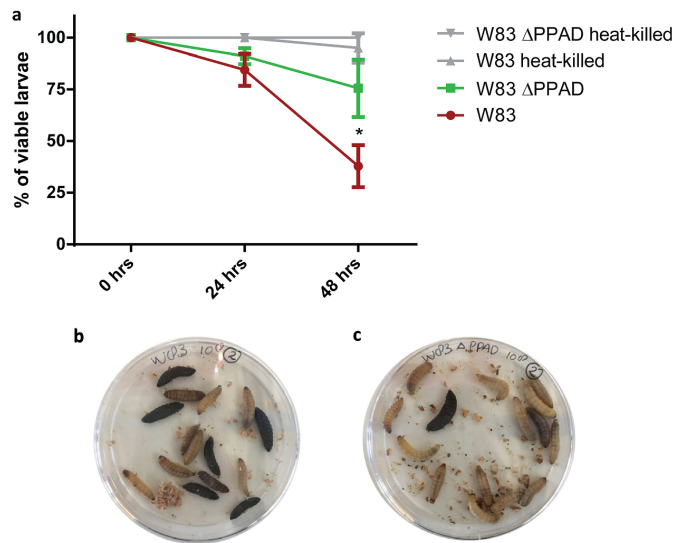


**FIG 7** PPAD is a critical virulence factor of *P. gingivalis*. Viability of *Galleria mellonella* larvae was measured 24 h and 48 h after infection with *P. gingivalis*. (a) The larvae were significantly less susceptible to *P. gingivalis* W83 ΔPPAD than to the wild-type strain W83. Heat-killed bacteria were used as a negative control. Data are means of three biological replicates ( $n = 15$ ). (b and c) Representative images of *G. mellonella* larvae infected with *P. gingivalis* W83 (b) or W83 ΔPPAD (c) \*,  $P < 0.05$ , two-tailed unpaired Student's  $t$  tests.

blocking of nonspecific antibody binding with 1% bovine serum albumin and 1% normal goat serum in phosphate-buffered saline (PBS). Next, samples were stained either with an in-house-produced PPAD-specific antibody (7, 8) or with the respective preimmune serum (1:100 in PBS, 1 h). Upon removal of excessive primary antibody by PBS, a secondary goat anti-rabbit IgG horseradish peroxidase (HRP) antibody (P0448; Dako, Santa Clara, CA, USA) was added at a concentration of 1:100 in PBS for 45 min, followed by washing and a developing reaction using a 3,3'-diaminobenzidine (DAB) kit (K3467; Dako). Sections were counterstained with hematoxylin and mounted with glycerine before microscopic evaluation.

***P. gingivalis* culture.** The *P. gingivalis* reference strain W83 and the respective PPAD-deficient mutant (W83 ΔPPAD) (37) were grown as described before (6). For infection experiments, liquid cultures were grown until stationary phase, which was reached after ~24 h. For several experiments, inoculation was performed by washing and diluting bacterial glycerol stocks stored at  $-80^{\circ}\text{C}$  in a 1:100 ratio into fresh brain heart infusion (BHI) medium (Oxoid, Basingstoke, UK).

**Neutrophil isolation.** Neutrophils were freshly isolated from four healthy donors (two females age 27 and 34 years and two males age 28 and 39 years) who had been medically examined. Lymphoprep buffer (StemCell Technologies, Vancouver, Canada) was used to separate cell types. EDTA-blood was first diluted 1:1 with PBS and then put gently on top of a volume of Lymphoprep (blood-to-Lymphoprep ratio, 2:1). Samples were centrifuged at 2,500 rpm at room temperature (RT) for 20 min without brake so as not to disrupt the separated cell layers. The plasma, Lymphoprep, and peripheral blood mononuclear cells were removed, and a layer of erythrocytes and neutrophils remained. The erythrocytes in this mixture were lysed by adding ammonium chloride 0.8% and 1 mM EDTA (pH 7.4) and shaking for 10 min on ice. After another centrifugation at 2,500 rpm for 3 min, the lysed erythrocytes were removed. These two steps were repeated once more to obtain a pellet of purified neutrophils.

**OMV and PPAD preparation.** *P. gingivalis* cultures in late-exponential phase were used for OMV collection. A first centrifugation step at  $8,000 \times g$  and  $4^{\circ}\text{C}$  for 20 min was performed to separate cells from OMV-containing supernatant. The supernatant was subjected to ultracentrifugation at  $100,000 \times g$  and  $4^{\circ}\text{C}$  for 3 h in an Optima MAX-XP ultracentrifuge 261 (Beckman Coulter, Brea, CA, USA) using an MLA-80 fixed-angle rotor. The pellet containing the OMVs was resuspended in PBS, and aliquots were frozen at  $-80^{\circ}\text{C}$  before use. Protein quantification was performed using a bicinchoninic acid (BCA) protein assay (Pierce, Waltham, MA, USA), according to the manufacturer's instructions, with the addition of 2.0% SDS to solubilize proteins. Sixteen micrograms of protein was used for the phagocytosis rescue experiment. Protein precipitation with 10% tricarboxylic acid (TCA) was performed as described before (6) to concentrate vesicles for Western blot analysis. Recombinant PPAD was purified from *Lactococcus lactis*, as previously described (7, 8).

**Neutrophil infections.** For neutrophil infection experiments followed by Western blotting or mass spectrometry analyses,  $3 \times 10^6$  neutrophils in 2.5 ml of RPMI 1640 medium (Gibco, Waltham, MA, USA)



with 2 mM L-glutamine and 10% autologous donor serum were seeded in each well of a 6-well plate. Phagocytosis experiments were carried out with  $5 \times 10^5$  neutrophils in 500  $\mu$ l of medium in 24-well plates. The neutrophils were allowed to rest on the plate at 37°C and 5% CO<sub>2</sub> for 1 h. When required, 100  $\mu$ l supernatant of W83, 100  $\mu$ l BHI medium, 2.5  $\mu$ g recombinant PPAD, 16  $\mu$ g OMs of W83, or 100  $\mu$ l PBS were added to the neutrophil suspension, and incubation was continued for 30 min. Subsequently, *P. gingivalis* was added at a multiplicity of infection (MOI) of 100. The neutrophils were exposed to the bacteria for 90 min. Extracellular bacteria were then removed, and the neutrophil layer was washed once with PBS before the addition of NP-40 lysis buffer (150 mM sodium chloride, 1.0% NP-40, 50 mM Tris [pH 8.0]) with cComplete mini protease inhibitor (Roche, Basel, Switzerland).

**Phagocytosis assay.** To determine whether PPAD impacts the association and/or internalization of *P. gingivalis* in neutrophils as defined by Lei et al. (38), a flow cytometry-based method was used as described previously (39). Briefly, a liquid bacterial culture was centrifuged for 10 min at  $7,000 \times g$  and 4°C and washed once in PBS before resuspending the bacterial pellet in 0.5 M NaHCO<sub>3</sub> (pH 8.0) to a concentration of  $2.5 \times 10^9$  CFU/ml before the addition of fluorescein isothiocyanate (FITC; Invitrogen, Carlsbad, USA). Bacterial concentrations were approximated by optical density readings at 600 nm according to a standard curve for each strain used.

An FITC concentration of 0.15 mg/ml was used for staining *P. gingivalis* W83 and W83  $\Delta$ PPAD (39, 40). The tubes with bacteria and FITC were subsequently incubated in the dark for 30 min at RT in a tube rotator. The bacteria were pelleted at  $7,000 \times g$  for 5 min, and the pellet was washed 3 times with PBS to remove unbound FITC. Finally, the bacteria were resuspended to the desired concentration in RPMI 1640–10% autologous donor serum–2 mM L-glutamine.

To measure the bacterial internalization rate, the extracellular fluorescence (representing associated but not internalized bacteria) was quenched using 0.2% trypan blue (Thermo Fisher Scientific, Waltham, MA, USA). Subsequently, two washing steps with PBS were performed to remove excessive trypan blue. Both quenched and nonquenched cell samples were fixed with 4% paraformaldehyde (PFA; Sigma-Aldrich, St. Louis, MO, USA) for 15 min prior to flow cytometric analyses and visualization by fluorescence microscopy.

An Accuri C6 flow cytometer was used to measure the mean fluorescence intensity (MFI) of the FITC-positive cells. The gating strategy to include only neutrophils in our analysis is shown in Fig. S1e to g. FITC-positive cells were identified by setting a fluorescence threshold in an uninfected neutrophil control sample, next to the autofluorescence peak, as shown in Fig. S1h to j. The association index of each *P. gingivalis* strain was calculated by multiplying the percentage of FITC-positive cells with associated bacteria (i.e. intracellular plus extracellularly bound bacteria) with the MFI of these cells, divided by 100, as previously described (41). The internalization index of each *P. gingivalis* strain was calculated by multiplying the percentage of cells with internalized bacteria (cells positive for FITC after trypan blue quenching) with the MFI of these cells, divided by 100 (38). For microscopic analyses, 10  $\mu$ l of the fixed cells was mounted on microscopy slides and visualized with an Axio Observer.Z1 fluorescence microscope (Zeiss, Jena, Germany) using  $\times 40$  or  $\times 65$  magnification. Images were recorded using an Axio Cam MRm Rev. 3 camera with FireWire.

**LDS-PAGE.** Lithium dodecyl sulfate (LDS)-PAGE was performed using 10% NuPAGE gels (Invitrogen, Carlsbad, CA, USA). Protein concentrations of cell lysates were determined with the Pierce BCA protein assay kit (Thermo Fisher Scientific, Waltham, MA, USA) and frozen at  $-20^\circ\text{C}$  until further use. Equal amounts of protein samples were incubated with LDS sample buffer for 10 min at 95°C, separated by LDS-PAGE, and either stained with SimplyBlue SafeStain (Life Technologies, Carlsbad, CA, USA) or processed further for Western blotting.

**Western blotting.** For Western blotting, proteins were transferred from the gel to a nitrocellulose membrane (Whatman, Buckinghamshire, UK) by semidry blotting. The transfer was performed at 200 mA for 75 min in the presence of methanol-containing buffers. Upon transfer, the nonspecific binding was blocked overnight at 4°C with 5% skim milk (Oxoid, Basingstoke, UK) in PBS. Afterwards, the blot was rinsed once with PBS-Tween 20 (PBS-T) to remove residual skim milk. Primary rabbit anti-RgpA/B, rabbit anti-PPAD antibodies (7, 8) or anti-histone H3 (ab18521; Abcam) in PBS-T (1:2,000) were added, and the blot was incubated for 1 h at RT. After removing the nonbound primary antibodies by 4 washes with PBS-T, the blot was incubated with IRDye 800CW goat anti-rabbit antibody (LI-COR Biosciences, Lincoln, NE, USA) in PBS-T (1:10,000) protected from light for 45 min. Last, background was reduced by washing 4 times with PBS-T and subsequently washing twice with PBS to remove the Tween. Fluorescence was measured with the LI-COR Odyssey infrared imaging system (LI-COR Biosciences, Lincoln, USA) and subsequently quantified using ImageJ (National Institutes of Health, Bethesda, MD, USA).

**Protease activity assay.** *P. gingivalis* was grown in BHI medium until stationary phase, and the growth medium was separated from the cells by centrifugation at  $7,000 \times g$  for 10 min. Recombinant human histone H3 (0.5  $\mu$ g; New England BioLabs, Ipswich, MA, USA) was incubated with 7.5  $\mu$ l of the growth medium fraction for 1, 5, 10, 15, 20, and 30 min at 37°C. Fresh BHI medium (7.5  $\mu$ l) was used as a negative control. The resulting protein samples were analyzed by Western blotting, as described above.

**Mass spectrometry of neutrophils.** Neutrophil lysates were processed for mass spectrometry analysis, as described before (42). Briefly, proteins were bound to StrataClean resins (Agilent Technologies, Santa Clara, CA, USA) and subsequently alkylated, reduced, and digested by trypsin. The resulting peptides were purified by C<sub>18</sub> stage-tip purification (Thermo Fisher Scientific, Waltham, MA, USA), according to the manufacturer's protocol, and dried until further use.

Purified peptides were analyzed by reversed-phase liquid chromatography (LC) electrospray ionization-tandem mass spectrometry (ESI-MS/MS) using an Orbitrap Elite mass spectrometer (Thermo Fisher Scientific, Waltham, MA, USA). In brief, in-house self-packed nano-LC columns (20 cm) were used

to perform LC with an EASY-nLC 1200 system (Thermo Fisher Scientific). The peptides were loaded with buffer A (0.1% [vol/vol] acetic acid) and subsequently eluted in 156 min using a 1% to 99% nonlinear gradient with buffer B (0.1% [vol/vol] acetic acid, 94.9% acetonitrile). After injection into the MS, a full scan was recorded in the Orbitrap MS with a resolution of 60,000. The 20 most abundant precursor ions were consecutively isolated in the linear ion trap and fragmented via collision-induced dissociation (CID). Unassigned charge states as well as singly charged ions were rejected, and the lock mass option was enabled.

Database searching was done with Sorcerer-Sequest 4 (Sage-N Research, Milpitas, CA, USA). After extraction from the raw files, \*.dta files were searched with Sequest against a target-decoy database with a set of common laboratory contaminants. A database for the respective peptide/protein search was created from the published genome sequences of the W83 strain and the human genome, which were downloaded from UniProt (<http://www.uniprot.org>) on 14 July 2016. The created database contained a total of 148,472 proteins. Database search was based on a strict trypsin digestion with two missed cleavages permitted. No fixed modifications were considered. Oxidation of methionine, carbamidomethylation of cysteine, and citrullination of arginine were considered variable modifications. The mass tolerance for precursor ions was set to 10 ppm and the mass tolerance for fragment ions to 1 Da. Validation of MS/MS-based peptide and protein identification was performed with Scaffold version 4 (Proteome Software, Portland, OR, USA). A false-discovery rate (FDR) of 0.1% was set for filtering the data. Protein identifications were accepted if at least 2 identified peptides were detected with the above-mentioned filter criteria in 2 out of 3 biological replicates. Protein data were exported from Scaffold and further curated in Microsoft Excel 2013 before further analysis.

Quantitative values of protein abundances in neutrophil samples were obtained by summing up all spectra associated with a specific protein within a sample, which includes also those spectra that are shared with other proteins. To allow comparisons, spectral counts were normalized by applying a scaling factor for each sample to each protein adjusting the values to normalized quantitative values.

**Mass spectrometry of histone H3 and LP9.** Recombinant human histone H3 (0.5  $\mu$ g; New England Biolabs, Ipswich, MA, USA) was incubated with recombinant PPAD (0.25  $\mu$ g) overnight at 37°C. Proteins were separated by LDS-PAGE and stained with SimplyBlue SafeStain, as described above. Histone H3-corresponding bands (Fig. S3b) were excised from the gel, dried, and further processed by trypsin digestion as described above.

LP9 was synthesized at EMC microcollections GmbH (Tübingen, Germany). The LP9 peptide (0.5  $\mu$ g) was incubated with recombinant PPAD (0.25  $\mu$ g) overnight at 37°C. Subsequently, the samples were processed by three different methods, as follows: (i) trypsin digestion, in which samples were alkylated, reduced, digested by trypsin, and purified by C<sub>18</sub> ZipTip purification, as described above; (ii) C<sub>4</sub> Exclusion of PPAD by C<sub>4</sub> ZipTip filtration using a slight modification of the manufacturer's protocol, where upon binding of PPAD to the ZipTip, the PPAD-containing tip was discarded and the LP9-containing flow-through was further processed by C<sub>18</sub> ZipTip filtration; and (iii) C<sub>18</sub> inclusion of LP9, where the LP9 peptides were immediately purified by C<sub>18</sub> ZipTip filtration following the manufacturer's protocol.

Purified peptides were analyzed by reversed-phase LC-ESI-MS/MS using an Orbitrap Elite spectrometer (Thermo Fisher Scientific, Waltham, MA, USA). In brief, in-house self-packed nano-LC columns (20 cm; packed with Aeris peptide material, 3.6- $\mu$ m XB-C<sub>18</sub>-100Å) were used to perform LC with an Easy-nLC 1200 system (Thermo Fisher Scientific). The peptides were loaded with buffer A (0.1% [vol/vol] acetic acid) and subsequently eluted in 80 min using a nonlinear gradient of 1% to 99% with buffer B (0.1% [vol/vol] acetic acid, 94.9% acetonitrile). After injection into the MS, a full scan was recorded in the Orbitrap spectrometer with a resolution of 60,000. The 20 most abundant precursor ions were consecutively isolated in the linear ion trap and fragmented via CID. Unassigned charge states and singly charged ions were rejected, and the lock mass option was enabled.

Database searching for the histone H3 and LP9 analyses was done with Sorcerer-Sequest 4 (Sage-N Research, Milpitas, CA, USA). After extraction from the raw files, \*.dta files were searched with Sequest against a target-decoy database with a set of common laboratory contaminants. For the peptide/protein search, the sequence of LP9 was added to the database that was used for analysis of the neutrophil MS data, and the database search was performed based on the same criteria as described above. For the histone H3 analysis, Sequest identifications required XCorr scores of greater than 2.2, 3.3, and 3.8 for doubly, triply, and all higher-charged peptides, respectively. For the LP9 analysis, Sequest identifications required XCorr scores of greater than 2.7, 3.5, and 3.5 for doubly, triply, and all higher-charged peptides, respectively. Protein data were exported from Scaffold. Spectra and fragmentation tables of the peptides identified to be citrullinated are presented in Fig. S5.

**Immunofluorescence microscopy of NET formation.** For microscopic analysis of infected neutrophils, sterile 12-mm-diameter coverslips (Menzel-Gläser, Braunschweig, Germany) were placed into 24-well plates (Corning, Corning, NY, USA). A total of  $2.5 \times 10^5$  neutrophils in 500  $\mu$ l RPMI 1640 medium were added to each well. To let the neutrophils adhere to the coverslips, plates were incubated for 1 h at 37°C and 5% CO<sub>2</sub>. Subsequently, cells were stimulated for 1 h with 20 mM phorbol myristate acetate (PMA; Sigma-Aldrich, St. Louis, MO, USA) to induce NETosis and then infected with *P. gingivalis* at an MOI of 100 for 90 min. Upon infection, 500  $\mu$ l of 8% PFA was added to each well to reach a final concentration of 4% PFA to fix the cells. Plates were stored at 4°C in the dark, and immunofluorescence staining was performed on the following day. For this, the fixative solution was removed, and the cell layer was washed carefully one time with PBS. A blocking step was performed by incubating cells at room temperature (RT) with 2% bovine serum albumin (BSA) in PBS for 1 h. Citrullinated histone H3 in NETs was stained with a rabbit anti-citrullinated histone H3 antibody (ab5103, 1:250; Abcam) and incubated for 1 h at RT in PBS, 0.05% Tween 20, and 0.5% BSA. Coverslips were washed with PBS before adding secondary



antibodies. The Alexa Fluor 568 goat anti-rabbit antibody (catalog no. A11011, 1:400; Invitrogen) was used to visualize the primary antibodies. Secondary antibodies were added in PBS with 4',6-diamidino-phenylindole (DAPI; product no. 10236276001, 1:5,000; Roche) and incubated for 30 min before mounting the coverslips in citifluor (CitiFluor, Hatfield, PA, USA). Slides were then analyzed using a Leica DFC450 C fluorescence microscope with the Leica Application Suite software version 4.2.0.

**NET survival assay.** NETosis was induced, and *P. gingivalis* was added to the NETs as described above, with the modification that no coverslips were placed into the wells. Upon 90 min of infection, NETs were isolated as described previously (43). Subsequently, different dilutions of bacteria trapped in the NETs were plated on blood agar base no. 2 (BA2) plates (Oxoid, Basingstoke, UK). The plates were incubated for 5 days at 37°C under anaerobic conditions, and *P. gingivalis* colonies were counted.

**Citrullination of LP9 and killing assay.** *Bacillus subtilis* strain 168 was grown overnight in BHI broth (Oxoid, Basingstoke, UK) with shaking at 37°C. The culture was diluted to an optical density at 600 nm of 0.1, and 100  $\mu$ l of this suspension was pipetted in each well of a 96-well plate. Bacteria were grown for 2 h shaking at 37°C in a Biotek Synergy 2 microplate reader (Biotek Instruments, Inc., Winooski, VT, USA) until they reached exponential phase, and LP9 (in PBS) was added at a final concentration of 200  $\mu$ g/ml. To investigate the effect of citrullination on its activity, LP9 was preincubated with PPAD or human peptidylarginine deiminase 2 (hPAD2) overnight at 37°C before its addition. Bacterial growth was monitored until stationary phase, and the respective growth curves were plotted with GraphPad Prism version 6 (GraphPad Software, La Jolla, CA, USA). The effect of LP9 on exponentially growing cells was determined by measuring the growth delay of *B. subtilis* upon the addition of LP9. The same procedure was applied for the killing assay of *P. gingivalis*. However, for *P. gingivalis*, standing cultures were grown for 48 h at 37°C.

**In vivo *Galleria mellonella* survival assay.** Larvae of *G. mellonella* were injected with the *P. gingivalis* W83 strain or the respective PPAD-deficient mutant. Bacteria were injected into the last proleg at a volume of 10  $\mu$ l using a HumaPen Luxura HD pen (Eli Lilly, Indianapolis, IN, USA). Viability was scored by one trained person at 24 h and 48 h postinfection based on pigmentation and mobility. To assess the virulence of the investigated *P. gingivalis* strains, the larvae were infected with 10<sup>8</sup> PBS-washed bacteria. Heat-killed bacteria (30 min, 90°C) were used as a negative control.

**Statistical analyses.** Statistical analyses were performed with GraphPad Prism version 6 (GraphPad Software, La Jolla, CA, USA) or with Scaffold version 4 (Proteome Software, Portland, OR, USA). Two groups were compared by performing an unpaired two-tailed Student's *t* test. Fisher's exact test was used to assess the significance of differences in normalized spectral counts of neutrophil proteins detected by MS. Significance was defined as a *P* value lower than or equal to 0.05.

**Medical ethics committee approval.** Blood donations from healthy volunteers were collected with approval of the medical ethics committee of the University Medical Center Groningen (UMCG; approval no. Metc2012-375). All blood donations were obtained after written informed consent from all volunteers and adhering to the Declaration of Helsinki guidelines.

**Biological and chemical safety.** *P. gingivalis* was handled following appropriate safety and containment procedures for biosafety level 2 microbiological agents. All experiments involving human cells were performed under appropriate safety conditions. All chemicals and reagents applied in this study were handled according to local guidelines for safe usage and protection of the environment.

**Data availability.** The mass spectrometry data are deposited in the ProteomeXchange repository PRIDE: <https://www.ebi.ac.uk/pride/archive/projects/PXD010798> (neutrophil infection) and <https://www.ebi.ac.uk/pride/archive/projects/PXD009081> (histone H3 and LP9).

## SUPPLEMENTAL MATERIAL

Supplemental material for this article may be found at <https://doi.org/10.1128/mBio.01704-18>.

**FIG S1**, PDF file, 1.5 MB.

**FIG S2**, PDF file, 3.1 MB.

**FIG S3**, PDF file, 2.1 MB.

**FIG S4**, PDF file, 0.8 MB.

**FIG S5**, PDF file, 44.6 MB.

**TABLE S1**, PDF file, 1 MB.

## ACKNOWLEDGMENTS

We thank Menke de Smit, Peter Heeringa, and Arjan Vissink for helpful discussions, and Putri Utari, Rita Setroikromo, and Wim J. Quax for support in setting up the *Galleria* infection model.

This work was funded by the Graduate School of Medical Sciences of the University of Groningen (to T. Stoberneck, M. du Teil Espina, L. M. Palma Medina, G. Gabarrini, and J. M. van Dijk), the Deutsche Forschungsgemeinschaft Grant GRK1870 (to L. M. Palma Medina and D. Becher), the China Scholarship Council (grant 201506170036 to X. Zhao), and the Center for Dentistry and Oral Hygiene of the University Medical Center Groningen (to G. Gabarrini and A. J. van Winkelhoff).

T. Stobernack, M. du Teil Espina, A. Otto, J. Westra, and J. M. van Dijk conceived and designed the experiments. T. Stobernack, M. du Teil Espina, L. M. Mulder, L. M. Palma Medina, D. R. Piebenga, G. Gabarrini, X. Zhao, K. M. J. Janssen, J. Hulzebos, T. Sura, and A. Otto performed the experiments and analyzed the data. D. Becher, F. Götz, and J. Westra contributed reagents. E. Brouwer applied for medical ethics approval and recruited volunteers. A. J. van Winkelhoff, J. Westra, and J. M. van Dijk supervised the project. T. Stobernack, M. du Teil Espina, and J. M. van Dijk wrote the manuscript. All authors have read and approved the manuscript.

We declare no financial competing interest.

## REFERENCES

1. Tonetti MS, Jepsen S, Jin L, Otomo-Corgel J. 2017. Impact of the global burden of periodontal diseases on health, nutrition and wellbeing of mankind: A call for global action. *J Clin Periodontol* 44:456–462. <https://doi.org/10.1111/jcpe.12732>.
2. Hajishengalis G. 2015. Periodontitis: from microbial immune subversion to systemic inflammation. *Nat Rev Immunol* 15:30–44. <https://doi.org/10.1038/nri3785>.
3. Cortés-Vieyra R, Rosales C, Uribe-Querol E. 2016. Neutrophil functions in periodontal homeostasis. *J Immunol Res* 2016:1396106. <https://doi.org/10.1155/2016/1396106>.
4. McGraw WT, Potempa J, Farley D, Travis J. 1999. Purification, characterization, and sequence analysis of a potential virulence factor from *Porphyromonas gingivalis*, peptidylarginine deiminase. *Infect Immun* 67:3248–3256.
5. Wegner N, Wait R, Sroka A, Eick S, Nguyen K-A, Lundberg K, Kinloch A, Culshaw S, Potempa J, Venables PJ. 2010. Peptidylarginine deiminase from *Porphyromonas gingivalis* citrullinates human fibrinogen and  $\alpha$ -enolase: implications for autoimmunity in rheumatoid arthritis. *Arthritis Rheum* 62:2662–2672. <https://doi.org/10.1002/art.27552>.
6. Stobernack T, Glasner C, Junker S, Gabarrini G, de Smit M, de Jong A, Otto A, Becher D, van Winkelhoff AJ, van Dijk JM. 2016. Extracellular proteome and citrullinome of the oral pathogen *Porphyromonas gingivalis*. *J Proteome Res* 15:4532–4543. <https://doi.org/10.1021/acs.jproteome.6b00634>.
7. Gabarrini G, Chlebowicz MA, Vega Quiroz ME, Veloo ACM, Rossen JWA, Harmsen HJM, Laine ML, van Dijk JM, van Winkelhoff AJ. 2018. Conserved citrullinating exoenzymes in *Porphyromonas* species. *J Dent Res* 97:556–562. <https://doi.org/10.1177/0022034517747575>.
8. Gabarrini G, Palma Medina LM, Stobernack T, Prins RC, Teil Espina Du M, Kuipers J, Chlebowicz MA, Rossen JWA, van Winkelhoff AJ, van Dijk JM. 2018. There's no place like OM: vesicular sorting and secretion of the peptidylarginine deiminase of *Porphyromonas gingivalis*. *Virulence* 9:456–464. <https://doi.org/10.1080/21505594.2017.1421827>.
9. de Smit M, Westra J, Vissink A, Meer der BD-V, Brouwer E, van Winkelhoff AJ. 2012. Periodontitis in established rheumatoid arthritis patients: a cross-sectional clinical, microbiological and serological study. *Arthritis Res Ther* 14:R222. <https://doi.org/10.1186/ar4061>.
10. Berthelot J-M, Le Goff B. 2010. Rheumatoid arthritis and periodontal disease. *Joint Bone Spine* 77:537–541. <https://doi.org/10.1016/j.jbspin.2010.04.015>.
11. Lundberg K, Wegner N, Yucel-Lindberg T, Venables PJ. 2010. Periodontitis in RA—the citrullinated enolase connection. *Nat Rev Rheumatol* 6:727–730. <https://doi.org/10.1038/nrrheum.2010.139>.
12. Neiders ME, Chen PB, Suido H, Reynolds HS, Zambon JJ, Shlossman M, Genco RJ. 1989. Heterogeneity of virulence among strains of *Bacteroides gingivalis*. *J Rheumatol Res* 24:192–198. <https://doi.org/10.1111/j.1600-0765.1989.tb02005.x>.
13. Potempa J, Sroka A, Imamura T, Travis J. 2003. Gingipains, the major cysteine proteinases and virulence factors of *Porphyromonas gingivalis*: structure, function and assembly of multidomain protein complexes. *Curr Protein Pept Sci* 4:397–407. <https://doi.org/10.2174/1389203033487036>.
14. Curtis MA, Thickett A, Slaney JM, Rangarajan M, Aduse-Opoku J, Shepherd P, Paramonov N, Hounsell EF. 1999. Variable carbohydrate modifications to the catalytic chains of the RgpA and RgpB proteases of *Porphyromonas gingivalis* W50. *Infect Immun* 67:3816–3823.
15. Otsuka A, Abe T, Watanabe M, Yagisawa H, Takei K, Yamada H. 2009. Dynam 2 is required for actin assembly in phagocytosis in Sertoli cells. *Biochem Biophys Res Commun* 378:478–482. <https://doi.org/10.1016/j.bbrc.2008.11.066>.
16. May RC, Caron E, Hall A, Machesky LM. 2000. Involvement of the Arp2/3 complex in phagocytosis mediated by Fc $\gamma$ RIII or CR3. *Nat Cell Biol* 2:246–248. <https://doi.org/10.1038/35008673>.
17. Park H, Cox D. 2009. Cdc42 regulates Fc $\gamma$  receptor-mediated phagocytosis through the activation and phosphorylation of Wiskott-Aldrich syndrome protein (WASP) and neural-WASP. *Mol Biol Cell* 20:4500–4508. <https://doi.org/10.1091/mbc.e09-03-0230>.
18. Löfgren R, Ng-Sikorski J, Sjölander A, Andersson T. 1993. Beta 2 integrin engagement triggers actin polymerization and phosphatidylinositol triphosphate formation in non-adherent human neutrophils. *J Cell Physiol* 123:1597–1605.
19. Mazzone A, Ricevuti G. 1995. Leukocyte CD11/CD18 integrins: biological and clinical relevance. *Haematologica* 80:161–175.
20. Ambruso DR, Cusack N, Thurman G. 2004. NADPH oxidase activity of neutrophil specific granules: requirements for cytosolic components and evidence of assembly during cell activation. *Mol Genet Metab* 81:313–321. <https://doi.org/10.1016/j.ymgme.2004.01.009>.
21. Hoeksema M, van Eijk M, Haagsman HP, Hartshorn KL. 2016. Histones as mediators of host defense, inflammation and thrombosis. *Future Microbiol* 11:441–453. <https://doi.org/10.2217/fmb.15.151>.
22. Papayannopoulos V. 2018. Neutrophil extracellular traps in immunity and disease. *Nat Rev Immunol* 18:134–147. <https://doi.org/10.1038/nri.2017.105>.
23. Sørensen OE, Borregaard N. 2016. Neutrophil extracellular traps—the dark side of neutrophils. *J Clin Invest* 126:1612–1620. <https://doi.org/10.1172/JCI84538>.
24. White PC, Chicca IJ, Cooper PR, Milward MR, Chapple ILC. 2016. Neutrophil extracellular traps in periodontitis: a web of intrigue. *J Dent Res* 95:26–34. <https://doi.org/10.1177/0022034515609097>.
25. Vitkov L, Hartl D, Minnich B, Hannig M. 2017. Janus-faced neutrophil extracellular traps in periodontitis. *Front Immunol* 8:1404. <https://doi.org/10.3389/fimmu.2017.01404>.
26. Wang Y, Li M, Stadler S, Correll S, Li P, Wang D, Hayama R, Leonelli L, Han H, Grigoryev SA, Allis CD, Coonrod SA. 2009. Histone hypercitrullination mediates chromatin decondensation and neutrophil extracellular trap formation. *J Cell Physiol* 184:205–213. <https://doi.org/10.1083/jcb.200806072>.
27. Li P, Li M, Lindberg MR, Kennett MJ, Xiong N, Wang Y. 2010. PAD4 is essential for antibacterial innate immunity mediated by neutrophil extracellular traps. *J Exp Med* 207:1853–1862. <https://doi.org/10.1084/jem.20100239>.
28. Janssen KJM, de Smit MJ, Witherath C, Brouwer E, van Winkelhoff AJ, Vissink A, Westra J. 2017. Autoantibodies against citrullinated histone H3 in rheumatoid arthritis and periodontitis patients. *J Clin Periodontol* 44:577–584. <https://doi.org/10.1111/jcpe.12727>.
29. Lollike K, Kjeldsen L, Sengeløv H, Borregaard N. 1995. Lysozyme in human neutrophils and plasma. A parameter of myelopoietic activity. *Leukemia* 9:159–164.
30. Fábán TK, Hermann P, Beck A, Fejérdy P, Fábán G. 2012. Salivary defense proteins: their network and role in innate and acquired oral immunity. *Int J Mol Sci* 13:4295–4320. <https://doi.org/10.3390/ijms13044295>.
31. Herbert S, Bera A, Nerz C, Kraus D, Peschel A, Goerke C, Meehl M, Cheung A, Götz F. 2007. Molecular basis of resistance to muramidase and cationic antimicrobial peptide activity of lysozyme in staphylococci. *PLoS Pathog* 3:e102. <https://doi.org/10.1371/journal.ppat.0030102>.

32. Gutner M, Chaushu S, Balter D, Bachrach G. 2009. Saliva enables the antimicrobial activity of LL-37 in the presence of proteases of *Porphyromonas gingivalis*. *Infect Immun* 77:5558–5563. <https://doi.org/10.1128/IAI.00648-09>.
33. Maisetta G, Brancatisano FL, Esin S, Campa M, Batoni G. 2011. Gingipains produced by *Porphyromonas gingivalis* ATCC49417 degrade human- $\beta$ -defensin 3 and affect peptide's antibacterial activity in vitro. *Peptides* 32:1073–1077. <https://doi.org/10.1016/j.peptides.2011.02.003>.
34. Browne N, Heelan M, Kavanagh K. 2013. An analysis of the structural and functional similarities of insect hemocytes and mammalian phagocytes. *Virulence* 4:597–603. <https://doi.org/10.4161/viru.25906>.
35. Bielecka E, Scavenius C, Kantyka T, Jusko M, Mizgalska D, Szmigielski B, Potempa B, Enghild JJ, Prossnitz ER, Blom AM, Potempa J. 2014. Peptidyl arginine deiminase from *Porphyromonas gingivalis* abolishes anaphylatoxin C5a activity. *J Biol Chem* 289:32481–32487. <https://doi.org/10.1074/jbc.C114.617142>.
36. Gabarrini G, de Smit M, Westra J, Brouwer E, Vissink A, Zhou K, Rossen JWA, Stobembach T, van Dijk JM, van Winkelhoff AJ. 2015. The peptidylarginine deiminase gene is a conserved feature of *Porphyromonas gingivalis*. *Sci Rep* 5:13936. <https://doi.org/10.1038/srep13936>.
37. Wegner N, Lundberg K, Kinloch A, Fisher B, Malmström V, Feldmann M, Venables PJ. 2010. Autoimmunity to specific citrullinated proteins gives the first clues to the etiology of rheumatoid arthritis. *Immunol Rev* 233:34–54. <https://doi.org/10.1111/j.0105-2896.2009.00850.x>.
38. Lei L, Li H, Yan F, Xiao Y. 2013. Hyperlipidemia impaired innate immune response to periodontal pathogen *Porphyromonas gingivalis* in apolipoprotein E knockout mice. *PLoS One* 8:e71849. <https://doi.org/10.1371/journal.pone.0071849>.
39. Pathirana RD, O'Brien-Simpson NM, Visvanathan K, Hamilton JA, Reynolds EC. 2007. Flow cytometric analysis of adherence of *Porphyromonas gingivalis* to oral epithelial cells. *Infect Immun* 75:2484–2492. <https://doi.org/10.1128/IAI.02004-06>.
40. Igboin CO, Griffen AL, Leys EJ. 2009. *Porphyromonas gingivalis* strain diversity. *J Clin Microbiol* 47:3073–3081. <https://doi.org/10.1128/JCM.00569-09>.
41. Rossi A, Lord J. 2013. Adiponectin inhibits neutrophil phagocytosis of *Escherichia coli* by inhibition of PKB and ERK 1/2 MAPK signalling and Mac-1 activation. *PLoS One* 8:e69108. <https://doi.org/10.1371/journal.pone.0069108>.
42. Bonn F, Bartel J, Büttner K, Hecker M, Otto A, Becher D. 2014. Picking vanished proteins from the void: how to collect and ship/share extremely dilute proteins in a reproducible and highly efficient manner. *Anal Chem* 86:7421–7427. <https://doi.org/10.1021/ac501189j>.
43. Barrientos L, Marin-Esteban V, de Chaisemartin L, Le-Moal VL, Sandré C, Bianchini E, Nicolas V, Pallardy M, Chollet-Martin S. 2013. An improved strategy to recover large fragments of functional human neutrophil extracellular traps. *Front Immunol* 4:166. <https://doi.org/10.3389/fimmu.2013.00166>.
44. Maekawa T, Krauss JL, Abe T, Jotwani R, Triantafilou M, Triantafilou K, Hashim A, Hoch S, Curtis MA, Nussbaum G, Lambris JD, Hajishengallis G. 2014. *Porphyromonas gingivalis* manipulates complement and TLR signaling to uncouple bacterial clearance from inflammation and promote dysbiosis. *Cell Host Microbe* 15:768–778.

## Manuscript II

### The global proteome and ubiquitinome of bacterial and viral co-infected bronchial epithelial cells

Sura T, Surabhi S, Maaß S, Hammerschmidt S, Siemens N, Becher D.

Published in *Journal of Proteomics* 2021,  
DOI: 10.1016/j.jprot.2021.104387

#### Author contributions:

Conceptualization, T.S., S.S., N.S. and D.B.; methodology, S.S., T.S.; validation, T.S.; formal analysis, T.S.; investigation, T.S.; resources, S.H., N.S. and D.B.; data curation, T.S.; writing—original draft preparation, T.S.; writing—review and editing, T.S., S.S., S.M., S.H., N.S., D.B.; visualization, T.S.; supervision, N.S., D.B.; project administration, D.B.; funding acquisition, D.B. and S.H.; All authors have read and agreed to the published version of the manuscript.

---

Thomas Sura

---

Prof. Dr. Dörte Becher



Contents lists available at ScienceDirect

Journal of Proteomics

journal homepage: [www.elsevier.com/locate/jprot](http://www.elsevier.com/locate/jprot)

## The global proteome and ubiquitinome of bacterial and viral co-infected bronchial epithelial cells

Thomas Sura<sup>a</sup>, Surabhi Surabhi<sup>b</sup>, Sandra Maaß<sup>a</sup>, Sven Hammerschmidt<sup>b</sup>, Nikolai Siemens<sup>b</sup>, Dörte Becher<sup>a,\*</sup>

<sup>a</sup> University of Greifswald, Center for Functional Genomics of Microbes, Institute of Microbiology, Department of Microbial Proteomics, Felix-Hausdorff-Str. 8, 17489 Greifswald, Germany

<sup>b</sup> University of Greifswald, Center for Functional Genomics of Microbes, Interfaculty Institute for Genetics and Functional Genomics, Department of Molecular Genetics and Infection Biology, Felix-Hausdorff-Str. 8, 17489 Greifswald, Germany

### ARTICLE INFO

#### Keywords:

Co-infection  
Ubiquitin  
Influenza A virus  
*Streptococcus pyogenes*  
*Staphylococcus aureus*  
16HBE  
Proteomics

### ABSTRACT

Viral infections facilitate bacterial trafficking to the lower respiratory tract resulting in bacterial-viral co-infections. Bacterial dissemination to the lower respiratory tract is enhanced by influenza A virus induced epithelial cell damage and dysregulation of immune responses. Epithelial cells act as a line of defense and detect pathogens by a high variety of pattern recognition receptors. The post-translational modification ubiquitin is involved in almost every cellular process. Moreover, ubiquitination contributes to the regulation of host immune responses, influenza A virus uncoating and transport within host cells. We applied proteomics with a special focus on ubiquitination to assess the impact of single bacterial and viral as well as bacterial-viral co-infections on bronchial epithelial cells. We used Tandem Ubiquitin Binding Entities to enrich polyubiquitinated proteins and assess changes in the ubiquitinome. Infecting 16HBE cells with *Streptococcus pyogenes* led to an increased abundance of proteins related to mitochondrial translation and energy metabolism in proteome and ubiquitinome. In contrast, influenza A virus infection mainly altered the ubiquitinome. Co-infections had no additional impact on protein abundances or affected pathways. Changes in protein abundance and enriched pathways were assigned to imprints of both infecting pathogens.

**Significance:** Viral and bacterial co-infections of the lower respiratory tract are a burden for health systems worldwide. Therefore, it is necessary to elucidate the complex interplay between the host and the infecting pathogens. Thus, we analyzed the proteome and the ubiquitinome of co-infected bronchial epithelial cells to elaborate a potential synergism of the two infecting organisms. The results presented in this work can be used as a starting point for further analyses.

### 1. Introduction

Community-acquired pneumonia (CAP) is one of the leading causes of morbidity and mortality constituting a major human health concern [1–3]. CAP is caused by a diverse range of pathogens, including bacteria and viruses. Many cases of primary viral infection result in bacterial trafficking to the lower respiratory tract leading to bacterial and viral co-infections [1,4], which are characterized by an increased severity of the disease [2,5]. Recent studies have shown that seasonal influenza infections and influenza A virus (IAV) related pandemics like the “Spanish Flu” and others constitute of bacterial and viral co-infections in more

than 30% of cases [6–11]. Bacterial pathogens, which are known to cause co-infections, are typical colonizers of the upper respiratory tract and include, amongst others, *Streptococcus pneumoniae*, *Streptococcus pyogenes* (group A streptococcus; GAS), and *Staphylococcus aureus* [12–14]. Within the lung, epithelial cells act as a physical barrier and play an important role in the clearance of inhaled particles [15–17]. IAV infection can induce impaired mucosal clearance and thereby promote bacterial dissemination of the lower respiratory tract [18,19]. Furthermore, disruption of the epithelial barrier predisposes bacterial invasive infection and promotes bacterial and viral co-infections [20]. In addition to the function as a barrier, epithelial cells are able to sense pathogens by

\* Corresponding author at: University of Greifswald, Center for Functional Genomics of Microbes, Institute of Microbiology, Department of Microbial Proteomics, Felix-Hausdorff-Str. 8, 17489 Greifswald, Germany.

E-mail address: [dbecher@uni-greifswald.de](mailto:dbecher@uni-greifswald.de) (D. Becher).

<https://doi.org/10.1016/j.jprot.2021.104387>

Received 16 June 2021; Received in revised form 26 August 2021; Accepted 22 September 2021

Available online 30 September 2021

1874-3919/© 2021 Elsevier B.V. All rights reserved.

a high variety of pattern recognition receptors (PRRs) and are involved in the innate immune response of the host [15,17].

Posttranslational modifications (PTMs) are key drivers in the regulation of protein activity, conformation, and localization within the cell. Ubiquitin, a protein that consists of 76 amino acids in length, is one of the most prominent PTMs. Ubiquitination is highly diverse, as this modification occurs as mono-, multimono- and polyubiquitination. In addition, there are many linkage types within polyubiquitination, each bearing different physiological functions [21]. Ubiquitination, therefore, does not only regulate the protein homeostasis within cells, it rather plays a role in almost every cellular process. Moreover, ubiquitination is involved in the regulation of the hosts innate and adaptive immune response [22–28] and participates in IAV uncoating and transport within host cells [29,30]. Bacteria like *Legionella pneumophila* and various viruses have been described to interfere with the host ubiquitin proteasome system (UPS), and thus are able to evade the host immune system [31,32].

Different tools have been developed to enable the mass spectrometry based investigation of ubiquitinated proteins. Here, we applied proteomics with an emphasis on ubiquitination events to elucidate the impact of single bacterial (*S. aureus*; *S. pyogenes*) and viral (IAV H1N1) as well as viral and bacterial co-infections on bronchial epithelial cells. We used Tandem-Ubiquitin-Binding-Entities (TUBEs) coupled to magnetic beads to assess changes in the abundances of polyubiquitinated proteins [33]. The pan-selective enrichment of polyubiquitinated proteins combined with LC-MS/MS based quantification provides further insights into the ubiquitination processes upon single- and co-infection at a global scale. To our knowledge, this is the first study that analyses the differential abundance of the proteome and the ubiquitinome of bronchial epithelial cells in response to bacterial-viral co-infection.

## 2. Materials and methods

### 2.1. Bacterial and viral strains, cell culture conditions, and infection experiments

*S. pyogenes* strain 5448 (GAS) is a streptococcal toxic shock syndrome isolate [34] and was cultured overnight in Todd-Hewitt broth (Invitrogen) supplemented with 1.5% (w/v) yeast extract (Invitrogen) at 37 °C. *S. aureus* strain LUG2012 (USA300 lineage) [35] was cultured overnight at 37 °C in casein hydrolysate and yeast extract (CCY) medium with agitation. Influenza A virus A/Germany-BY/74/2009 (H1N1) was propagated and cultivated as described by Eisfeld and colleagues [36].

16HBE14o- (16HBE) cells (kindly provided from Dieter Gruenert, Mt. Zion, Cancer Center, San Francisco, CA, USA) were cultured in MEM medium (Gibco) supplemented with 10% (v/v) fetal bovine serum (FBS; Life Technologies), 2 mM L-glutamine (Invitrogen), 10 mM HEPES (GE Healthcare) and 1% (v/v) Minimal Essential Amino Acids (GE Healthcare) in fibronectin coated flasks (Corning) at 37 °C and 5% CO<sub>2</sub> atmosphere.

16HBE cells were seeded in T175 culture flasks and grown to approximately 80% confluence. For calculation of the multiplicity of infection (MOI), cell counts of the control flask were determined. The flasks were either left untreated or were infected with H1N1 at MOI 0.1 for 24 h. This amount of virus and the time point were determined as an optimal infection with no significant cell death. After 24 h, bacterial infections of uninfected and H1N1 infected cells were performed. Both, *S. pyogenes* 5448 and *S. aureus* LUG2012 infections were conducted at MOI 10 for 2 h. Uninfected or H1N1 infected cells served as controls and were treated exactly in the same way. After 2 h of bacterial infection, cells were detached using a scraper and counted. Cell counts were determined by light microscopic quantification of cell viability. Cells were stained with 0.4% (v/v) trypan blue under serum-free conditions and visually examined. All experiments were performed in triplicates.

### 2.2. Preparation of cell lysate

Whole cell extracts were prepared by adding 1.5 ml of lysis buffer (50 mM Tris-HCl [pH 7.5], 0.15 M NaCl, 1 mM EDTA, 1% (v/v) NP-40, 10% glycerol, 1× cOmplete Protease Inhibitor Cocktail (Roche), 1 mM PMSF, 10 mM N-ethylmaleimide, 20 μM MG132) to the cells. Samples were incubated on ice for 30 min with vortexing every 5 min. Lysates were sonicated two times for 1 min (probe MS72; 0.1 s pulse; 0.5 s cycle, 20% amplitude) (SONOPULS HD 3100, Bandelin) to shear DNA. Lysates were cleared by high-speed centrifugation (20,000 ×g; 10 min). Protein concentration was determined using the BCA assay (Thermo Fisher).

### 2.3. Enrichment of polyubiquitinated proteins

For the enrichment of polyubiquitinated proteins magnetic beads from 65 μl magnetic TUBE 2 slurry (LifeSensors) were washed two times with TBS-T (20 mM Tris-HCl [pH 8.0], 150 mM NaCl, 0.1% (v/v) Tween-20) and collected with a magnetic stand. Lysate containing 1 mg of protein was added to the beads. The final volume was adjusted to 900 μl using freshly prepared lysis buffer. Samples were incubated overnight in a rotator (10 rpm; 4 °C). Beads were collected using a magnetic stand, the unbound fraction was removed, and the beads were washed four times with 1 ml TBS-T. After the final washing step, the magnetic beads were suspended in 50 μl SDS buffer (5% (w/v) SDS; 50 mM triethylammonium bicarbonate [TEAB]; 5 mM Tris(2-carboxyethyl)phosphine [TCEP]) and incubated at 65 °C for 45 min with agitation (300 rpm). The magnetic beads were pelleted by centrifugation and the supernatant was transferred to a new tube.

### 2.4. Proteolytic digest for total proteome samples

Proteins were digested on micro S-Traps (Protifi) following the vendor's protocol with slight modifications. Briefly, lysates containing 50 μg protein were transferred into new tubes and the volume was adjusted to 50 μl using freshly prepared lysis buffer. SDS and TEAB have been added to final concentrations of 5% (w/v) and 50 mM, respectively. Disulfide bonds were reduced by adding TCEP (5 mM final concentration; 45 min; 65 °C). Thiol groups were alkylated by adding iodoacetamide (IAA; 10 mM final concentration; 15 min; RT; in the dark). Phosphoric acid was added to the samples to a final concentration of 1.2%. Afterwards, 500 μl S-Trap-binding-buffer (90% methanol, 100 mM TEAB) were added to the acidified samples. The protein colloid solution was subsequently loaded onto the S-Trap micro columns by centrifugation (4000 ×g). Trapped proteins were washed three times with 165 μl S-Trap-binding-buffer. Proteins were digested by adding 25 μl digestion-buffer (50 mM TEAB) containing 2 μg trypsin (Promega) followed by an incubation for 3 h at 47 °C. Peptides were subsequently eluted with 40 μl 50 mM TEAB; 0.1% (v/v) acetic acid; 60% (v/v) ACN in 0.1% (v/v) acetic acid. All eluted fractions of a sample were pooled and dried in a vacuum concentrator. Dry peptides were stored at –80 °C.

### 2.5. Proteolytic digest of polyubiquitinated proteins

Enriched polyubiquitinated proteins were digested on micro S-Traps (Protifi) following the vendor's protocol with slight modifications. In brief, thiol groups of eluted proteins were alkylated by adding IAA (10 mM final concentration) followed by an incubation of 15 min at room temperature in the dark. Phosphoric acid was added to the samples to a final concentration of 1.2%. Hereafter, 316 μl of S-Trap-binding-buffer (90% methanol, 100 mM TEAB) were added to the acidified samples. The protein colloid solution was subsequently loaded onto the S-Trap micro columns by centrifugation (4000 ×g). Trapped proteins were washed three times with 165 μl S-Trap-binding-buffer. Proteins were digested by adding 25 μl digestion-buffer (50 mM TEAB) containing 1 μg trypsin (Promega) followed by an incubation for 3 h at 47 °C. Peptides were subsequently eluted with 40 μl of 50 mM TEAB; 0.1% (v/v) acetic



acid; 60% (v/v) ACN in 0.1% (v/v) acetic acid. All fractions of one sample were pooled and dried in a vacuum concentrator. Dry peptides were stored at  $-80^{\circ}\text{C}$ .

### 2.6. Peptide fractionation by basic reversed-phase chromatography

Peptides were fractionated using Pierce Micro-Spin Columns (Thermo Fisher) packed with 15 mg of Dr. Maisch Reprosil-Gold 300 C18, 5  $\mu\text{m}$  (Dr. Maisch) particles. Columns were washed three times with 300  $\mu\text{l}$  acetonitrile and equilibrated two times with 300  $\mu\text{l}$  0.1% (v/v) TFA by centrifugation (5000  $\times$ g; 2 min). Dried peptides were reconstituted in 300  $\mu\text{l}$  0.1% (v/v) TFA and loaded onto the spin column by centrifugation (4 min; 3000  $\times$ g). Peptides were subsequently eluted with 5%; 7.5%; 10%; 12.5%; 15%; 17.5%; 20% and 60% (v/v) acetonitrile in 0.1% (v/v) triethylamine, 300  $\mu\text{l}$  each (4 min; 3000  $\times$ g). Fractions were concatenated using the scheme: 5% and 15%; 7.5% and 17.5%; 10% and 20%; 12.5% and 60%. Concatenated fractions were dried by vacuum centrifugation and resolved with 20  $\mu\text{l}$  0.1% (v/v) acetic acid containing iRT peptides (Biognosys). From the proteome samples, 5  $\mu\text{l}$  of each fraction were pooled for validation of the label free quantification by parallel reaction monitoring (PRM).

### 2.7. LC-MS/MS

LC-MS/MS was applied to uncover peptide compositions and quantities. Therefore, an EASY-nLC 1200 (Thermo Fischer) was coupled to a QExactive mass spectrometer (Thermo Fisher). Peptides were loaded onto in-house packed fused silica columns of 20 cm length and an inner diameter of 75  $\mu\text{m}$ , filled with Dr. Maisch Reprosil-Pur 120 C18-AQ 1.9  $\mu\text{m}$  (Dr. Maisch). Peptides were eluted using a non-linear binary gradient of 166 min from 2% to 99% solvent B (0.1% (v/v) acetic acid in acetonitrile) in solvent A (0.1% (v/v) acetic acid). Detailed information on the LC setup is provided in supplementary table S1. The full scan was recorded with a mass range from 300 to 1650  $m/z$  and a resolution of 140,000 at 200  $m/z$ . The 15 most abundant ions were isolated with an isolation width of 2 Th and fragmented by higher-energy collisional dissociation (HCD) at a normalized collision energy of 27. Fragment ion spectra were recorded with a resolution of 17,500 at 200  $m/z$ . Ions with unassigned charge states as well as charge 1 and higher than 6 were excluded from fragmentation. Fragmented ions were excluded from fragmentation for 30 s. Lock mass correction was enabled. Detailed information is provided in supplementary table S2.

For PRM measurements of selected proteins precursor ions were isolated with an isolation width of 1.4 Th and fragmented by higher-energy collisional dissociation (HCD) at a normalized collision energy of 27. Fragment ion spectra were recorded with a resolution of 70,000 at 200  $m/z$ . Selected precursor ions were time scheduled. A detailed list of applied MS settings and selected precursor ions is provided in supplementary table S3.

### 2.8. Data analysis

Datasets for enriched ubiquitinated proteins and for the total proteome were processed separately. Raw data were searched with MaxQuant (version 1.6.14.0) against the UniProt databases for human, *S. aureus* USA300 and Influenza A virus (A/Germany-BY/74/2009 (H1N1)) as well as the NCBI database for *S. pyogenes* M1 GAS [37–39]. The maximum number of allowed missed cleavages was 2 and precursor mass tolerance was set to 4.5 ppm. Carbamidomethylation (C) was set as a fixed modification, oxidation (M) and acetylation (protein N-termini) were set as variable modifications for both datasets. GlyGly (K) was set as an additional variable modification for TUBE enriched samples. Match between runs was applied and protein abundances were calculated by the MaxLFQ algorithm. A detailed table of applied parameters for database searching can be found in supplementary table S4 and supplementary table S5.

Identified protein groups were analyzed with Perseus (version 1.6.14.0) [40]. Only identified by site and reverse hits as well as potential contaminations were removed. To assess differentially expressed proteins, a two-tailed *t*-test was applied for proteins with “LFQintensity” values in three out of three replicates of the compared groups. Proteins were considered as differentially expressed with a *p*-value  $<0.05$  and a fold change  $>1.5$ . Quantification results and summary statistics can be found in supplementary table S6. Enrichment analysis of GO-direct terms was performed with the Database for Annotation, Visualization and Integrated Discovery v6.8 (DAVID) [41,42]. Data were visualized using Inkscape (version 0.92.2) and RStudio (version 1.3.1073) with the ggplot2 (version 3.3.2) and dplyr (version 1.0.1) packages [43]. Networks were created with STRING v11 [44]. Skyline (version 20.2.0.343) was used to analyze the PRM experiment [45]. Protein abundances were exported from Skyline and imported in Excel. Protein abundances were log2 transformed and normalized by subtraction of the abundance value of the housekeeping protein VCP. A fold change was calculated by subtracting the averaged protein abundance of the control samples from the averaged protein abundance of the infected samples. The calculated fold changes were compared to the fold changes calculated from MaxLFQ values.

## 3. Results and discussion

This study was performed to elaborate the global effect of bacterial and viral co-infections on protein abundances and polyubiquitination occurrence. As a first step, we separately analyzed bacterial and viral infections to generate data that can be compared to the co-infection results. Indeed, the presented study was not specifically designed to quantify ubiquitination site occupancies. For that reason, we have used TUBEs to enrich polyubiquitinated proteins and have not used antibodies against diGLY remnant peptides.

### 3.1. Cell survival post infections

First, 16HBE cells were mono-infected with the selected pathogens and cell counts were obtained at final time point post infection. H1N1 and *S. aureus* LUG2012 infections were characterized by minor but not significant changes in cell viability. In contrast, *S. pyogenes* 5448 infection led to a decrease in 16HBE cell counts by more than 60% (Supplementary Fig. 1). Next, co-infections were performed. Irrespective of the prior H1N1 infection, a similar pattern in 16HBE cell counts was observed (Supplementary Fig. 1). 16HBE cell survival post *S. aureus* LUG2012 or H1N1 infections was within the range measured in a recent study published by Schultz et al. [46].

### 3.2. Proteome and Ubiquitinome of mono-infections

In order to characterize the global impact of single bacterial and viral infections we performed mass-spectrometry based label-free quantification (LFQ) to determine changes on proteome and ubiquitinome level of human bronchial epithelial cells. Data reproducibility was assessed by calculating CV's from the abundances of proteins that have been quantified in three biological replicates (Supplementary Fig. 4). MaxLFQ quantification of the proteome was confirmed by independent PRM measurements of selected proteins (Supplementary table S7).

Quantified proteins have been considered as differentially expressed with a fold change  $>1.5$  and a *p*-value  $<0.05$ . The global proteome analysis conducted in this study resulted in 4873–5088 quantified proteins depending on the pathogen used for the infection. Thus, the total number of quantified proteins is within the same range for all performed infections (Supplementary Fig. 2). Nevertheless, the fraction of proteins that have been found to be differentially expressed is different for each of the performed infections (Supplementary Fig. 3). In congruence with the cytotoxicity data, the strongest effects on the proteome were observed in *S. pyogenes* 5448 infections. In total, 400 proteins were

differentially expressed in *S. pyogenes* 5448 infected 16HBE cells, whereas 65 and 63 differentially expressed proteins were detected upon *S. aureus* LUG2012 and IAV infection, respectively. Moreover, every infection resulted in a unique pattern of proteins with significantly altered abundances. This is represented by a low overlap of differentially expressed proteins (Fig. 1A).

Influenza viruses are described to interfere with the host ubiquitin proteasome system at many stages of the viral life cycle [30]. Hence, it was expected to detect a high number of proteins with alterations in ubiquitination frequency. Additionally, several bacterial pathogens can hijack components of the UPS to evade the hosts immunity [47]. Therefore, it was expected to see changes in the abundances of UPS components and ubiquitination incidences induced by bacterial infections. The enrichment of polyubiquitinated proteins by TUBE 2 magnetic beads enabled the quantification of polyubiquitinated proteins. In contrast to the proteome, the ubiquitinome comprises a higher number of proteins with significantly altered abundances. The highest number was observed for IAV H1N1 infected cells (498 differentially expressed proteins), followed by *S. pyogenes* 5448 (417 differentially expressed proteins) and the *S. aureus* LUG2012 infections (137 differentially expressed proteins). Depending on the infecting organism a specific pattern of differentially expressed proteins has been noticed for enriched polyubiquitinated proteins (Fig. 1B).

Next, gene-annotation enrichment analysis was applied to the proteins with increased and reduced abundances to determine the affected biological pathways. Again, a unique pattern of over-represented pathways for each infection was detected, which is represented by a minor overlap (Fig. 2A and B). Only one pathway, *protein transport*, was enriched in the proteomes of all single infections. In IAV H1N1 infection *protein transport* was enriched from three proteins with decreased abundance without a tendency towards a specific pathway (Supplementary Table S8). In contrast to the viral infection, the term *protein transport* is enriched from proteins with increased abundance in bacterial infections. Here, proteins that are Rab GTPases and Rab associated were detected in both infections (Supplementary Table S8). Rab GTPases are involved in endolysosomal trafficking and were shown to be involved in host pathogen interactions, but also that they are manipulated by bacterial pathogens [48–50].

Furthermore, proteins related to *protein transport into mitochondrial matrix* were over-represented by proteins of increased abundance in both bacterial infections. An increase in the abundance of Tom22, the central receptor component of the TOM-complex, was detected for both bacterial infections [51,52] (Supplementary Table S6). In addition to the increase in Tom22 abundance, Tom40 was detected with increased abundance in GAS infection, as well. Both, Tom22 and Tom40, were found to be crucial for *Chlamydia* propagation in HeLa 229 cells [53]. This may indicate a potential role of the mitochondrial protein import machinery in *S. pyogenes* and *S. aureus* infections, as well. No further overlap was detected by the enrichment analysis of total proteome data

from single infections (Fig. 2A). Similarly, there was only a minor overlap of over-represented gene ontology biological process terms (GOBP) terms for polyubiquitinated proteins. The following terms have been enriched for polyubiquitinated proteins with altered abundances by all investigated single infections: *mitochondrial electron transport*, *mitochondrial respiratory chain complex I assembly*, *cell-cell adhesion*, *rRNA processing*, *translation* and *translation initiation* (Fig. 2B).

Single *S. aureus* LUG2012 infections resulted only in a small number of differentially expressed proteins. Moreover, the number of over-represented GOBP terms is relatively low, too. Still, it is worth mentioning that terms enriched from proteins with increased abundance after *S. aureus* LUG2012 infection are mainly ascribed to HLA-A and B2M. Four out of seven enriched terms uniquely assigned to *S. aureus* LUG2012 refer exclusively to these two proteins (Supplementary Table S8). These data indicate a higher abundance of MHC-I already two hours post infection (hpi) compared to the uninfected control. However, *S. aureus* infections are mostly linked to antigen presentation by MHC-II and their expressed homologue Map [54,55]. Since the *S. aureus* LUG2012 mono-infection of 16HBE cells induced only minor changes in the protein abundance, a higher MOI or a prolonged infection period would probably induce a stronger effect. It can be assumed that the percentage of cells that have been infected intracellularly by *S. aureus* LUG2012 is relatively low in the chosen setup and therefore, the induced changes in the proteome and ubiquitinome are superimposed by the proteome and ubiquitinome of unaffected cells. Another study analyzed the proteome of *S. aureus* infected 16HBE cells over a time course of 96 h. This analysis showed that apoptosis of the host cells is induced 24 hpi. In accordance with our data, even fewer changes in the host proteome were detected at 2.5 hpi [56]. In contrast to our approach, the aforementioned study applied antibiotic treatment to solely focus on the impact of intracellular staphylococci. Due to the different experimental setup and the addition of the ubiquitination analysis, we expected to discover more proteins with changes in abundance at the early onset of infection. The infection period of two hours was chosen to analyze an early time point of infection and to have the same setup for both bacterial infections. Thus, in the following part we will mainly focus on H1N1 and *S. pyogenes* mono-infections.

Even if there were only a few changes observed in the proteome of IAV infected cells (Fig. 2C), 498 proteins were detected with significant alteration in ubiquitination incidence. The most significant enriched GOBP-term was *mRNA splicing, via spliceosome*, which is represented by more than 30 proteins with decreased abundance in TUBE 2 enrichment (Fig. 2D). Billare et al. demonstrated the involvement of ubiquitination in pre-mRNA splicing by mutating ubiquitin at 144A, which led to a stalled spliceosome assembly at the B complex [57]. Furthermore, influenza A viruses are known to misuse, alter, and relocate the host mRNA splicing machinery [58]. Interestingly, proteins related to GTPases and Rho signaling are over-represented from proteins with increased abundance in ubiquitinome samples. Thus, the viral replication cycle seems to be connected to Rho GTPase signaling at almost every step [59] (Fig. 2D).

*S. pyogenes* 5448 infections had the greatest impact on proteins related to the GOBP-direct terms *mitochondrial translational elongation* and *mitochondrial translational termination*, indicating mitochondrial dysfunction (Fig. 2E and F). In contrast to the viral infection, these terms were highly enriched in both, proteome and ubiquitinome analyses. This leads to the assumption that the abundance of polyubiquitinated proteins results from changes in the protein abundance. Furthermore, *cell-cell adhesion* was most significantly enriched for proteins with decreased abundance within both data sets of *S. pyogenes* 5448 infections (Fig. 2E and F). Adhesion of streptococci can cause alterations in the cytoskeleton of the host cell [60]. Thus, adhesion and of streptococci might explain the changes in *cell-cell adhesion* related proteins. The STRING network generated from proteins with higher abundances of the ubiquitinome contains clusters of proteins representing *rRNA processing*; *metabolism of lipids*; *mitochondrial translation*; *mitochondrial protein*

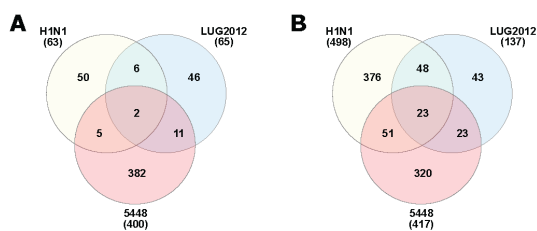


Fig. 1. Overlap of proteins with significantly changed abundance. Overlap of proteins that were found to be significantly changed in abundance ( $p$ -value  $< 0.05$ ;  $FC > 1.5$ ) in proteome (A) and ubiquitinome (B) of 16HBE cells infected with Influenza A virus (H1N1), *Staphylococcus aureus* (LUG2012) or *Streptococcus pyogenes* (5448) [ $n = 3$ ].



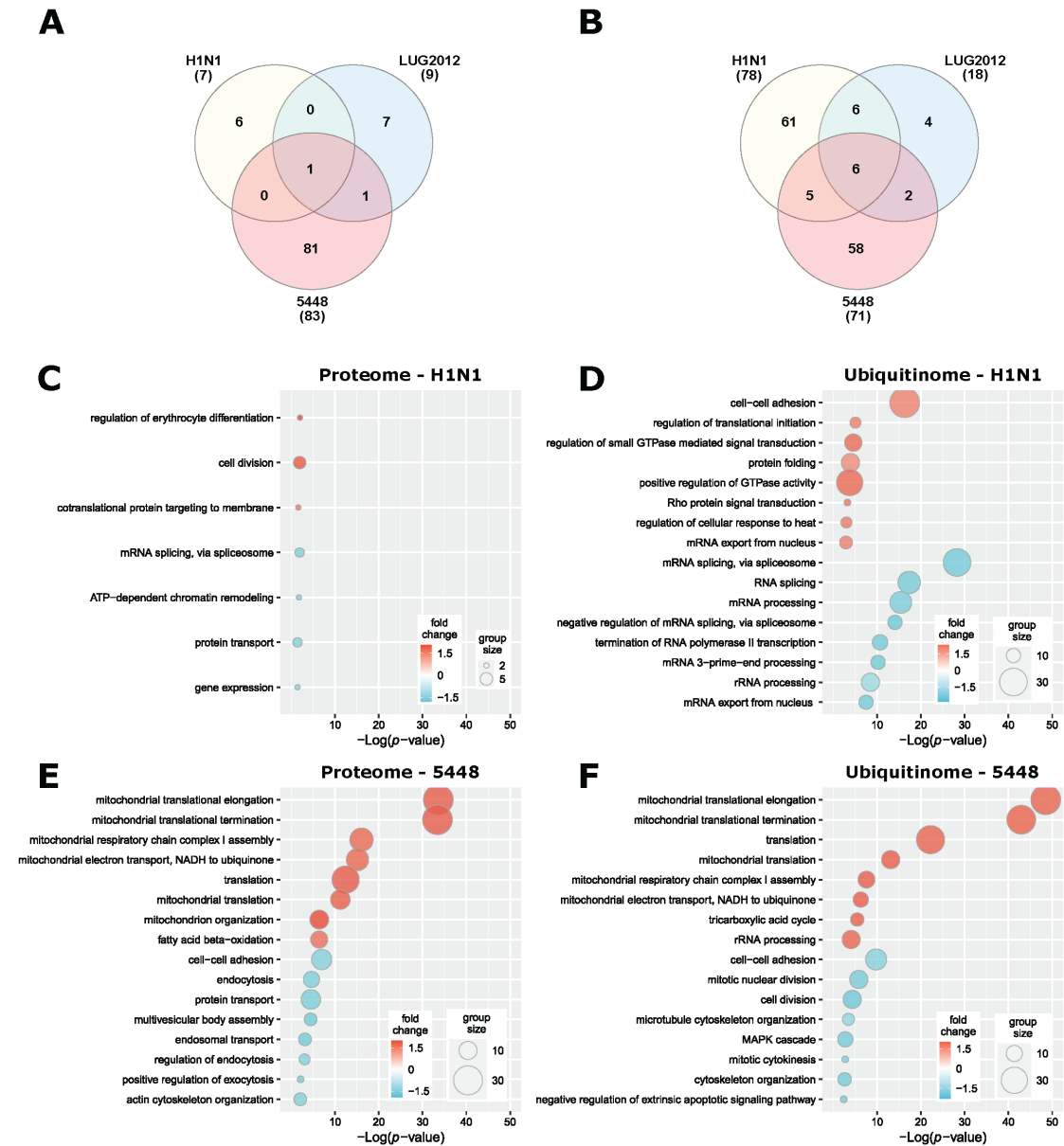


Fig. 2. GOBP terms enriched from proteins with significantly changed abundance. Categorical annotation enrichment ( $p$ -value  $< 0.05$ ) of gene ontology biological process terms (GOBP) from proteins significantly changed in abundance ( $p$ -value  $< 0.05$ ; FC  $> 1.5$ ) in the proteome (A) and the ubiquitinome (B) of 16HBE cells infected with Influenza A virus (H1N1), *Staphylococcus aureus* (LUG2012) or *Streptococcus pyogenes* (5448) [ $n = 3$ ]. (C–F) displays the top hits of the enriched GOBP terms from proteins with increased and decreased abundance, ranked by  $p$ -value, colored according to their fold change and sized by the number of proteins that are included within each enriched term.

import- and respiratory electron transport, ATP synthesis-reactome pathways (Supplementary Fig. 5). Enriched mitochondria related terms could be explained by the induction of apoptosis and increased mitochondrial dysfunction [61,62]. Mitochondrial dysfunction and induction of epithelial cell death can be induced by the secretion of the Streptococcal pyrogenic exotoxin B (SpeB), streptolysin S (SLS) and

streptolysin O (SLO) by *S. pyogenes*. SLO produced by extracellular streptococci forms pores in host cell membranes and eventually results in loss of mitochondrial outer membrane potential [63]. SLS production allows GAS to escape from the endosome [63]. Moreover, SLS can induce mitochondrial dysfunction and induces cell death by elevated mitochondrial ROS levels [64,65]. Expression of SpeB, a secreted and

membrane associated cysteine protease that acts as a virulence factor, prevents ubiquitin mediated recognition and selective autophagy of cytosolic streptococci [64,65].

The proteomic data on bacterial and viral mono-infections generated in the first part of this study are fundamental for the interpretation of the co-infection data.

### 3.3. Proteome and Ubiquitinome of co-infected 16HBE cells

In certain cases it has been described that viral infection might pave the way for subsequent bacterial infection of the lower respiratory tract [19]. Therefore, we performed co-infection experiments. 16HBE cells were infected with IAV for 24 h followed by a bacterial infection for additional two hours. Co-infection with *S. aureus* and IAV H1N1 resulted in reduced killing of 16HBE cells compared to the bacterial single infection (Supplementary Fig. S1). This leads to the assumption that we have observed a protective effect of the IAV H1N1 infection in our analysis. Protective effects of the viral infections in bacterial superinfections were described as well in several previous studies and were summarized by Paget and Trottein [66]. An increased survival rate upon co-infection was also observed by Schultz et al. [46]. In comparison to our results, murine model based studies have shown a synergistic effect of IAV and *S. aureus* co-infection [67–69]. Our proteomic analyses revealed that co-infection mostly mirrors single bacterial infection. Although, the number of proteins detected with differential abundance was slightly increased in the proteome samples of *S. aureus* LUG2012 co-infected samples, only minor changes in the overall numbers of proteins with significantly altered abundance were observed (Supplementary Fig. 2 and 3). While the amount of overrepresented pathways in proteome samples increased after *S. aureus* LUG2012 co-infection, we were not able to identify pathways that enable the prediction of synergism of the pathogens (Supplementary Table S8). This is particularly apparent when comparing the numbers of polyubiquitinated proteins with differential abundance in response to single and co-infections with *S. aureus* LUG2012. Variations in the ubiquitination pattern of 16HBE cells, which were observed after single IAV infection have mostly disappeared upon IAV and *S. aureus* LUG2012 co-infection (Supplementary Table S9; Supplementary Fig. S3). Currently, we cannot explain our observation apart from assuming a protective effect of the co-infection in the selected experimental setup. As mentioned before, extension of the infection period or application of an increased MOI during the *S. aureus* LUG2012 infection would possibly be required to induce potential changes in proteome and ubiquitinome responses by 16HBE cells. However, this would also lead to an increase in host cell damage.

At the analyzed period of infection and the selected MOI, *S. pyogenes* 5448 and IAV H1N1 co-infection is more cytotoxic towards 16HBE cells than *S. aureus* LUG2012 and IAV H1N1 co-infection (Supplementary Fig. 1). Still, we were not able to detect reduced survival of 16HBE cells in *S. pyogenes* 5448 co-infection. Thus, a potential synergistic effect of the co-infection cannot be assumed based on the cell survival. In experiments conducted in murine models a synergistic effect of viral and bacterial co-infection has been shown by an increased mortality [70–72]. Moreover, Li and coworkers have demonstrated that IAV infection results in an increase of fibronectin and  $\alpha 5$  integrin in a TGF $\alpha$  dependent manner, vacillating increased bacterial adherence to host cells [73]. In our study we have not detected an altered abundance of fibronectin or  $\alpha 5$  integrin upon viral infection (Supplementary table S6). This might explain the lack of decreased cell survival upon co-infection in our study.

Here, enriched pathways noticed in *S. pyogenes* 5448 co-infection originate from both, viral and bacterial infections (Fig. 3). This imprint is particularly apparent in ubiquitinome analyses (Fig. 3D). While alterations observed in the proteome samples derive mostly from the bacterial pathogen (Fig. 3C and Fig. 4A), the detected changes in the abundance of polyubiquitinated proteins are influenced by both pathogens (Fig. 3D, Fig. 4B and Supplementary Fig. 5).

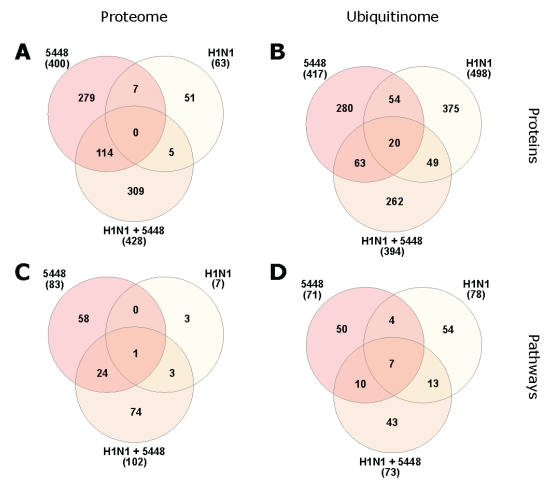


Fig. 3. Overlap in proteins and enriched GOBP terms of proteins with significantly changed abundance in 16HBE cells infected with IAV, *Streptococcus pyogenes* 5448 or both. Overlap from proteins found to be significantly changed in abundance ( $p$ -value  $< 0.05$ ; FC  $> 1.5$ ) in the proteome (A) and the ubiquitinome (B). Categorical annotation enrichment ( $p$ -value  $< 0.05$ ) of GOBP terms from proteins with significant changes in abundance ( $p$ -value  $< 0.05$ ; FC  $> 1.5$ ) in proteome (C) and ubiquitinome (D) [ $n = 3$ ].

Even if the detected variations within the composition of the proteome and the ubiquitinome of the IAV and *S. pyogenes* 5448 co-infection can be traced back to both infecting pathogens, there is no distinct tendency whether the co-infection enhances or weakens the changes in protein abundances for specific pathways. Consequently, this phenotype might explain why no increased severity of co-infection was observed in the investigated model (Supplementary Fig. 1).

### 3.4. Concluding remarks

As far as we are aware, this is the first global description of the ubiquitinome in response to bacterial-viral co-infection in 16HBE cells. We believe that this study provides a complex and comprehensive protein repository of high-quality proteome data for 16HBE cells after bacterial and viral mono- as well as co-infections. Furthermore, it includes identification and quantification of putatively polyubiquitinated proteins, which will facilitate further investigations of this important post-translational modification event.

Challenging 16HBE cells with the Gram-positive pathogen *S. pyogenes* 5448 reduced the number of viable cells in a rapid manner. The infection led to an increased abundance of proteins related to mitochondrial translation and energy metabolism in the proteome and ubiquitinome. *S. aureus* LUG2012 infection induced only minor changes in the proteome. Nevertheless, an increased abundance of MHC-I proteins was detected upon staphylococcal infection. Similar to the *S. aureus* LUG2012 infection, IAV H1N1 infection caused only minor effects on the host's proteome abundance. In contrast to the staphylococcal infection, viral infection dramatically altered the abundance of polyubiquitinated proteins. Reduced polyubiquitination was mostly recognized for proteins related to mRNA splicing whereas proteins related to GTPase and Rho signaling had higher levels of polyubiquitination.

Alterations within the ubiquitinome observed upon viral infection were not detected after co-infection with *S. aureus* LUG2012 and IAV H1N1. In addition, we detected an increase in cell survival in the co-infection. Taken together, this might indicate a protective effect of the IAV H1N1 infection in the presented work.

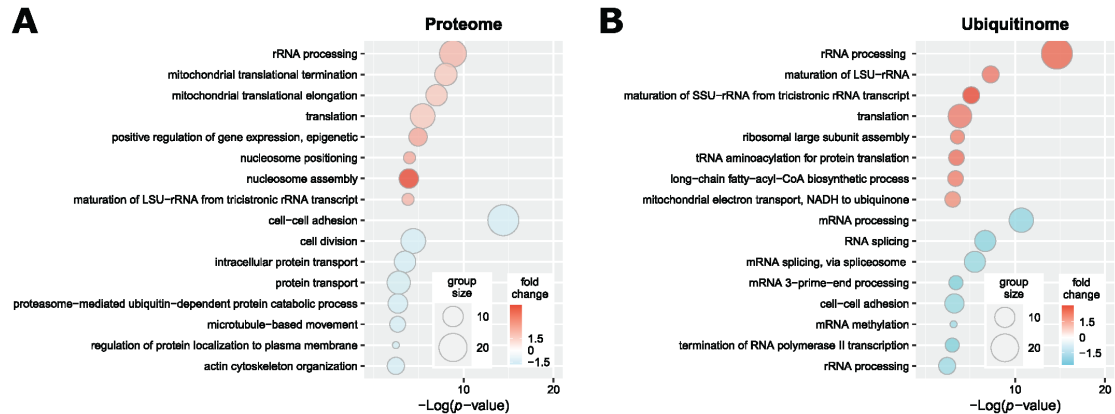


Fig. 4. GOBP terms enriched from proteins with significantly changed abundance after co-infection of 16HBE cells with Influenza A virus (H1N1) and *Streptococcus pyogenes* (5448). Categorical annotation ( $p$ -value  $< 0.05$ ) of gene ontology biological process terms (GOBP) from proteins significantly changed in abundance ( $p$ -value  $< 0.05$ ; FC  $> 1.5$ ) in the proteome (A) and the ubiquitinome (B) [ $n = 3$ ]. Displayed are the top hits of the GOBP term enrichment from proteins with increased and decreased abundance, ranked by  $p$ -value, colored according to their fold change and sized by the number of proteins that are included within each enriched term.

*S. pyogenes* 5448 co-infection had no additional significant impact on protein abundances or enriched pathways. The findings of this work indicate that most changes in protein abundance and over-represented pathways were assigned to imprints of both infecting pathogens. Moreover, it can be concluded that the *S. pyogenes* 5448 and IAV H1N1 co-infection in the presented study shows an additive, rather than a synergistic effect. This might be caused by the selected pathogens as the outcome of a co-infection strongly depends on the selected viral and bacterial strains [70,72].

Further studies using advanced cell culture system like air liquid interface will be important to elaborate the effects of co-infection in a more *in vivo* like infection. Moreover, the usage of different IAV subtypes will enable the elucidation of subtype specific and general effects on the ubiquitinome. This should also show differences in the outcome of the co-infection due to the usage of different IAV subtypes.

**Associated data**

The mass spectrometry proteomics data have been deposited to the ProteomeXchange Consortium (<http://proteomecentral.proteomexchange.org>) via the PRIDE partner repository [74] with the dataset identifier PXD025146 (reviewer\_pxd025146@ebi.ac.uk).

Data from the PRM-based validation measurements were deposited to the ProteomeXchange Consortium via Panorama Public and are available through the identifier PXD026625 or directly via the Panorama web service ([http://www.panoramaweb.org/16HBE\\_Co\\_infection.url](http://www.panoramaweb.org/16HBE_Co_infection.url)) (reviewer37@proteinms.net).

**Author contributions**

Conceptualization, T.S., S.S., N.S. and D.B.; methodology, S.S., T.S.; validation, T.S.; formal analysis, T.S.; investigation, T.S.; resources, S.H., N.S. and D.B.; data curation, T.S.; writing—original draft preparation, T.S.; writing—review and editing, T.S., S.S., S.M., S.H., N.S., D.B.; visualization, T.S.; supervision, N.S., D.B.; project administration, D.B.; funding acquisition, D.B. and S.H.; All authors have read and agreed to the published version of the manuscript.

**Funding**

This research was funded by the Mecklenburg-Pomerania Excellence

Initiative (Germany) and European Social Fund (ESF) Grant Kolnfekt (ESF/14-BM-A55-0008/16 and ESF/14-BM-A55-0001/16).

**Conflicts of interest**

The authors declare no conflict of interest. The funders had no role in the design of the study; in the collection, analyses, or interpretation of data; in the writing of the manuscript, or in the decision to publish the results.

**Data availability**

The mass spectrometry proteomics data have been deposited to the ProteomeXchange Consortium (<http://proteomecentral.proteomexchange.org>) via the PRIDE partner repository [74] with the dataset identifier PXD025146. Data from the PRM-based validation measurements were deposited to the ProteomeXchange Consortium via Panorama Public and are available through the identifier PXD026625 or directly via the Panorama web service ([http://www.panoramaweb.org/16HBE\\_Co\\_infection.url](http://www.panoramaweb.org/16HBE_Co_infection.url)).

**Acknowledgments**

The authors want to acknowledge all partners of the collaborative project “Kolnfekt”. Furthermore, the authors thank Nicolas Stelling for supporting the cell culture experiments. We thank Elisa Teichmann for testing the TUBE enrichment protocols and Claudia Hirschfeld for revising the manuscript.

**Appendix A. Supplementary data**

Supplementary data to this article can be found online at <https://doi.org/10.1016/j.jprot.2021.104387>.

**References**

[1] W.H. Self, R.A. Balk, C.G. Grijalva, D.J. Williams, Y. Zhu, E.J. Anderson, G. W. Waterer, D.M. Courtney, A.M. Bramley, C. Trabue, S. Fakhran, A.J. Blaschke, S. Jain, K.M. Edwards, R.G. Wunderink, Procalcitonin as a marker of etiology in adults hospitalized with community-acquired pneumonia, *Clin. Infect. Dis.* 65 (2017) 183–190, <https://doi.org/10.1093/cid/cix317>.  
 [2] K. Cawcutt, A.C. Kalil, Pneumonia with bacterial and viral coinfection, *Curr. Opin. Crit. Care* 23 (2017) 385–390, <https://doi.org/10.1097/MCC.0000000000000435>.

- [3] J.C. Brealey, P.D. Sly, P.R. Young, K.J. Chappell, Viral bacterial co-infection of the respiratory tract during early childhood, *FEMS Microbiol. Lett.* 362 (2015), <https://doi.org/10.1093/femsle/fuv062>.
- [4] O. Ruuskanen, A. Järvinen, What is the real role of respiratory viruses in severe community-acquired pneumonia? *Clin. Infect. Dis.* 59 (2014) 71–73, <https://doi.org/10.1093/cid/ciu242>.
- [5] S. Hammerschmidt, Special issue on 'Microbe-host interactions', *FEBS Lett.* 590 (2016) 3703–3704, <https://doi.org/10.1002/1873-3468.12466>.
- [6] J.F. Brundage, Interactions between influenza and bacterial respiratory pathogens: implications for pandemic preparedness, *Lancet Infect. Dis.* 6 (2006) 303–312, [https://doi.org/10.1016/S1473-3099\(06\)70466-2](https://doi.org/10.1016/S1473-3099(06)70466-2).
- [7] D.M. Morens, J.K. Taubenberger, A.S. Fauci, Predominant role of bacterial pneumonia as a cause of death in pandemic influenza: implications for pandemic influenza preparedness, *J. Infect. Dis.* 198 (2008) 962–970, <https://doi.org/10.1086/591708>.
- [8] Y.-W. Chien, K.P. Klugman, D.M. Morens, Bacterial pathogens and death during the 1918 influenza pandemic, *N. Engl. J. Med.* 361 (2009) 2582–2583, <https://doi.org/10.1056/NEJMc0908216>.
- [9] G. Palacios, M. Hornig, D. Cisterna, N. Savji, A.V. Bussetti, V. Kapoor, J. Hui, R. Tokarz, T. Briese, E. Baumeister, W.I. Lipkin, *Streptococcus pneumoniae* coinfection is correlated with the severity of H1N1 pandemic influenza, *PLoS One* 4 (2009), e8540, <https://doi.org/10.1371/journal.pone.0008540>.
- [10] J.R. Gill, Z.-M. Sheng, S.F. Ely, D.G. Guinee, M.B. Beasley, J. Suh, C. Deshpande, D. J. Mollura, Pulmonary pathologic findings of fatal 2009 pandemic influenza A/H1N1 viral infections, *Arch. Pathol. Lab. Med.* 134 (2010) 235, <https://doi.org/10.5858/134.2.235>.
- [11] A.J. Kallen, J. Brunkard, Z. Moore, P. Budge, K.E. Arnold, G. Fosheim, L. Finelli, S. E. Beekmann, P.M. Polgreen, R. Gorwitz, J. Hageman, *Staphylococcus aureus* community-acquired pneumonia during the 2006 to 2007 influenza season, *Ann. Emerg. Med.* 53 (2009) 358–365, <https://doi.org/10.1016/j.annemergmed.2008.04.027>.
- [12] C.Y. Okumura, V. Nizet, Subterfuge and sabotage: evasion of host innate defenses by invasive gram-positive bacterial pathogens, *Annu. Rev. Microbiol.* 68 (2014) 439–458, <https://doi.org/10.1146/annurev-micro-092412-155711>.
- [13] J.A. McCullers, Insights into the interaction between influenza virus and pneumococcus, *Clin. Microbiol. Rev.* 19 (2006) 571–582, <https://doi.org/10.1128/CMR.00058.05>.
- [14] A. van Belkum, D.C. Melles, J. Nouwen, W.B. van Leeuwen, W. van Wamel, M. C. Vos, H.F. Wertheim, H.A. Verbrugh, Co-evolutionary aspects of human colonisation and infection by *Staphylococcus aureus*, *Infect. Genet. Evol.* 9 (2009) 32–47, <https://doi.org/10.1016/j.meegid.2008.09.012>.
- [15] R.G. Crystal, S.H. Randell, J.F. Engelhardt, J. Vovnoy, M.E. Sunday, Airway epithelial cells: current concepts and challenges, *Proc. Am. Thorac. Soc.* 5 (2008) 772–777, <https://doi.org/10.1513/pats.200805-041HR>.
- [16] P.S. Hiemstra, P.B. McCray, R. Bals, The innate immune function of airway epithelial cells in inflammatory lung disease, *Eur. Respir. J.* 45 (2015) 1150–1162, <https://doi.org/10.1183/09031936.00141514>.
- [17] M. Vareille, E. Kieninger, M.R. Edwards, N. Regamey, The airway epithelium: soldier in the fight against respiratory viruses, *Clin. Microbiol. Rev.* 24 (2011) 210–229, <https://doi.org/10.1128/CMR.00014-10>.
- [18] N. Sharma-Chavla, V. Sender, O. Kershaw, A.D. Gruber, J. Volckmar, B. Henriques-Normark, S. Stegemann-Koniszewski, D. Bruder, Influenza A virus infection predisposes hosts to secondary infection with different *Streptococcus pneumoniae* serotypes with similar outcome but serotype-specific manifestation, *Infect. Immun.* 84 (2016) 3445–3457, <https://doi.org/10.1128/IAI.00422.16>.
- [19] N. Siemens, S. Oehmcke-Hecht, T.C. Mettenleiter, B. Kreikemeyer, P. Valentin-Weigand, S. Hammerschmidt, Port d'Entrée for respiratory infections - does the influenza A virus pave the way for bacteria? *Front. Microbiol.* 8 (2017) 2602, <https://doi.org/10.3389/fmicb.2017.02602>.
- [20] M.E. Nickol, J. Ciric, S.D. Falcinelli, D.S. Chertow, J. Kindrachuk, Characterization of host and bacterial contributions to lung barrier dysfunction following co-infection with 2009 pandemic influenza and methicillin resistant *Staphylococcus aureus*, *Viruses* 11 (2019) 116, <https://doi.org/10.3390/v11020116>.
- [21] M. Akutsu, I. Dikic, A. Bremm, Ubiquitin chain diversity at a glance, *J. Cell Sci.* 129 (2016) 875–880, <https://doi.org/10.1242/jcs.183954>.
- [22] K.P. Bhat, S.F. Greer, Proteolytic and non-proteolytic roles of ubiquitin and the ubiquitin proteasome system in transcriptional regulation, *Biochim. Biophys. Acta (BBA) - Gene Regul. Mech.* 1809 (2011) 150–155, <https://doi.org/10.1016/j.bbagr.2010.11.006>.
- [23] C. Gómez-Díaz, F. Ikeda, Roles of ubiquitin in autophagy and cell death, *Semin. Cell Dev. Biol.* 93 (2019) 125–135, <https://doi.org/10.1016/j.semcdb.2018.09.004>.
- [24] J. Zinngrebe, A. Montinaro, N. Peltzer, H. Walczak, Ubiquitin in the immune system, *EMBO Rep.* 15 (2014) 322, <https://doi.org/10.1002/embr.201470030>.
- [25] G. Lopez-Gastejon, Control of the inflammasome by the ubiquitin system, *FEBS J.* 287 (2020) 11–26, <https://doi.org/10.1111/febs.15118>.
- [26] H. Hu, S.-C. Sun, Ubiquitin signaling in immune responses, *Cell Res.* 26 (2016) 457–483, <https://doi.org/10.1038/cr.2016.40>.
- [27] G. Courtis, M.-O. Fauvarque, The many roles of ubiquitin in NF- $\kappa$ B signaling, *Biomedicines* 6 (2018) 43, <https://doi.org/10.3390/biomedicines6020043>.
- [28] A. Neutznier, S. Li, S. Xu, M. Karbowski, The ubiquitin/proteasome system-dependent control of mitochondrial steps in apoptosis, *Semin. Cell Dev. Biol.* 23 (2012) 499–508, <https://doi.org/10.1016/j.semcdb.2012.03.019>.
- [29] Y. Yamauchi (Ed.), *Influenza A virus Uncoating*, 2020.
- [30] A. Rudnicka, Y. Yamauchi, Ubiquitin in influenza virus entry and innate immunity, *Viruses* 8 (2016) 293, <https://doi.org/10.3390/v8100293>.
- [31] T. Kubori, X.T. Bui, A. Hubber, H. Nagai, *Legionella* RavZ plays a role in preventing ubiquitin recruitment to bacteria-containing vacuoles, *Front. Cell. Infect. Microbiol.* 7 (2017) 384, <https://doi.org/10.3389/fcimb.2017.00384>.
- [32] T. Seissler, R. Marquet, J.C. Paillart, Hijacking of the ubiquitin/proteasome pathway by the HIV auxiliary proteins, *Viruses* 9 (2017) 322, <https://doi.org/10.3390/v9110322>.
- [33] R. Hjerpe, F. Aillet, F. Lopitz-Otsoa, V. Lang, P. England, M.S. Rodriguez, Efficient protection and isolation of ubiquitylated proteins using tandem ubiquitin binding entities, *EMBO Rep.* 10 (2009) 1250–1258, <https://doi.org/10.1038/embo.2009.192>.
- [34] N. Siemens, B. Chakraborty, S.M. Shambat, M. Morgan, H. Bergsten, O. Hyldegaard, S. Skrede, P. Arnell, M.B. Madsen, L. Johansson, J. Juarez, L. Bosnjak, M. Mörgelein, M. Svensson, A. Norrby-Teglund, Biofilm in group A streptococcal necrotizing soft tissue infections, *JCI Insight* 1 (2016), e87882, <https://doi.org/10.1172/jci.insight.87882>.
- [35] S. Mairpady Shambat, P. Chen, A.T. Nguyen Hoang, H. Bergsten, F. Vandenesch, N. Siemens, G. Lina, I.R. Monk, T.J. Foster, G. Arakere, M. Svensson, A. Norrby-Teglund, Modelling staphylococcal pneumonia in a human 3D lung tissue model system delineates toxin-mediated pathology, *Dis. Model. Mech.* 8 (2015) 1413–1425, <https://doi.org/10.1242/dmm.021923>.
- [36] A.J. Eisfeld, G. Neumann, Y. Kawaoka, Influenza A virus isolation, culture and identification, *Nat. Protoc.* 9 (2014) 2663–2681, <https://doi.org/10.1038/nprot.2014.180>.
- [37] J. Cox, M. Mann, MaxQuant enables high peptide identification rates, individualized p.p.b.-range mass accuracies and proteome-wide protein quantification, *Nat. Biotechnol.* 26 (2008) 1367–1372, <https://doi.org/10.1038/nbt.1511>.
- [38] S. Tyanova, T. Temu, J. Cox, The MaxQuant computational platform for mass spectrometry-based shotgun proteomics, *Nat. Protoc.* 11 (2016) 2301–2319, <https://doi.org/10.1038/nprot.2016.136>.
- [39] J. Cox, M.Y. Hein, C.A. Luber, I. Paron, N. Nagaraj, M. Mann, Accurate proteome-wide label-free quantification by delayed normalization and maximal peptide ratio extraction, termed MaxLFQ, *Mol. Cell. Proteomics* 13 (2014) 2513–2526, <https://doi.org/10.1074/mcp.M113.031591>.
- [40] S. Tyanova, T. Temu, P. Sinitcyn, A. Carlson, M.Y. Hein, T. Geiger, M. Mann, J. Cox, The Perseus computational platform for comprehensive analysis of (prote)omics data, *Nat. Methods* 13 (2016) 731–740, <https://doi.org/10.1038/nmeth.3901>.
- [41] D.W. Huang, B.T. Sherman, R.A. Lempicki, Bioinformatics enrichment tools: paths toward the comprehensive functional analysis of large gene lists, *Nucleic Acids Res.* 37 (2009) 1–13, <https://doi.org/10.1093/nar/gkn923>.
- [42] D.W. Huang, B.T. Sherman, R.A. Lempicki, Systematic and integrative analysis of large gene lists using DAVID bioinformatics resources, *Nat. Protoc.* 4 (2009) 44–57, <https://doi.org/10.1038/nprot.2008.211>.
- [43] RStudio Team, *RStudio: Integrated Development Environment for R*, Boston, MA, <http://www.rstudio.com/>, 2020.
- [44] D. Szklarczyk, A.L. Gable, D. Lyon, A. Junge, S. Wyder, J. Huerta-Cepas, M. Simonovic, N.T. Doncheva, J.H. Morris, P. Bork, L.J. Jensen, C. von Mering, STRING v11: protein-protein association networks with increased coverage, supporting functional discovery in genome-wide experimental datasets, *Nucleic Acids Res.* 47 (2019) D607–D613, <https://doi.org/10.1093/nar/gky1131>.
- [45] L.K. Pino, B.C. Searle, J.G. Bollinger, B. Nunn, B. MacLean, M.J. MacCoss, The skyline ecosystem: informatics for quantitative mass spectrometry proteomics, *Mass Spectrom. Rev.* 39 (2020) 229–244, <https://doi.org/10.1002/mas.21540>.
- [46] D. Schultz, S. Surabhi, N. Stelling, M. Rothe, K.S. Group, K. Methling, S. Hammerschmidt, N. Siemens, M. Lalk, 16HBE cell lipid mediator responses to mono and co-infections with respiratory pathogens, *Metabolites* 10 (2020) 113, <https://doi.org/10.3390/metabo10030113>.
- [47] T. Maculins, E. Fiskin, S. Bhogaraju, I. Dikic, Bacteria host relationship: ubiquitin ligases as weapons of invasion, *Cell Res.* 26 (2016) 499–510, <https://doi.org/10.1038/cr.2016.30>.
- [48] A. Guichard, V. Nizet, E. Bier, RAB11-mediated trafficking in host-pathogen interactions, *Nat. Rev. Microbiol.* 12 (2014) 624–634, <https://doi.org/10.1038/nrmicro3325>.
- [49] M.-P. Stein, M.P. Müller, A. Wandinger-Ness, Bacterial pathogens commandeering Rab GTPases to establish intracellular niches, *Traffic* 13 (2012) 1565–1588, <https://doi.org/10.1111/tra.12000>.
- [50] S. Spanò, J.E. Galán, Taking control: hijacking of Rab GTPases by intracellular bacterial pathogens, *Small GTPases* 9 (2018) 182–191, <https://doi.org/10.1080/21541248.2017.1336192>.
- [51] H. Sakaue, T. Shiota, N. Ishizaka, S. Kawano, Y. Tamura, K.S. Tan, K. Imai, C. Motono, T. Hirokawa, K. Taki, N. Miyata, O. Kuge, T. Lithgow, T. Endo, Porin Associates with Tom22 to regulate the mitochondrial protein gate assembly, *Mol. Cell* 73 (2019) 1044–1055, e8, <https://doi.org/10.1016/j.molcel.2019.01.003>.
- [52] M. Yano, N. Hoogenraad, K. Terada, M. Mori, Identification and functional analysis of human Tom22 for protein import into mitochondria, *Mol. Cell. Biol.* 20 (2000) 7205–7213, <https://doi.org/10.1128/MCB.20.19.7205-7213.2000>.
- [53] I. Derré, M. Pypaert, A. Dautry-Varsat, H. Agaisse, RNAi screen in *Drosophila* cells reveals the involvement of the Tom complex in Chlamydia infection, *PLoS Pathog.* 3 (2007) 1446–1458, <https://doi.org/10.1371/journal.ppat.0030155>.
- [54] L.Y. Lee, Y.J. Miyamoto, B.W. McIntyre, M. Höök, K.W. McCrea, D. McDevitt, E. L. Brown, The *Staphylococcus aureus* Map protein is an immunomodulator that interferes with T cell-mediated responses, *J. Clin. Invest.* 110 (2002) 1461–1471, <https://doi.org/10.1172/JCI16318>.
- [55] Y. Si, F. Zhao, P. Beesetty, D. Weiskopf, Z. Li, Q. Tian, M.-L. Alegre, A. Sette, A. S. Chong, C.P. Montgomery, Inhibition of protective immunity against

- Staphylococcus aureus* infection by MHC-restricted immunodominance is overcome by vaccination, *Sci. Adv.* 6 (2020), <https://doi.org/10.1126/sciadv.aaw7713> eaaw7713.
- [56] L.M. Palma Medina, A.-K. Becker, S. Michalik, H. Yedavally, E.J.M. Raineri, P. Hildebrandt, M. Gesell Salazar, K. Surmann, H. Pfortner, S.A. Mekonnen, A. Salvati, L. Kaderali, J.M. van Dijk, U. Völker, Metabolic cross-talk between human bronchial epithelial cells and internalized *Staphylococcus aureus* as a driver for infection, *Mol. Cell. Proteomics* 18 (2019) 892–908, <https://doi.org/10.1074/mcp.RA118.001138>.
- [57] P. Bellare, E.C. Small, X. Huang, J.A. Wohlschlegel, J.P. Staley, E.J. Sontheimer, A role for ubiquitin in the spliceosome assembly pathway, *Nat. Struct. Mol. Biol.* 15 (2008) 444–451, <https://doi.org/10.1038/nsmb.1401>.
- [58] J. Dubois, O. Terrier, M. Rosa-Calatrava, Influenza viruses and mRNA splicing: doing more with less, *MBio* 5 (2014), <https://doi.org/10.1128/mBio.00070.14> e00070-14.
- [59] C. van den Broeke, T. Jacob, H.W. Favoreel, Rho'ing in and out of cells: viral interactions with the GTPase signaling, *Small GTPases* 5 (2014), e28318, <https://doi.org/10.4161/sntp.28318>.
- [60] Q. Jiang, X. Zhou, L. Cheng, M. Li, The adhesion and invasion mechanisms of streptococci, *Curr. Issues Mol. Biol.* 32 (2019) 521–560, <https://doi.org/10.21775/cimb.032.521>.
- [61] N. Mai, Z.M.A. Chrzanowska Lightowlers, R.N. Lightowlers, The process of mammalian mitochondrial protein synthesis, *Cell Tissue Res.* 367 (2017) 5–20, <https://doi.org/10.1007/s00441-016-2456-0>.
- [62] D.-F. Suen, K.L. Norris, R.J. Youle, Mitochondrial dynamics and apoptosis, *Genes Dev.* 22 (2008) 1577–1590, <https://doi.org/10.1101/gad.1658508>.
- [63] J.A. Tsatsaronis, M.J. Walker, M.L. Sanderson-Smith, Host responses to group A streptococcus: cell death and inflammation, *PLoS Pathog.* 10 (2014), e1004266, <https://doi.org/10.1371/journal.ppat.1004266>.
- [64] C. Aikawa, T. Nozawa, F. Maruyama, K. Tsumoto, S. Hamada, I. Nakagawa, Reactive oxygen species induced by *Streptococcus pyogenes* invasion trigger apoptotic cell death in infected epithelial cells, *Cell. Microbiol.* 12 (2010) 814–830, <https://doi.org/10.1111/j.1462-5822.2010.01435.x>.
- [65] N. Tsao, C.-F. Kuo, M.-H. Cheng, W.-C. Lin, C.-F. Lin, Y.-S. Lin, Streptolysin S induces mitochondrial damage and macrophage death through inhibiting degradation of glycogen synthase kinase-3 $\beta$  in *Streptococcus pyogenes* infection, *Sci. Rep.* 9 (2019) 5371, <https://doi.org/10.1038/s41598-019-41853-3>.
- [66] C. Paget, F. Trottein, Mechanisms of bacterial superinfection post-influenza: a role for unconventional T cells, *Front. Immunol.* 10 (2019) 336, <https://doi.org/10.3389/fimmu.2019.00336>.
- [67] L. Jia, J. Zhao, C. Yang, Y. Liang, P. Long, X. Liu, S. Qiu, L. Wang, J. Xie, H. Li, H. Liu, W. Guo, S. Wang, P. Li, B. Zhu, R. Hao, H. Ma, Y. Jiang, H. Song, Severe pneumonia caused by coinfection with influenza virus followed by methicillin-resistant *Staphylococcus aureus* induces higher mortality in mice, *Front. Immunol.* 9 (2018) 3189, <https://doi.org/10.3389/fimmu.2018.03189>.
- [68] T.R. Borgogna, B. Hissey, E. Heitmann, J.J. Obar, N. Meissner, J.M. Voyich, Secondary bacterial pneumonia by *Staphylococcus aureus* following influenza A infection is SaeR/S dependent, *J. Infect. Dis.* 218 (2018) 809–813, <https://doi.org/10.1093/infdis/jiy210>.
- [69] C.-L. Small, C.R. Shaler, S. McCormick, M. Jeyanathan, D. Damjanovic, E.G. Brown, P. Arck, M. Jordana, C. Kaushic, A.A. Ashkar, Z. Xing, Influenza infection leads to increased susceptibility to subsequent bacterial superinfection by impairing NK cell responses in the lung, *J. I. 184* (2010) 2048–2056, <https://doi.org/10.4049/jimmunol.0902772>.
- [70] J.N. Weeks-Gorospe, H.R. Hurtig, A.R. Iverson, M.J. Schuneman, R.J. Webby, J. A. McCullers, V.C. Huber, Naturally occurring swine influenza A virus PB1-F2 phenotypes that contribute to superinfection with Gram-positive respiratory pathogens, *J. Virol.* 86 (2012) 9035–9043, <https://doi.org/10.1128/JVI.00369-12>.
- [71] S. Okamoto, S. Kawabata, Y. Terao, H. Fujitaka, Y. Okuno, S. Hamada, The *Streptococcus pyogenes* capsule is required for adhesion of bacteria to virus-infected alveolar epithelial cells and lethal bacterial-viral superinfection, *Infect. Immun.* 72 (2004) 6068–6075, <https://doi.org/10.1128/IAI.72.10.6068-6075.2004>.
- [72] S. Okamoto, S. Kawabata, I. Nakagawa, Y. Okuno, T. Goto, K. Sano, S. Hamada, Influenza A virus-infected hosts boost an invasive type of *Streptococcus pyogenes* infection in mice, *J. Virol.* 77 (2003) 4104–4112, <https://doi.org/10.1128/JVI.77.7.4104-4112.2003>.
- [73] N. Li, A. Ren, X. Wang, X. Fan, Y. Zhao, G.F. Gao, P. Cleary, B. Wang, Influenza viral neuraminidase primes bacterial coinfection through TGF  $\beta$ -mediated expression of host cell receptors, *Proc. Natl. Acad. Sci. U. S. A.* 112 (2015) 238–243, <https://doi.org/10.1073/pnas.1414422112>.
- [74] Y. Perez-Riverol, A. Csordas, J. Bai, M. Bernal-Llinares, S. Hewapathirana, D. J. Kundu, A. Inuganti, J. Griss, G. Mayer, M. Eisenacher, E. Pérez, J. Uszkoreit, J. Pfeuffer, T. Sachsenberg, S. Yilmaz, S. Tiwary, J. Cox, E. Audain, M. Walzer, A. F. Jarnuczak, T. Ternent, A. Brazma, J.A. Vizcaíno, The PRIDE database and related tools and resources in 2019: improving support for quantification data, *Nucleic Acids Res.* 47 (2019) D442–D450, <https://doi.org/10.1093/nar/gky1106>.

## Manuscript III

*Streptococcus pneumoniae* and influenza A virus co-infection induces altered polyubiquitination in A549 cells

Sura T, Gering V, Cammann C, Hammerschmidt S, Maaß S, Seifert U, Becher D.

Published in *Frontiers in Cellular and Infection Microbiology* 2022,  
DOI: 10.3389/fcimb.2022.817532

### Author contributions:

Conceptualization: TS, US, and DB. Formal analysis: TS. Funding acquisition: SH, US and DB. Methodology: TS and VG. Data analysis: TS. Writing—first draft: TS. Writing—review and editing: TS, VG, CC, SM, SH, US, and DB. All authors contributed to the article and approved the submitted version.

---

Thomas Sura

---

Prof. Dr. Dörte Becher





# Streptococcus pneumoniae and Influenza A Virus Co-Infection Induces Altered Polyubiquitination in A549 Cells

Thomas Sura<sup>1</sup>, Vanessa Gering<sup>2</sup>, Clemens Cammann<sup>2</sup>, Sven Hammerschmidt<sup>3</sup>, Sandra Maaß<sup>1</sup>, Ulrike Seifert<sup>2</sup> and Dörte Becher<sup>1\*</sup>

<sup>1</sup> Department of Microbial Proteomics, Institute of Microbiology, University of Greifswald, Greifswald, Germany, <sup>2</sup> Friedrich Loeffler-Institute of Medical Microbiology-Virology, University Medicine Greifswald, Greifswald, Germany, <sup>3</sup> Department of Molecular Genetics and Infection Biology, Interfaculty Institute for Genetics and Functional Genomics, University of Greifswald, Greifswald, Germany

## OPEN ACCESS

### Edited by:

Jason W. Rosch,  
St. Jude Children's Research Hospital,  
United States

### Reviewed by:

Hannah Rowe,  
Oregon State University, United States  
Tomoko Sumitomo,  
Osaka University, Japan

### \*Correspondence:

Dörte Becher  
dbecher@uni-greifswald.de

### Specialty section:

This article was submitted to  
Molecular Bacterial Pathogenesis,  
a section of the journal  
Frontiers in Cellular and  
Infection Microbiology

**Received:** 18 November 2021

**Accepted:** 25 January 2022

**Published:** 24 February 2022

### Citation:

Sura T, Gering V, Cammann C,  
Hammerschmidt S, Maaß S, Seifert U  
and Becher D (2022) Streptococcus  
pneumoniae and Influenza A Virus Co-  
Infection Induces Altered  
Polyubiquitination in A549 Cells.  
Front. Cell. Infect. Microbiol. 12:817532.  
doi: 10.3389/fcimb.2022.817532

Epithelial cells are an important line of defense within the lung. Disruption of the epithelial barrier by pathogens enables the systemic dissemination of bacteria or viruses within the host leading to severe diseases with fatal outcomes. Thus, the lung epithelium can be damaged by seasonal and pandemic influenza A viruses. Influenza A virus infection induced dysregulation of the immune system is beneficial for the dissemination of bacteria to the lower respiratory tract, causing bacterial and viral co-infection. Host cells regulate protein homeostasis and the response to different perturbances, for instance provoked by infections, by post translational modification of proteins. Aside from protein phosphorylation, ubiquitination of proteins is an essential regulatory tool in virtually every cellular process such as protein homeostasis, host immune response, cell morphology, and in clearing of cytosolic pathogens. Here, we analyzed the proteome and ubiquitinome of A549 alveolar lung epithelial cells in response to infection by either *Streptococcus pneumoniae* D39Δcps or influenza A virus H1N1 as well as bacterial and viral co-infection. Pneumococcal infection induced alterations in the ubiquitination of proteins involved in the organization of the actin cytoskeleton and Rho GTPases, but had minor effects on the abundance of host proteins. H1N1 infection results in an anti-viral state of A549 cells. Finally, co-infection resembled the imprints of both infecting pathogens with a minor increase in the observed alterations in protein and ubiquitination abundance.

**Keywords:** co-infection, ubiquitin, influenza A virus, *Streptococcus pneumoniae* D39, A549

## INTRODUCTION

Respiratory tract infections are among the most prevalent causes of death worldwide (Roth et al., 2018). These infections are mainly caused by influenza A virus (IAV), *Streptococcus pneumoniae* and other pathogens (Aliberti and Kaye, 2013; Troeger et al., 2019). Infections with IAV can cause dissemination of bacteria to the lower respiratory tract allowing viral and bacterial co-infection (Ruuskanen and Järvinen, 2014; Self et al., 2017). Thus, viral and bacterial co-infection is related to

increased mortality compared to single infections (Palacios et al., 2009; Hammerschmidt, 2016; Cawcutt and Kalil, 2017). Recently, it has been shown that co-infection occurs in seasonal and pandemic IAV infection in more than 30% of all cases (Brundage, 2006; Morens et al., 2008). The Gram-positive bacterium *S. pneumoniae* is mainly associated as secondary infection in IAV infected patients (Palacios et al., 2009). Influenza A virus infection can cause disruption of the epithelial barrier and impaired immune response causing bacterial spreading and reduced bacterial killing (Siemens et al., 2017). In the lung, epithelial cells act as an important line of defense and are involved in pathogen sensing and initiation of the host immune response (Vareille et al., 2011; Hiemstra et al., 2015). Among others, posttranslational modifications of proteins, like protein phosphorylation and ubiquitination, regulate processes within the host cell. Proteins can be modified with various types of ubiquitination like monoubiquitination and polyubiquitination. Ubiquitin, a protein of 76 amino acids, is covalently linked to the  $\epsilon$ -amine group of lysine residues in target proteins and thus, regulates their stability, localization or interaction properties. The function of ubiquitination depends on the length and linkage type of the ubiquitin chain. Furthermore, ubiquitin is involved in the regulation of immunity and clearance of intracellular pathogens (Bhat and Greer, 2011; Zinngrebe et al., 2014; Hu and Sun, 2016). It was demonstrated previously that bacterial and viral pathogens are able to manipulate the ubiquitin proteasome system (UPS) to evade the host defense. Moreover, host ubiquitin is misused by influenza A viruses to facilitate particle uncoating and transport within the host cell (Rudnicka and Yamauchi, 2016; Yamauchi, 2020). Here, we infected type 2 lung epithelial cells (A549) with a pandemic IAV, with *S. pneumoniae* D39 $\Delta$ cps, and conducted viral and bacterial co-infection to elaborate the effects of these infections on protein abundance and on protein ubiquitination. We enriched for K48 and K63 polyubiquitinated proteins, because these ubiquitin chains are the most dominant within the lung tissue, and applied label free LC-MS/MS based quantification. The results of this study contribute to the understanding of the ubiquitin mediated regulatory processes during viral and bacterial co-infection.

## MATERIALS AND METHODS

### Bacterial and Viral Strains

*Streptococcus pneumoniae* D39 $\Delta$ cps, a non-encapsulated mutant of D39 was described earlier (Saleh et al., 2013).

The pandemic influenza A/H1N1 virus [A/Germany-BY/74/2009(H1N1)] was kindly provided by the Institute of Immunology (FLI, Federal Research Institute for Animal Health) (Greifswald-Insel Riems, Germany).

### Cell Culture and Infections

A549 alveolar type 2 lung epithelial cells (ATCC CCL-185) were cultured in T75 flasks in RPMI medium (Invitrogen)

supplemented with 10% fetal calf serum (FCS) at 37°C in 5% CO<sub>2</sub> atmosphere. For infection experiments, cells were seeded into T75 flasks and grown to 80-90% confluence. 2 h before all infections the medium of A549 cells was exchanged by RPMI without FCS.

Bacteria were grown at 37°C in Todd Hewitt broth supplemented with 0.5% yeast extract (THY) to mid-exponential phase (OD<sub>600</sub> of 0.35-0.40). Pneumococci were washed and resuspended in PBS prior to infection. A549 cells were infected with *S. pneumoniae* D39 $\Delta$ cps at a MOI of 15 and were harvested 6 h post infection.

For viral infections, A549 cells were infected at a MOI of 5. After 2 h the medium was replaced by RPMI supplemented with 10% FCS and cells were harvested 24 hours post infection. Viral replication was confirmed *via* qRT-PCR (**Supplementary Figure S1**).

For co-infections, A549 cells were infected with IAV followed by bacterial infection. Cells were infected with IAV at a MOI of 5. After 2 h the medium was replaced by RPMI supplemented with 10% FCS and infected cells were cultured for additional 20 h at 37°C in 5% CO<sub>2</sub> atmosphere. Then, 2 h before bacterial infection, media was changed to RPMI without FCS. Hereafter, A549 cells were infected with *S. pneumoniae* D39 $\Delta$ cps (MOI 15) for 6 h.

At the end of the infection period cells were washed with PBS and cells were detached using trypsin and counted. Cell counts were determined by light microscopic quantification of cell viability. Cells were stained with 0.4% (v/v) trypan blue under serum-free conditions and visually examined.

All experiments were performed in triplicates (n=3).

### Interleukin ELISA

ELISA plates (Human IL-6/IL-8 Max Deluxe Set [BioLegend]) were coated with capture antibody and incubated for 16-18 h at 4°C. Plates were washed (PBS + 0.5% Tween-20). Hereafter, plates were blocked with blocking solution for 1 h with shaking at 200 rpm. Furthermore, standard series were prepared (IL-8: 1000 pg/ml – 15.6 pg/ml, IL-6: 500 pg/ml – 7.8 pg/ml). Non-specific bindings were blocked, blocking solution was removed and plates were washed. Standards and cell culture medium samples were added to the plates and incubated for 2 h with shaking. After the plates were washed, they were incubated with the detection antibody for 1 h. The detection antibody solution was removed and plates were washed. Avidin-HRP solution was added and incubated for 30 min with shaking. Avidin-HRP solution was removed and plates were washed. TMB substrate solution was added and incubated for 15 min in the dark. Stop solution (2 N H<sub>2</sub>SO<sub>4</sub>) was added and absorbance was measured at 450 nm and 570 nm within 15 min.

### Protein Extraction

Protein extraction was performed as described elsewhere (Sura et al., 2021). Briefly, harvested cells were resuspended in 1 ml lysis buffer (50 mM Tris HCl [pH 7.5], 0.15 M NaCl, 1 mM EDTA, 1% NP 40, 10% glycerol, 1x cOmplete Protease Inhibitor Cocktail [Roche], 1 mM PMSF, 10 mM N-ethylmaleimide, 20  $\mu$ M MG132), sonicated to shear DNA and cleared by



centrifugation. Protein concentration of the samples was determined by the BCA assay.

### Selective Enrichment of K48 and K63 Ubiquitinated Proteins

Lysates containing 500 µg of total protein were transferred into new tubes and filled to 300 µl with lysis buffer. To reduce unspecific binding of proteins to magnetic beads, 10 µl of magnetic control beads (LifeSensors) have been added to the samples and were incubated in an overhead shaker for 1 h at 10 rpm and 4°C. Afterwards, supernatants were transferred into new tubes. For the enrichment of K48 ubiquitinated proteins, 40 µl of K48 magnetic TUBE HF (LifeSensors), washed with Tris-buffered saline with Tween20 (TBS-T), were added, followed by an incubation for 3 h at 10 rpm and 4°C. To enrich K63 polyubiquitinated proteins, 700 µl water and K63 Flag-TUBE (LifeSensors) with a final concentration of 50 nM were added to the precleared sample and incubated for 2 h at 10 rpm and 4°C. Subsequently, 8 µl of magnetic anti-Flag beads were added and samples were incubated for additional 2 h. The unbound fraction of both enrichments was removed and the beads were washed three times with 500 µl TBS-T. To elute the enriched proteins, beads were resuspended in 25 µl SDS buffer (5% SDS; 50 mM TEAB; 5 mM TCEP) and incubated at 65°C for 45 min with 300 rpm shaking. Finally, the supernatants were transferred into new tubes.

### Proteolytic Digest

Extracted and enriched ubiquitinated proteins were digested by suspension trapping on micro S Traps (Protifi) as described elsewhere (Sura et al., 2021). Briefly, lysates containing 30 µg protein were transferred into new tubes and disulfide bonds were reduced by adding TCEP. Thiol groups were alkylated by adding iodoacetamide for proteome samples or chloroacetamide for ubiquitinome samples. Proteins were digested by adding 25 µl digestion buffer (50 mM TEAB) containing 1.2 µg trypsin for proteome samples and 600 ng trypsin (Promega) for ubiquitin enriched samples followed by an incubation for 3 h at 47°C. Peptides were subsequently eluted with 40 µl 50 mM TEAB; 0.1% acetic acid; 60% ACN in 0.1% acetic acid. All eluted fractions of a sample were pooled and dried in a vacuum concentrator. Dried peptides were stored at -80°C

### Peptide Fractionation

Peptides generated from crude protein extracts were fractionated by off-line high pH reversed phase chromatography as described elsewhere (Sura et al., 2021).

### LC-MS/MS Analysis

The peptide composition of the generated samples was analyzed by LC-MS/MS with an EASY-nLC 1000 (Thermo Fisher Scientific) coupled to a QExactive mass spectrometer (Thermo Fisher Scientific). Peptides were loaded onto in-house packed fused silica columns of 20 cm length and an inner diameter of 75 µm, filled with ReproSil Pur 120 C18-AQ 1.9 µm (Dr. Maisch). Peptides were subsequently eluted by a non-linear binary gradient of 165 min from 2% to 99% solvent B (0.1% acetic

acid in acetonitrile) in solvent A (0.1% acetic acid). Detailed information on the gradient and LC setup can be found in **Supplementary Table S1**. MS/MS data for the proteome and the K48 ubiquitin chain enriched samples were acquired as previously described (Sura et al., 2021). For the K63 ubiquitin chain enriched samples the mass spectrometer was operated in DDA mode. The survey scan was acquired from 300-1650 m/z with a resolution of 70,000 at 200 m/z. The 10 most abundant ions were selected for fragmentation *via* HCD with a normalized collision energy of NCE 27. The AGC target was set to 1E5 with an underfill ratio of 10% and a maximum injection time of 180 ms. MS/MS spectra were acquired in centroid mode with a resolution of 17,500 at 200 m/z. Ions with unassigned charge states as well as charge 1 and higher than 6 were excluded from fragmentation. Dynamic exclusion was set to 30 s and lock mass correction was enabled. Detailed information on the MS/MS acquisition parameters for all datasets are provided in **Supplementary Tables S2** and **S3**.

### Database Search

Datasets of enriched polyubiquitinated and total proteome samples were processed separately. Raw data were searched with MaxQuant (version 1.6.17.0) (Cox and Mann, 2008; Cox et al., 2014) against the UniProt databases for human (July 2019, UP000005640, 20,416 entries), Influenza A virus (A/Germany-BY/74/2009(H1N1)) (December 2017, UP000153067, 10 entries) and for *S. pneumoniae* D39 (September 2020, UP000001452, 1,915 entries). The maximum number of allowed missed cleavages was 2 and precursor mass tolerance was set to 4.5 ppm. Carbamidomethylation (C) was set as a fixed modification, oxidation (M) and acetylation (protein N-termini) were set as variable modifications for both datasets. GlyGly (K) was set as an additional variable modification for K48 and K63 ubiquitin chain enriched samples. Proteins were identified with at least two unique peptides, and peptide-spectrum match (PSM) and protein false discovery rate (FDR) were set to 0.01. Match between runs was applied and protein abundances were calculated by the MaxLFQ algorithm. A detailed table of applied parameters for database searching can be found in **Supplementary Tables S4** and **S5**.

### Data Analysis

Identified protein groups were analyzed with Perseus (version 1.6.15.0) (Tyanova et al., 2016; Tyanova and Cox, 2018). Only identified by site and reverse hits, as well as potential contaminations were removed. To assess differentially expressed proteins, a two tailed *t* test was applied for proteins with "LFQ intensity" values in three out of three replicates of the compared groups. Proteins were considered as differentially expressed with a *p* value < 0.05 and a fold change > 1.5. Quantification results and summary statistics can be found in **Supplementary Table S6**. Functional annotation enrichment of proteins with significantly changed abundance was performed with the Database for Annotation, Visualization and Integrated Discovery (DAVID v6.8) (Da Huang et al., 2009a; Da Huang et al., 2009b) and Reactome (Jassal et al., 2020). Protein interaction networks were created with STRING (v11.0)

(Szkłarczyk et al., 2019). Data were visualized using Inkscape (version 0.92.2) and RStudio (version 1.3.1073) with the packages ggplot2 (version 3.3.5), dplyr (version 1.0.6), EnhancedVolcano (version 1.4.0), splitstackshape (version 1.4.8), shadowtext (version 0.0.8) and ggpubr (version 0.4.0). Data variance was assessed by calculation of CVs from proteins with quantitative values in all three replicates (Supplementary Figure S2).

## RESULTS

To investigate the effect of bacterial or viral mono-infections and bacto-viral co-infections we infected A549 cells at a MOI that does not kill the majority of the A549 cells within the analyzed time frame. Also, we aimed to explore, whether the co-infection will be more severe to A549 cells than the infections with a single pathogen. Therefore, we analyzed the proteome and ubiquitinome of mono- and co-infected A549 cells.

### Cell Count and Interleukin Secretion

A549 cells were grown to 80%-90% confluence. Hereafter, cells were challenged either with the influenza A virus H1N1, *S. pneumoniae* D39Δcps, or both pathogens in a viral bacterial co-infection. After 24 h of viral infection the A549 cell count significantly increased by more than 25% (Supplementary Figure S3). This indicates that IAV propagation does not interfere with A549 proliferation within the observed time frame. In contrast, a 25% reduced cell count was observed after 6 h of *S. pneumoniae* infection. After co-infection the number of cells did not change compared to the uninfected control.

Cell culture supernatants of each infection were used to determine the levels of secreted immune modulating effectors. The average (n=3) level of IL-6 and IL-8 was increased after *S. pneumoniae* infection and bacto-viral co-infection (Supplementary Figure S4), but not after single viral infection. In detail, there is a difference in IL-6 and IL-8 levels when comparing the bacterial single infection or the co-infection with the corresponding mock infection. In contrast, there is no difference between the single H1N1 infection and the associated mock infection. Therefore, the H1N1 infection does not lead to an increased interleukin production.

### Differentially Abundant Proteins in Proteome and Ubiquitinome

For all experiments, the PSM FDR and the protein FDR have been set to 0.01. Proteins were considered as significantly changed in abundance, when they were quantified in all three replicates of the compared groups with a fold change greater than 1.5 and a *p*-value below 0.05. This, in total, resulted in the identification of more than 90,000 peptides, enabling quantification of more than 5,800 proteins for the proteome data set. In the proteome of A549 cells 74, 37 and 107 proteins were found to be significantly changed in abundance upon H1N1 infection, *S. pneumoniae* infection, and co-infection, respectively (Figure 1A). H1N1 infection induced the accumulation

of various proteins, whereas the *S. pneumoniae* infection mainly led to decreasing protein abundances. Moreover, different sets of proteins were effected by viral or bacterial infection. This is also reflected by the low overlap between these infections (Figure 1B).

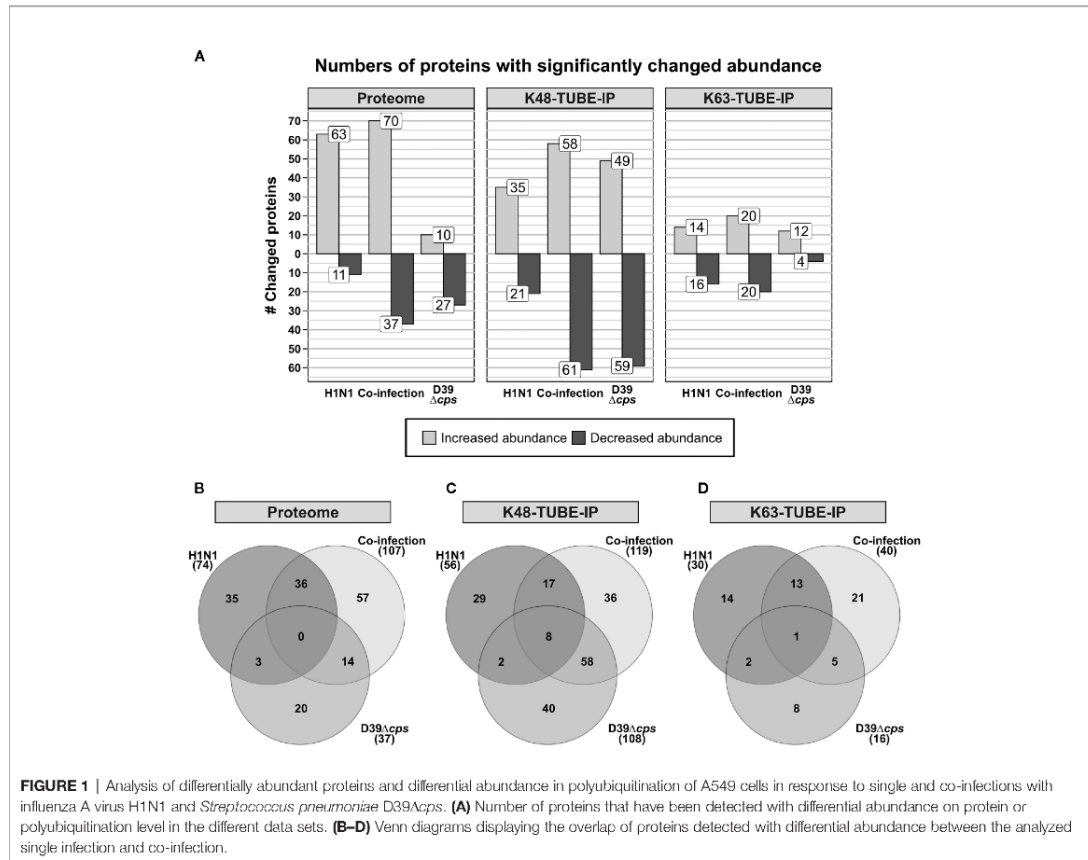
After enrichment of polyubiquitinated proteins we were able to identify more than 34,000 and 9,800 peptides, from the K48 and K63 enriched samples, respectively. This enabled the quantification of more than 2,800 proteins after K48 enrichment and more than 850 proteins in the K63 enriched data set (Figure 1A). In contrast to the proteome and K63 polyubiquitin enriched data sets, *S. pneumoniae* infection induced more changes than H1N1 infection in the K48 polyubiquitin enriched data set. Comparison of the proteins, which were differentially expressed upon viral and bacterial infection, revealed only a limited number of shared proteins between the single infections (Figures 1A, C, D). To elaborate whether altered abundance detected for proteins in the polyubiquitin enriched data sets originates from alterations in protein abundance in general, we examined the overlap of proteins that were detected with altered abundance in those data sets (Supplementary Figure S5). Whereas upon pneumococcal infection three proteins were detected with differential expression in the proteome and K48 enriched samples, 18 and 15 proteins were differentially expressed in the proteome and K48 enriched data set upon viral and co-infection, respectively (Supplementary Figure S5). This indicates that in most cases altered abundance in polyubiquitin enriched samples is independent of variations in the abundance of the respective proteins. Hence, differential abundance in polyubiquitin enriched data sets is caused by changing polyubiquitination incidence rather than by changing protein abundance. Volcano plots and MA plots, comparing the different conditions are shown in Supplementary Figures S6–S8.

### Functional Analysis of Proteins Differentially Expressed in the Total Proteome Samples

To get detailed insights into the processes driving the cellular response to the infecting pathogens, we used the Database for Annotation, Visualization and Integrated Discovery (DAVID) to perform annotation enrichment on proteins with significantly changed abundance.

Infected A549 cells with H1N1 significantly altered the abundance of 74 proteins within the proteome samples. The abundance of 63 proteins was increased and decreased for eleven proteins. Functional annotation enrichment revealed that *type I interferon*, *ISG* and other terms, which represent a response to viruses, were mainly enriched within proteins of increased abundance (Figure 2A). No terms have been enriched from proteins with reduced abundance (Figure 2A).

In the proteome of *S. pneumoniae* infected A549 cells only 37 proteins were detected with significantly altered abundance, among them we detected ten with increased abundance and 27 with decreased abundance. Here, the terms *oxidation-reduction process* (*p*-value = 0.00022) and *regulation of translation* (*p*-value =



0.0055) were enriched from proteins with reduced abundance. In contrast to the H1N1 infection, no terms were enriched from proteins with increased abundance.

Viral and bacterial co-infections of A549 cells mainly affected Gene Ontology Biological Process-terms (GOBP-terms) similar to those enriched in single infections. Proteins with increased abundance were annotated for GOBP terms *defense to virus*, *type I interferon signaling pathway* and *ISG15-protein conjugation*. The term *oxidation-reduction process* was enriched from proteins with decreased abundance (Figure 2B). In general, there is a reasonable quantity of proteins detected with the same regulation between the single infection and the co-infection (Figure 1B). Additionally, several proteins were quantified in the H1N1 and co-infection, but were missing in uninfected and *S. pneumoniae* infected samples. These proteins are MX1, MX2, IFI44, IFIT1, IFIT2, IFIT3 and IFI11, which are all involved in *type I interferon signaling* and viral defense.

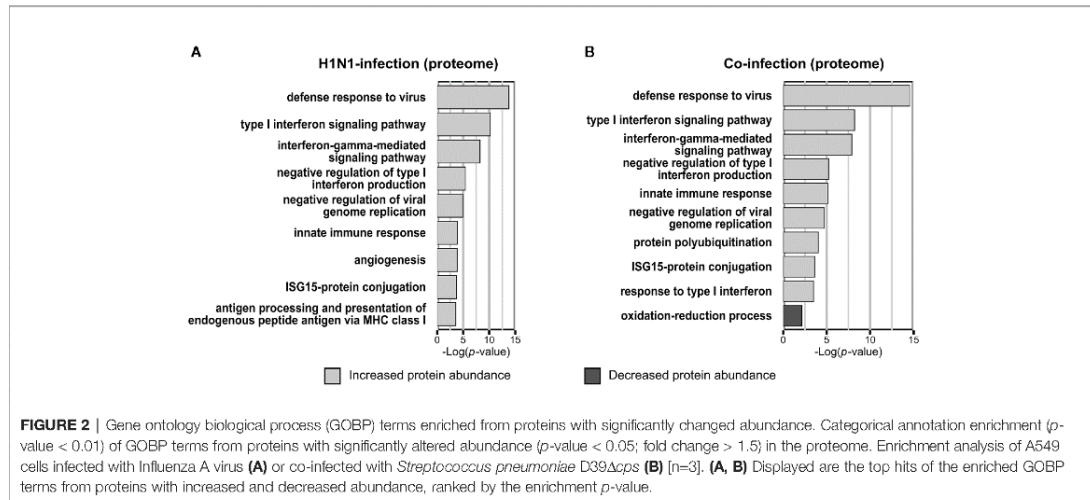
Furthermore, 17 proteins that are included in the integrated annotations for Ubiquitin and Ubiquitin-like Conjugation Database (iUUCD 2.0) (Zhou et al., 2018) and 2 proteins that are catalytically active subunits of the immunoproteasome as well as

the proteasome activator subunit beta (PA28beta) were detected with altered protein abundance upon infection (Table 1).

### Functional Analysis of Differentially Abundant Proteins in K48 Enriched Samples

As ubiquitination is involved in the regulation of nearly every cellular process, we selectively enriched for K48 and K63 polyubiquitinated proteins. It was demonstrated that K48 and K63 polyubiquitin chains are the most abundant chain types in murine primary macrophages and in murine lung tissue (Heunis et al., 2020). K48 ubiquitination has a variety of functions in the eukaryotic cell. Still, the primary function is to mark proteins for proteasomal degradation.

After 24 h of H1N1 infection, there were fewer changes in protein abundance detected in K48 enriched samples compared to total proteome samples. GOBP terms that were most significantly overrepresented from proteins with increased abundance in the K48 enriched samples were *defense response to virus*, *type I interferon signaling pathway* and *negative*



regulation of viral genome replication, while RNA splicing was most significantly overrepresented from proteins with decreased abundance.

Upon *S. pneumoniae* infection we detected altered abundance of 108 putatively K48 polyubiquitinated proteins. Fifty-nine proteins were quantified with decreased abundance and 49 with increased abundance after infection. Only three out of 37 proteins detected with differential expression in the proteome samples were detected with altered abundance in the K48 polyubiquitin enrichment. Proteins with decreased abundance in K48 polyubiquitination mostly affected processes involved in

mRNA splicing and rRNA processing. Arp2/3 complex mediated actin nucleation and other processes related to actin filament organization were highly overrepresented by proteins with increased K48 polyubiquitination. In addition to actin filament related processes, FC-gamma receptor signaling pathway involved in phagocytosis was enriched from proteins with increased K48 polyubiquitination, as well.

In the viral and bacterial co-infection the pattern of proteins with significantly changed abundance after K48 enrichment is similar to both of the single infections. Moreover, the co-infection shares ~50% and ~15% of differentially expressed

**TABLE 1 |** List of proteins that were detected with differential abundance upon infection and are listed in the iUUCD 2.0 database or related to the immunoproteasome and proteasome regulation (highlighted with an asterisk).

Protein	iUUCD 2.0		fold change		
	family	ID	H1N1	Co-infection	D39
TMF1	E3 adaptor	IUUC-Hsa-046889	1.09	<b>-1.81</b>	-1.33
CIAO1	E3 adaptor	IUUC-Hsa-046528	–	<b>-1.79</b>	-1.43
CORO7	E3 adaptor	IUUC-Hsa-045847	1.43	<b>1.93</b>	<b>1.94</b>
MNAT1	E3	IUUC-Hsa-045876	<b>1.58</b>	1.34	1.19
RBCK1	E3	IUUC-Hsa-045738	<b>1.66</b>	1.77	-1.45
IRF2BPL	E3	IUUC-Hsa-046942	1.16	1.51	1.13
TRIM56	E3	IUUC-Hsa-046238	<b>1.59</b>	<b>1.55</b>	1.08
TRIM25	E3	IUUC-Hsa-045828	<b>1.67</b>	<b>1.58</b>	1.03
RNF213	E3	IUUC-Hsa-046140	<b>1.64</b>	<b>1.99</b>	-1.10
RNF121	E3	IUUC-Hsa-046468	–	1.53	<b>1.57</b>
PML	E3	IUUC-Hsa-045861	<b>3.57</b>	<b>4.19</b>	1.08
TRIM21	E3	IUUC-Hsa-046583	<b>5.17</b>	<b>4.62</b>	-1.44
DTX3L	E3	IUUC-Hsa-045921	<b>19.49</b>	<b>18.17</b>	-1.10
HERC5	E3	IUUC-Hsa-046342	<b>12.21</b>	<b>28.65</b>	–
UBE2T	E2	IUUC-Hsa-046513	1.31	-1.41	<b>-1.54</b>
UBE2E1	E2	IUUC-Hsa-046576	1.04	-1.95	<b>-1.53</b>
UBE2L6	E2	IUUC-Hsa-045943	<b>5.23</b>	<b>7.72</b>	<b>1.33</b>
PSME2*	–	–	1.27	<b>1.53</b>	1.15
PSMB9*	–	–	1.67	<b>1.95</b>	-1.11
PSMB8*	–	–	<b>1.76</b>	<b>2.34</b>	-1.02

The fold change upon each infection is given and highlighted in bold if the detected change is statistically significant (students t-test;  $p$ -value  $< 0.05$ ; fold change  $> 1.5$ ;  $n=3$ ).

proteins with the bacterial and the viral infection, respectively (Figure 1C). Proteins that were shared between the single infections change their abundance into the same direction. Although the STRING network, which was generated from the co-infection (Figure 3B) data, has a high similarity to the network generated from the bacterial infection (Figure 3A), it also contains a cluster of proteins that has been detected upon viral infection (*response to virus*) (Figure 3B). Furthermore, eight proteins were found to be changed significantly in all infections and three of them are related to *RNA splicing* (Figure 1C). Ten proteins were only quantified in the viral and in co-infection samples. These proteins affect the processes of *response to virus*, *type I interferon signaling pathway* and *interferon-gamma-mediated signaling pathway*.

### Functional Analysis of Differentially Abundant Proteins in K63 Enriched Samples

In contrast to K48 polyubiquitination, K63 polyubiquitin chains are thought to mediate non-proteasomal signals for endocytosis and immune responses. The K63 enriched data set displays the lowest number of quantified proteins within the three data sets obtained in this work. Accordingly, the K63 data set reveals fewer proteins detected with altered abundance. H1N1 infection induced variations in the K63 polyubiquitination level of 30 proteins. Proteins with reduced K63 ubiquitination affect *mRNA splicing* processes and proteins with increased K63 ubiquitination affect *redox* processes. Changes induced by the *S. pneumoniae* infection do not affect multiple pathways, only *negative regulation of mitochondrial outer membrane permeabilization involved in apoptotic signaling pathway* is affected by proteins with increased K63 polyubiquitination. Co-infection most significantly affected processes involved in *mRNA processing* from proteins with decreased polyubiquitination.

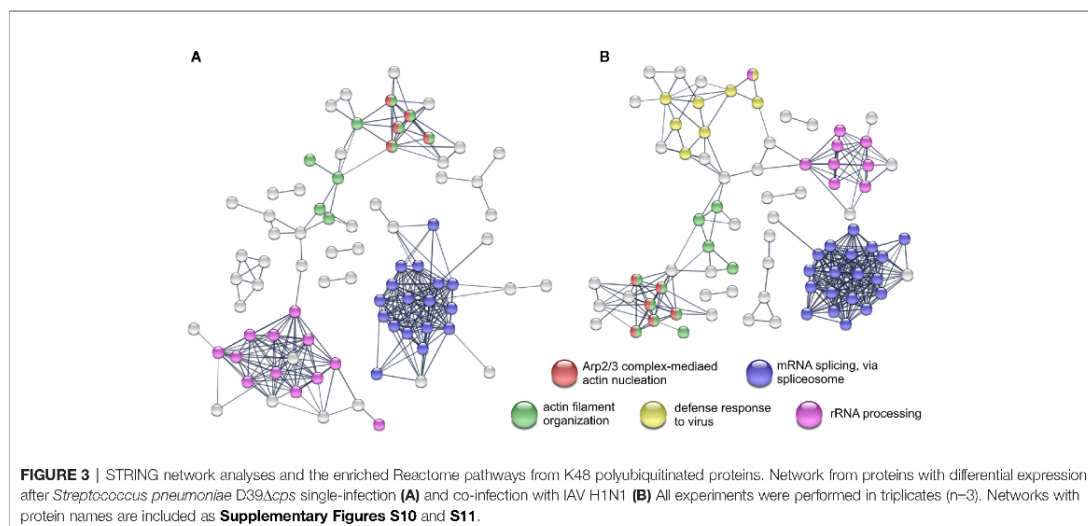
Proteins with increased polyubiquitination affected *redox* processes and *response to ER stress*.

## DISCUSSION

In the work presented, we used *in vitro* cell culture based infection experiments to examine potential synergistic effects of the infecting pathogens in viral and bacterial co-infections on human lung epithelial cells. Therefore, we analyzed viral and bacterial mono-infections, along with bacto-viral co-infections of A549 cells, focusing on the proteome, as well as the selective enrichment of polyubiquitinated proteins. Infecting A549 cells with H1N1 for 24 h induced a pronounced immune response and viral defense of the host. The additional bacterial infection was performed at MOI 15 to be able to elaborate a potential synergisms of the pathogens.

### Response to IAV H1N1 Infection

Influenza H1N1 infection induced a strong viral defense response of the A549 cells. This was established by the induction of the JAK-STAT cascade, type I interferon signaling, interferon  $\gamma$  signaling and induction of the ISG15 protein conjugation. Induction of the type I interferon production mediated by RIG-I and MAVS, which leads to the induction of a wide array of genes, can be assumed from increased protein abundance of interferon stimulated genes (Schoggins et al., 2011; Zhang et al., 2020). In addition, we detected a 25 fold increase in the abundance of DDX60 which was shown to be required for RIG-I mediated type I interferon expression after viral infection (Miyashita et al., 2011). From the proteins with higher abundance after viral infection, nine show E3 ligase activity and one protein is described as an E2 enzyme (Zhou et al., 2018) (Table 1). Among these proteins are HERC5 and TRIM25, both acting as E3 ligating enzymes for ISG15



(Wong et al., 2006; Mathieu et al., 2021), which increased twelve and five times in abundance in our experiments, respectively. UBE2L6, the ISG15 E2 transferring enzyme, was detected to be fivefold more abundant after viral infection. These results are in concordance with previously published data where an up-regulation of UPS genes in response to Interferon-stimulation was detected (Seifert et al., 2010). This, together with the increased abundance of the transcription factor IRF9, which induces the transcription of interferon stimulated genes (ISG) when forming a complex with STAT1 and STAT2, underpins the interferon mediated activation of the JAK-STAT pathway. OAS1-3 are degraders of viral RNA (Shim et al., 2017) and were also detected with increased abundance after viral infection. Moreover, increased protein abundance of the ubiquitin E3 ligase DTX3L and the interacting protein PARP9 as well as of PARP10, 12 and 14 was observed in IAV infected A549 cells. These results confirm the findings on increased protein abundances of PARP9 and PARP14 upon viral infection, first observed by Becker and colleagues (Becker et al., 2018). We were able to confirm these results using a different influenza strain, but the same cell line. It is reported by others that the outcome of the IAV infection depends not only on the MOI and the duration of the infection, but also on the cell line, as well as the employed viral stain (Becker et al., 2018; Wu et al., 2019). Influenza virus infection predispose the host cell to secondary bacterial infections, which was shown from mice and *in vitro* experiments (Sharma-Chawla et al., 2016; Bai et al., 2021). Bai and coworkers demonstrated that viral infection induced an increase in the abundance of PPIA, which interacts and mediates protection from proteasomal degradation of PTK2. Ultimately, this results in increased integrin  $\alpha 5$  expression and actin rearrangement, which renders the host cell more susceptible for secondary bacterial infection (Bai et al., 2021). In contrast, we have not detected significant changes in the abundance of PPIA and integrin- $\alpha 5$  in the proteome nor in the abundance of PTK2 in the proteome and K48 enriched data set. These differences in the outcome of the viral infection can potentially be caused by several reasons. First, observed differences were caused by the use of different influenza strains. The second reason can be the infection duration and the MOI at which the experiments were conducted. Bai et al. showed that the mRNA level of PPIA reached its maximum at 12 hpi and decreased afterwards (Bai et al., 2021). The use of a higher MOI may result in a shifted maximal mRNA level and CypA expression. The reason causing the observed differences remains unclear. We can exclude the cell line as a cause, as we used A549, too. In addition, Becker et al. have not observed changes in the protein abundance of CypA or ITGA5 after IAV infection of A549 cells, as well (Becker et al., 2018).

### Response to *Streptococcus pneumoniae* Infection

The pneumococcal infection induced differential abundance of 37 proteins. Furthermore, we detected 108 and 16 proteins with significantly altered abundance in K48 and K63 polyubiquitination, respectively.

The protein that showed the most prominent increase in abundance (about four fold) was PTGS2 or COX-2, being an inducible protein involved in the initial step of prostaglandin synthesis. In type II alveolar epithelial cells the induction of the COX-2 expression in response to pneumococci is controlled in a p38 MAPK and NF $\kappa$ B dependent manner (N'Guessan et al., 2006; Szymanski et al., 2012). Bootsma and colleagues also observed an induction of COX-2 by the  $\Delta$ cps mutant of *S. pneumoniae* analyzing the transcriptional response of Detroit 562 pharyngeal epithelial cells to the adherence of different pneumococcal strains (Bootsma et al., 2007). They have shown that *S. pneumoniae* D39 and its isogenic  $\Delta$ cps mutant alter the expression of different gene sets. Infection with the  $\Delta$ cps mutant changed the expression of 156 genes (28 upregulated and 128 downregulated) (Bootsma et al., 2007). Given the fact that Detroit 562 cells are of pharyngeal origin and A549 cells are lung epithelial cells, the published results cannot be entirely transferred to our study. Nevertheless, Bootsma et al. also observed an increase in IL-6 and IL-8 levels upon *S. pneumoniae* D39 $\Delta$ cps infection (Bootsma et al., 2007) (**Supplementary Figure S4**).

Bacterial pathogens such as *S. pneumoniae* use different strategies like transmigration or transcytosis to cross epithelial or endothelial barriers of the host. Pneumococcal uptake by A549 cells is low, however, A549 cells show increased uptake of *S. pneumoniae* D39 $\Delta$ cps compared to the wild type strain (Talbot et al., 1996; Bootsma et al., 2007). Still, it was shown that pneumococcal phosphorylcholine mimics the natural ligand of PAFr initiating bacterial uptake in a  $\beta$ -arrestin dependent manner (Radin et al., 2005; Bertuzzi et al., 2019). Pneumococcal endocytosis is clathrin and caveolae mediated and the vast majority of endocytosed pneumococci is killed by lysosomal fusion of the endosome (Gradstedt et al., 2013). Pneumolysin, a cholesterol-dependent cytolysin expressed on the pneumococcal surface and released by autolysis, disables the acidification of the endosome by the formation of pores in the endosomal membrane (Barnett et al., 2015; Ogawa et al., 2018). The ubiquitin-proteasome system (UPS) is involved in the autophagosomal entrapment and killing of cytosolic pneumococci (Iovino et al., 2014; Ogawa et al., 2018). Additionally, pneumolysin directly interacts with actin and activates small GTPases leading to remodeling of the actin network (Hupp et al., 2013). Rho GTPases act upstream of the Arp2/3 complex, which facilitate actin nucleation and is involved in clathrin-mediated endocytosis and phagocytosis (Sirotkin, 2011; Sumida and Yamada, 2015; Jin et al., 2021). In our study, we observed increased abundance in K48 polyubiquitination of proteins belonging to the Arp2/3 complex and other actin and cytoskeleton organization related GO terms (**Figure 3A**). Moreover, the Reactome analysis revealed that Rho-GTPase signaling is affected by proteins with increased K48 polyubiquitination, as well. Thereby, polyubiquitination bridges the host proteome and ubiquitinome in response to pneumococcal infection. These results are not in contrast to the finding that *S. pneumoniae* D39 effectively overcomes the epithelial barrier by transmigration (Attali et al., 2008). We have not observed any changes in the abundance of junction proteins as it was described

by Peter and colleagues (Peter et al., 2017). This could be due to the use of a single cell line and no lung tissue.

In our K48 polyubiquitin analysis we detected reduced polyubiquitination in proteins involved in mRNA splicing and rRNA processing. Proteins involved in mRNA splicing mainly belong to the spliceosomal E complex. Changes in the spliceosome composition may indicate an early apoptotic state of the epithelial cells, linking the spliceosome and apoptosis (Schwerk and Schulze-Osthoff, 2005). It remains unclear what causes these effects upon pneumococcal infection and is a subject of future studies.

In addition to the K48 polyubiquitin analysis, Reactome analysis of proteins with altered abundance in K63 polyubiquitination also indicated involvement of the Rho-GTPase cycle, whereas the functional annotation enrichment analysis of K63 polyubiquitinated proteins showed only *negative regulation of mitochondrial outer membrane permeabilization involved in apoptotic signaling pathway* as an overrepresented GOBP term.

### Viral and Bacterial Co-Infection

Bacterial and viral co-infections are related to increased severity of disease, increased morbidity and mortality (Siemens et al., 2017; Lim et al., 2019). Influenza A virus infection, caused by pandemic or seasonal strains, predispose the host to secondary bacterial infections (Sharma-Chawla et al., 2016; Siemens et al., 2017; LeMessurier et al., 2020). In our experiments we could not observe an increased cytotoxicity of the co-infection compared to bacterial or viral single infection (**Supplementary Figure S3**). Following the co-infection we observed similar IL6 and IL8 level compared to the bacterial single infection (**Supplementary Figure S4**). Unexpectedly, preceding viral infection reduced pneumococcal adherence to A549 epithelial cells in our experimental setup (**Supplementary Figure S9**). Still, viral and bacterial co-infection resulted in the highest number of proteins with significantly altered abundance on protein and polyubiquitination level. Interestingly, we did not detect over representation of pathways that have not been identified upon one of the two single infections. For all obtained data sets the pathways affected by co-infection resembles both of the single infections. This is in congruence with a previous study where we reported additive effects of IAV H1N1 and *Streptococcus pyogenes* co-infection of 16HBE cells (Sura et al., 2021). Nevertheless, here we have detected enhanced alteration of protein abundance and polyubiquitination incidence upon co-infection. This effect on protein abundance was also noticed for PSMB8, PSMB9 and for PSME2 (**Table 1**). These proteins are immunoproteasome subunits and proteasome activator PA28beta and are involved in altered generation of MHC I antigenic peptides presented to CD8 T-cells (Keller et al., 2015; McCarthy and Weinberg, 2015). The further increase in protein abundance upon co-infection might be induced by enhanced IFN- $\gamma$  production caused by the bacterial superinfection as it was reported by Strehlitz and coworkers from mice experiments (Strehlitz et al., 2018). Upon co-infection higher numbers of proteins with significantly altered abundance were detected in all data sets when compared to the single infections. Still, these

observations are not reflected by an increased cytotoxicity of the viral bacterial co-infection.

In the presented study we used *S. pneumoniae* D39 $\Delta$ cps, an isogenic mutant that lacks the capsular polysaccharides. Thus, the outcome of the study and the observed alterations in the proteome and the ubiquitinome were potentially influenced by the absence of capsular polysaccharides. However, the interaction between A549 cells and the pneumococci is mainly based on bacterial adherence to the cell surface (Agarwal et al., 2010). It has been shown that the intimate contact of pneumococci with host cells is associated with a reduction of CPS (Hammerschmidt et al., 2005). While encapsulated wild-type pneumococci interact only moderately with non-professional host cells under *in vitro* conditions, binding can be enhanced using isogenic non-encapsulated mutants. Thereby, the induced signal transduction cascades can be elucidated and the host responses analyzed. Although this is not related to the pathophysiological conditions under *in vivo* conditions, important discoveries were made in the last decades using this combination of bacteria and host cells.

Importantly, we chose a MOI of only 15 bacteria per host cell to reduce the level of host cell damage caused by pneumolysin and hydrogen peroxide to a minimum in the bacterial single infections and co-infections. In *in vivo* studies higher bacterial infection doses are applied to study the effects in experimental acute pneumonia or septicemia infection models.

In *in vivo* experiments, co-infection appears to be adverse for the host, caused by the IAV induced expression of type I interferons suppressing the bacterial clearance by disturbed recruitment of immune cells (LeMessurier et al., 2020; Park et al., 2021). On the other hand, type I interferons increase the expression of tight junction proteins and decrease the expression of PAFr, reducing pneumococcal uptake and hindering transmigration (LeMessurier et al., 2013). The *in vitro* study presented here is based on A549 cells grown as a monolayer. Due to the lack of immune cells and their interaction with the epithelial barrier in our setup, this adverse effect was probably not observed. Furthermore, A549 cells grown as a monolayer do not form tight junctions (Carterson et al., 2005). The scarcity of tight junctions might explain the fact that we did not observe changes in the expression of tight junction proteins, whether induced by type I interferons, or by pneumococcal infection, as it was observed in lung tissue (LeMessurier et al., 2013; Peter et al., 2017).

It can be concluded that IAV and *S. pneumoniae* D39 $\Delta$ cps co-infection of monolayer grown A549 cells shows additive, but in the current setup no observable synergistic effects. It would be interesting to investigate whether this changes in polarized, 3D grown A549 cells and to determine the impact of the pneumococcal virulence factor pneumolysin.

### DATA AVAILABILITY STATEMENT

The mass spectrometry proteomics data have been deposited to the ProteomeXchange Consortium (<http://proteomecentral.proteomexchange.org>) via the PRIDE (Perez-



Riverol et al., 2019) partner repository with the dataset identifier PXD028465.

## AUTHOR CONTRIBUTIONS

Conceptualization: TS, US, and DB. Formal analysis: TS. Funding acquisition: SH, US and DB. Methodology: TS and VG. Data analysis: TS. Writing—first draft: TS. Writing—review and editing: TS, VG, CC, SM, SH, US, and DB. All authors contributed to the article and approved the submitted version.

## FUNDING

This research was funded by the Mecklenburg-Pomerania Excellence Initiative (Germany), the European Social Fund (ESF) Grant KoInfekt (ESF/14-BM-A55-0008/16 and ESF/14-

## REFERENCES

- Agarwal, V., Asmat, T. M., Luo, S., Jensch, I., Zipfel, P. F., and Hammerschmidt, S. (2010). Complement Regulator Factor H Mediates a Two-Step Uptake of *Streptococcus Pneumoniae* by Human Cells. *J. Biol. Chem.* 285, 23486–23495. doi: 10.1074/jbc.M110.142703
- Aliberti, S., and Kaye, K. S. (2013). The Changing Microbiologic Epidemiology of Community-Acquired Pneumonia. *Postgrad. Med.* 125, 31–42. doi: 10.3810/pgm.2013.11.2710
- Attali, C., Durmort, C., Vernet, T., and Di Guilmi, A. M. (2008). The Interaction of *Streptococcus Pneumoniae* With Plasmin Mediates Transmigration Across Endothelial and Epithelial Monolayers by Intercellular Junction Cleavage. *Infect. Immun.* 76, 5350–5356. doi: 10.1128/IAI.00184-08
- Bai, X., Yang, W., Luan, X., Li, H., Li, H., Tian, D., et al. (2021). Induction of Cyclophilin A by Influenza A Virus Infection Facilitates Group A *Streptococcus* Coinfection. *Cell Rep.* 35, 109159. doi: 10.1016/j.celrep.2021.109159
- Barnett, T. C., Cole, J. N., Rivera-Hernandez, T., Henningham, A., Paton, J. C., Nizet, V., et al. (2015). Streptococcal Toxins: Role in Pathogenesis and Disease. *Cell Microbiol.* 17, 1721–1741. doi: 10.1111/cmi.12531
- Becker, A. C., Gannagé, M., Giese, S., Hu, Z., Abou-Eid, S., Roubaty, C., et al. (2018). Influenza A Virus Induces Autophagosomal Targeting of Ribosomal Proteins. *Mol. Cell Proteomics* 17, 1909–1921. doi: 10.1074/mcp.RA117.000364
- Bertuzzi, M., Hayes, G. E., and Bignell, E. M. (2019). Microbial Uptake by the Respiratory Epithelium: Outcomes for Host and Pathogen. *FEMS Microbiol. Rev.* 43, 145–161. doi: 10.1093/femsre/fuy045
- Bhat, K. P., and Greer, S. F. (2011). Proteolytic and non-Proteolytic Roles of Ubiquitin and the Ubiquitin Proteasome System in Transcriptional Regulation. *Biochim. Biophys. Acta* 1809, 150–155. doi: 10.1016/j.bbagr.2010.11.006
- Bootsma, H. J., Egmont-Petersen, M., and Hermans, P. W. M. (2007). Analysis of the *In Vitro* Transcriptional Response of Human Pharyngeal Epithelial Cells to Adherent *Streptococcus Pneumoniae*: Evidence for a Distinct Response to Encapsulated Strains. *Infect. Immun.* 75, 5489–5499. doi: 10.1128/IAI.01823-06
- Brundage, J. F. (2006). Interactions Between Influenza and Bacterial Respiratory Pathogens: Implications for Pandemic Preparedness. *Lancet Infect. Dis.* 6, 303–312. doi: 10.1016/S1473-3099(06)70466-2
- Carterson, A. J., Höner zu Bentrup, K., Ott, C. M., Clarke, M. S., Pierson, D. L., Vanderburg, C. R., et al. (2005). A549 Lung Epithelial Cells Grown as Three-Dimensional Aggregates: Alternative Tissue Culture Model for *Pseudomonas Aeruginosa* Pathogenesis. *Infect. Immun.* 73, 1129–1140. doi: 10.1128/IAI.73.2.1129-1140.2005
- Cawcutt, K., and Kalil, A. C. (2017). Pneumonia With Bacterial and Viral Coinfection. *Curr. Opin. Crit. Care* 23, 385–390. doi: 10.1097/MCC.0000000000000435
- BM-A55-0009/16), and the Helmholtz Institute (ZoonFlu). We acknowledge support for the Article Processing Charge from the German Research Foundation and the Open Access Publication Fund of the University of Greifswald.

## ACKNOWLEDGMENTS

The authors want to acknowledge all partners of the collaborative project “KoInfekt”. Furthermore, the authors thank Claudia Hirschfeld for revising the manuscript.

## SUPPLEMENTARY MATERIAL

The Supplementary Material for this article can be found online at: <https://www.frontiersin.org/articles/10.3389/fcimb.2022.817532/full#supplementary-material>

- Cox, J., Hein, M. Y., Luber, C. A., Paron, I., Nagaraj, N., and Mann, M. (2014). Accurate Proteome-Wide Label-Free Quantification by Delayed Normalization and Maximal Peptide Ratio Extraction, Termed MaxLFQ. *Mol. Cell Proteomics* 13, 2513–2526. doi: 10.1074/mcp.M113.031591
- Cox, J., and Mann, M. (2008). MaxQuant Enables High Peptide Identification Rates, Individualized P.P.B.-Range Mass Accuracies and Proteome-Wide Protein Quantification. *Nat. Biotechnol.* 26, 1367–1372. doi: 10.1038/nbt.1511
- Da Huang, W., Sherman, B. T., and Lempicki, R. A. (2009a). Bioinformatics Enrichment Tools: Paths Toward the Comprehensive Functional Analysis of Large Gene Lists. *Nucleic Acids Res.* 37, 1–13. doi: 10.1093/nar/gkn923
- Da Huang, W., Sherman, B. T., and Lempicki, R. A. (2009b). Systematic and Integrative Analysis of Large Gene Lists Using DAVID Bioinformatics Resources. *Nat. Protoc.* 4, 44–57. doi: 10.1038/nprot.2008.211
- Gradstedt, H., Iovino, F., and Bijlsma, J. J. E. (2013). *Streptococcus Pneumoniae* Invades Endothelial Host Cells via Multiple Pathways and Is Killed in a Lysosome Dependent Manner. *PLoS One* 8, e65626. doi: 10.1371/journal.pone.0065626
- Hammerschmidt, S. (2016). Special Issue on ‘Microbe-Host Interactions’. *FEBS Lett.* 590, 3703–3704. doi: 10.1002/1873-3468.12466
- Hammerschmidt, S., Wolff, S., Hocke, A., Rosseau, S., Müller, E., and Rohde, M. (2005). Illustration of Pneumococcal Polysaccharide Capsule During Adherence and Invasion of Epithelial Cells. *Infect. Immun.* 73, 4653–4667. doi: 10.1128/IAI.73.8.4653-4667.2005
- Heunis, T., Lamoliatte, F., Marin-Rubio, J. L., Dannoura, A., and Trost, M. (2020). Technical Report: Targeted Proteomic Analysis Reveals Enrichment of Atypical Ubiquitin Chains in Contractile Murine Tissues. *J. Proteomics* 229, 103963. doi: 10.1016/j.jpro.2020.103963
- Hiemstra, P. S., McCray, P. B., and Bals, R. (2015). The Innate Immune Function of Airway Epithelial Cells in Inflammatory Lung Disease. *Eur. Respir. J.* 45, 1150–1162. doi: 10.1183/09031936.00141514
- Hupp, S., Förtsch, C., Wippel, C., Ma, J., Mitchell, T. J., and Iliev, A. I. (2013). Direct Transmembrane Interaction Between Actin and the Pore-Competent, Cholesterol-Dependent Cytolysin Pneumolysin. *J. Mol. Biol.* 425, 636–646. doi: 10.1016/j.jmb.2012.11.034
- Hu, H., and Sun, S.-C. (2016). Ubiquitin Signaling in Immune Responses. *Cell Res.* 26, 457–483. doi: 10.1038/cr.2016.40
- Iovino, F., Gradstedt, H., and Bijlsma, J. J. E. (2014). The Proteasome-Ubiquitin System is Required for Efficient Killing of Intracellular *Streptococcus Pneumoniae* by Brain Endothelial Cells. *mBio* 5, e00984–14. doi: 10.1128/mBio.00984-14
- Jassal, B., Matthews, L., Viteri, G., Gong, C., Lorente, P., Fabregat, A., et al. (2020). The Reactome Pathway Knowledgebase. *Nucleic Acids Res.* 48, D498–D503. doi: 10.1093/nar/gkz11031



- Jin, M., Shirazinejad, C., Wang, B., Yan, A., Schöneberg, J., Upadhyayula, S., et al. (2021). Asymmetric Arp2/3-Mediated Actin Assembly Facilitates Clathrin-Mediated Endocytosis at Stalled Sites in Genome-Edited Human Stem Cells. *bioRxiv*. doi: 10.1101/2021.07.16.452693
- Keller, I. E., Vosyka, O., Takenaka, S., Klob, A., Dahlmann, B., Willems, L. I., et al. (2015). Regulation of Immunoproteasome Function in the Lung. *Sci. Rep.* 5, 10230. doi: 10.1038/srep10230
- LeMessurier, K. S., Hans, H., Lying, C., Elaine, T., and Vanessa, R. (2013). Type I Interferon Protects Against Pneumococcal Invasive Disease by Inhibiting Bacterial Transmigration Across the Lung. *PLoS Pathog.* 9, e1003727. doi: 10.1371/journal.ppat.1003727
- LeMessurier, K. S., Tiwary, M., Morin, N. P., and Samarasinghe, A. E. (2020). Respiratory Barrier as a Safeguard and Regulator of Defense Against Influenza A Virus and *Streptococcus Pneumoniae*. *Front. Immunol.* 11. doi: 10.3389/fimmu.2020.00003
- Lim, Y. K., Kweon, O. J., Kim, H. R., Kim, T.-H., and Lee, M.-K. (2019). Impact of Bacterial and Viral Coinfection in Community-Acquired Pneumonia in Adults. *Diagn. Microbiol. Infect. Dis.* 94, 50–54. doi: 10.1016/j.diagmicrobio.2018.11.014
- Mathieu, N. A., Papparisto, E., Barr, S. D., and Spratt, D. E. (2021). HERC5 and the ISGylation Pathway: Critical Modulators of the Antiviral Immune Response. *Viruses* 13, 1102. doi: 10.3390/v13061102
- McCarthy, M. K., and Weinberg, J. B. (2015). The Immunoproteasome and Viral Infection: A Complex Regulator of Inflammation. *Front. Microbiol.* 6. doi: 10.3389/fmicb.2015.00021
- Miyashita, M., Oshiumi, H., Matsumoto, M., and Seya, T. (2011). DDX60, a DEXD/H Box Helicase, is a Novel Antiviral Factor Promoting RIG-I-Like Receptor-Mediated Signaling. *Mol. Cell Biol.* 31, 3802–3819. doi: 10.1128/MCB.01368-10
- Morens, D. M., Taubenberger, J. K., and Fauci, A. S. (2008). Predominant Role of Bacterial Pneumonia as a Cause of Death in Pandemic Influenza: Implications for Pandemic Influenza Preparedness. *J. Infect. Dis.* 198, 962–970. doi: 10.1086/591708
- N'Guessan, P. D., Hippenstiel, S., Etouem, M. O., Zahlten, J., Beerhmann, W., Lindner, D., et al. (2006). *Streptococcus Pneumoniae* Induced P38 MAPK- and NF-kappaB-Dependent COX-2 Expression in Human Lung Epithelium. *Am. J. Physiol. Lung Cell Mol. Physiol.* 290, L1131–L1138. doi: 10.1152/ajplung.00383.2005
- Ogawa, M., Matsuda, R., Takada, N., Tomokiyo, M., Yamamoto, S., Shizukuishi, S., et al. (2018). Molecular Mechanisms of *Streptococcus Pneumoniae*-Targeted Autophagy via Pneumolysin, Golgi-Resident Rab41, and Nedd4-1-Mediated K63-Linked Ubiquitination. *Cell Microbiol.* 20, e12846. doi: 10.1111/cmi.12846
- Palacios, G., Hornig, M., Cisterna, D., Savji, N., Bussetti, A. V., Kapoor, V., et al. (2009). *Streptococcus Pneumoniae* Coinfection is Correlated With the Severity of H1N1 Pandemic Influenza. *PLoS One* 4, e8540. doi: 10.1371/journal.pone.0008540
- Park, S.-S., Gonzalez-Juarbe, N., Riegler, A. N., Im, H., Hale, Y., Platt, M. P., et al. (2021). *Streptococcus Pneumoniae* Binds to Host GAPDH on Dying Lung Epithelial Cells Worsening Secondary Infection Following Influenza. *Cell Rep.* 35, 109267. doi: 10.1016/j.celrep.2021.109267
- Perez-Riverol, Y., Csordas, A., Bai, J., Bernal-Llinares, M., Hewapathirana, S., Kundu, D. J., et al. (2019). The PRIDE Database and Related Tools and Resources in 2019: Improving Support for Quantification Data. *Nucleic Acids Res.* 47, D442–D450. doi: 10.1093/nar/gky1106
- Peter, A., Fatykhova, D., Kershaw, O., Gruber, A. D., Rueckert, J., Neudecker, J., et al. (2017). Localization and Pneumococcal Alteration of Junction Proteins in the Human Alveolar-Capillary Compartment. *Histochem Cell Biol.* 147, 707–719. doi: 10.1007/s00418-017-1551-y
- Radin, J. N., Orihuela, C. J., Murti, G., Guglielmo, C., Murray, P. J., and Tuomanen, E. I. (2005). Beta-Arrestin 1 Participates in Platelet-Activating Factor Receptor-Mediated Endocytosis of *Streptococcus Pneumoniae*. *Infect. Immun.* 73, 7827–7835. doi: 10.1128/IAI.73.12.7827-7835.2005
- Roth, G. A., Abate, D., Abate, K. H., Abay, S. M., Abbafati, C., Abbasi, N., et al. (2018). Global, Regional, and National Age-Sex-Specific Mortality for 282 Causes of Death in 195 Countries and Territories—2017: A Systematic Analysis for the Global Burden of Disease Study 2017. *Lancet* 392, 1736–1788. doi: 10.1016/S0140-6736(18)32203-7
- Rudnicka, A., and Yamauchi, Y. (2016). Ubiquitin in Influenza Virus Entry and Innate Immunity. *Viruses* 8, 293. doi: 10.3390/v8100293
- Ruuskanen, O., and Järvinen, A. (2014). What is the Real Role of Respiratory Viruses in Severe Community-Acquired Pneumonia? *Clin. Infect. Dis.* 59, 71–73. doi: 10.1093/cid/ciu242
- Saleh, M., Bartual, S. G., Abdullah, M. R., Jensch, I., Asmat, T. M., Petruschka, L., et al. (2013). Molecular Architecture of *Streptococcus Pneumoniae* Surface Thioredoxin-Fold Lipoproteins Crucial for Extracellular Oxidative Stress Resistance and Maintenance of Virulence. *EMBO Mol. Med.* 5, 1852–1870. doi: 10.1002/emmm.201202435
- Schoggins, J. W., Wilson, S. J., Panis, M., Murphy, M. Y., Jones, C. T., Bieniasz, P., et al. (2011). A Diverse Range of Gene Products Are Effectors of the Type I Interferon Antiviral Response. *Nature* 472, 481–485. doi: 10.1038/nature09907
- Schwark, C., and Schulze-Osthoff, K. (2005). Regulation of Apoptosis by Alternative pre-mRNA Splicing. *Mol. Cell* 19, 1–13. doi: 10.1016/j.molcel.2005.05.026
- Seifert, U., Bialy, L. P., Ebstein, F., Bech-Otschir, D., Voigt, A., Schröter, F., et al. (2010). Immunoproteasomes Preserve Protein Homeostasis Upon Interferon-Induced Oxidative Stress. *Cell* 142, 613–624. doi: 10.1016/j.cell.2010.07.036
- Self, W. H., Balk, R. A., Grijalva, C. G., Williams, D. J., Zhu, Y., Anderson, E. J., et al. (2017). Procalcitonin as a Marker of Etiology in Adults Hospitalized With Community-Acquired Pneumonia. *Clin. Infect. Dis.* 65, 183–190. doi: 10.1093/cid/cix317
- Sharma-Chawla, N., Sender, V., Kershaw, O., Gruber, A. D., Volckmar, J., Henriques-Normark, B., et al. (2016). Influenza A Virus Infection Predisposes Hosts to Secondary Infection With Different *Streptococcus Pneumoniae* Serotypes With Similar Outcome But Serotype-Specific Manifestation. *Infect. Immun.* 84, 3445–3457. doi: 10.1128/IAI.00422-16
- Shim, J. M., Kim, J., Tenson, T., Min, J.-Y., and Kainov, D. E. (2017). Influenza Virus Infection, Interferon Response, Viral Counter-Response, and Apoptosis. *Viruses* 9, 223. doi: 10.3390/v9080223
- Siemens, N., Oehmcke-Hecht, S., Mettenleiter, T. C., Kreikemeyer, B., Valentini-Weigand, P., and Hammerschmidt, S. (2017). Port D'entrée for Respiratory Infections - Does the Influenza A Virus Pave the Way for Bacteria? *Front. Microbiol.* 8. doi: 10.3389/fmicb.2017.02602
- Sirotkin, V. (2011). Cell Biology: Actin Keeps Endocytosis on a Short Leash. *Curr. Biol.* 21, R552–R554. doi: 10.1016/j.cub.2011.06.029
- Strehlitz, A., Goldmann, O., Pils, M. C., Pessler, F., and Medina, E. (2018). An Interferon Signature Discriminates Pneumococcal From Staphylococcal Pneumonia. *Front. Immunol.* 9. doi: 10.3389/fimmu.2018.01424
- Sumida, G. M., and Yamada, S. (2015). Rho GTPases and the Downstream Effectors Actin-Related Protein 2/3 (Arp2/3) Complex and Myosin II Induce Membrane Fusion at Self-Contacts. *J. Biol. Chem.* 290, 3238–3247. doi: 10.1074/jbc.M114.612168
- Sura, T., Surabhi, S., MaaB, S., Hammerschmidt, S., Siemens, N., and Becher, D. (2021). The Global Proteome and Ubiquitinome of Bacterial and Viral Co-Infected Bronchial Epithelial Cells. *J. Proteomics* 250, 104387. doi: 10.1016/j.jprot.2021.104387
- Szklarczyk, D., Gable, A. L., Lyon, D., Junge, A., Wyder, S., Huerta-Cepas, J., et al. (2019). STRING V11: Protein-Protein Association Networks With Increased Coverage, Supporting Functional Discovery in Genome-Wide Experimental Datasets. *Nucleic Acids Res.* 47, D607–D613. doi: 10.1093/nar/gky1131
- Szymanski, K. V., Toennies, M., Becher, A., Fatykhova, D., N'Guessan, P. D., Gutbier, B., et al. (2012). *Streptococcus Pneumoniae*-Induced Regulation of Cyclooxygenase-2 in Human Lung Tissue. *Eur. Respir. J.* 40, 1458–1467. doi: 10.1183/09031936.00186911
- Talbot, U. M., Paton, A. W., and Paton, J. C. (1996). Uptake of *Streptococcus Pneumoniae* by Respiratory Epithelial Cells. *Infect. Immun.* 64, 3772–3777. doi: 10.1128/iai.64.9.3772-3777.1996
- Troeger, C. E., Blacker, B. F., Khalil, I. A., Zimsen, S. R. M., Albertson, S. B., Abate, D., et al. (2019). Mortality, Morbidity, and Hospitalisations Due to Influenza Lower Respiratory Tract Infection: An Analysis for the Global Burden of Disease Study 2017. *Lancet Respir. Med.* 7, 69–89. doi: 10.1016/S2213-2600(18)30496-X
- Tyanova, S., and Cox, J. (2018). Perseus: A Bioinformatics Platform for Integrative Analysis of Proteomics Data in Cancer Research. *Methods Mol. Biol.* 1711, 133–148. doi: 10.1007/978-1-4939-7493-1\_7

- Tyanova, S., Temu, T., Sinitcyn, P., Carlson, A., Hein, M. Y., Geiger, T., et al. (2016). The Perseus Computational Platform for Comprehensive Analysis of (Prote)Omics Data. *Nat. Methods* 13, 731–740. doi: 10.1038/nmeth.3901
- Varcille, M., Kieninger, E., Edwards, M. R., and Regamey, N. (2011). The Airway Epithelium: Soldier in the Fight Against Respiratory Viruses. *Clin. Microbiol. Rev.* 24, 210–229. doi: 10.1128/CMR.00014-10
- Wong, J. J. Y., Pung, Y. F., Sze, N. S.-K., and Chin, K.-C. (2006). HFERC5 is an IFN-Induced HECT-Type E3 Protein Ligase That Mediates Type I IFN-Induced ISGylation of Protein Targets. *Proc. Natl. Acad. Sci. U. S. A.* 103, 10735–10740. doi: 10.1073/pnas.0600397103
- Wu, H., Zhang, S., Huo, C., Zou, S., Lian, Z., and Hu, Y. (2019). iTRAQ-Based Proteomic and Bioinformatic Characterization of Human Mast Cells Upon Infection by the Influenza A Virus Strains H1N1 and H5N1. *FEBS Lett.* 593, 2612–2627. doi: 10.1002/1873-3468.13523
- Yamauchi, Y. (2020). *Influenza A Virus Uncoating*. In: T. Mettenleiter, M. Kielian and M. Roossinck. *Advances in Virus Research* 106:1–38 (Advances in virus research). doi: 10.1016/bs.aivir.2020.01.001
- Zhang, Y., Xu, Z., and Cao, Y. (2020). Host-Virus Interaction: How Host Cells Defend Against Influenza A Virus Infection. *Viruses* 12, 376. doi: 10.3390/v12040376
- Zhou, J., Xu, Y., Lin, S., Guo, Y., Deng, W., Zhang, Y., et al. (2018). iUUCD 2.0: An Update With Rich Annotations for Ubiquitin and Ubiquitin-Like Conjugations. *Nucleic Acids Res.* 46, D447–D453. doi: 10.1093/nar/gkx1041
- Zinngrebe, J., Montinaro, A., Peltzer, N., and Walczak, H. (2014). Ubiquitin in the Immune System. *EMBO Rep.* 15, 322. doi: 10.1002/embr.201470030

**Conflict of Interest:** The authors declare that the research was conducted in the absence of any commercial or financial relationships that could be construed as a potential conflict of interest.

**Publisher's Note:** All claims expressed in this article are solely those of the authors and do not necessarily represent those of their affiliated organizations, or those of the publisher, the editors and the reviewers. Any product that may be evaluated in this article, or claim that may be made by its manufacturer, is not guaranteed or endorsed by the publisher.

Copyright © 2022 Sura, Gering, Cammann, Hammerschmidt, Maaß, Seifert and Becher. This is an open-access article distributed under the terms of the Creative Commons Attribution License (CC BY). The use, distribution or reproduction in other forums is permitted, provided the original author(s) and the copyright owner(s) are credited and that the original publication in this journal is cited, in accordance with accepted academic practice. No use, distribution or reproduction is permitted which does not comply with these terms.

## Appendix

### Published peer-reviewed manuscripts included in this thesis

- **Sura T**, Gering V, Cammann C, Hammerschmidt S, Maaß S, Seifert U, Becher D. *Streptococcus pneumoniae* and influenza A virus co-infection induces altered polyubiquitination in A549 cells  
Published in *Frontiers in Cellular and Infection Microbiology* 2022  
10.3389/fcimb.2022.817532
- **Sura T**, Surabhi S, Maaß S, Hammerschmidt S, Siemens N, Becher D. The global proteome and ubiquitinome of bacterial and viral co-infected bronchial epithelial cells  
Published in *Journal of Proteomics* 2021  
10.1016/j.jprot.2021.104387
- Stobernack T, du Teil Espina M, Mulder LM, Palma Medina LM, Piebenga DR, Gabarrini G, Zhao X, Janssen KMJ, Hulzebos J, Brouwer E, **Sura T**, Becher D, van Winkelhoff AJ, Götz F, Otto A, Westra J, van Dijl JM. A secreted bacterial peptidylarginine deiminase can neutralize human innate immune defenses  
Published in *mBio* 2018  
10.1128/mBio.01704-18

### Published peer-reviewed manuscripts not included in this thesis

- Hochstrasser R, Michaelis S, Brülisauer S, **Sura T**, Fan M, Maaß S, Becher D, Hilbi H. Migration of acanthamoeba through legionella biofilms is regulated by the bacterial Lqs-LvbR network, effector proteins and the flagellum  
Published in *Environmental Microbiology* 2022  
10.1111/1462-2920.16008
- Graf AC, Striesow J, Pané-Farré J, **Sura T**, Wurster M, Lalk M, Pieper DH, Becher D, Kahl BC, Riedel K. An innovative protocol for metaproteomic analyses of microbial pathogens in cystic fibrosis sputum  
Published in *Frontiers in Cellular and Infection Microbiology* 2021  
10.3389/fcimb.2021.724569

- Biran D, **Sura T**, Otto A, Yair Y, Becher D, Ron EZ.  
Surviving serum: the *Escherichia coli iss* gene of extraintestinal pathogenic *E. coli* is required for the synthesis of group 4 capsule  
Published in *Infection and Immunity* 2021  
10.1128/IAI.00316-21
- Maaß S, Bartel J, Mücke PA, Schlüter R, **Sura T**, Zschke-Kriesche J, Smits SHJ, Becher D.  
Proteomic adaptation of *Clostridioides difficile* to treatment with the antimicrobial peptide nisin  
Published in *Cells* 2021  
10.3390/cells10020372
- Francis TB, Bartosik D, **Sura T**, Sichert A, Hehemann JH, Markert S, Schweder T, Fuchs BM, Teeling H, Amann RI, Becher D.  
Changing expression patterns of TonB-dependent transporters suggest shifts in polysaccharide consumption over the course of a spring phytoplankton bloom  
Published in *ISME Journal* 2021  
10.1038/s41396-021-00928-8
- Bartel J, Varadarajan AR, **Sura T**, Ahrens CH, Maaß S, Becher D.  
Optimized proteomics workflow for the detection of small proteins  
Published in *Journal Proteome Research* 2020  
10.1021/acs.jproteome.0c00286
- Antelo-Varela M, Aguilar Suárez R, Bartel J, Bernal-Cabas M, Stobernack T, **Sura T**, van Dijl JM, Maaß S, Becher D.  
Membrane modulation of super-secreting "midiBacillus" expressing the major *Staphylococcus aureus* antigen - a mass-spectrometry-based absolute quantification approach  
Published in *Frontiers in Bioengineering and Biotechnology* 2020  
10.3389/fbioe.2020.00143
- Antelo-Varela M, Bartel J, Quesada-Ganuza A, Appel K, Bernal-Cabas M, **Sura T**, Otto A, Rasmussen M, van Dijl JM, Nielsen A, Maaß S, Becher D.  
Ariadne's thread in the analytical labyrinth of membrane proteins: integration of Targeted and shotgun proteomics for global absolute quantification of membrane proteins  
Published in *Analytical Chemistry* 2019  
10.1021/acs.analchem.9b02869

- 
- Guerrero Montero I, Dolata KM, Schlüter R, Malherbe G, Sievers S, Zühlke D, **Sura T**, Dave E, Riedel K, Robinson C.  
Comparative proteome analysis in an *Escherichia coli* CyDisCo strain identifies stress responses related to protein production, oxidative stress and accumulation of misfolded protein  
Published in *Microbial Cell Factories* 2019  
10.1186/s12934-019-1071-7
  - Dolata KM, Montero IG, Miller W, Sievers S, **Sura T**, Wolff C, Schlüter R, Riedel K, Robinson C.  
Far-reaching cellular consequences of tat deletion in *Escherichia coli* revealed by comprehensive proteome analyses  
Published in *Microbiological Research* 2019  
10.1016/j.micres.2018.10.008
  - Shulman A, Yair Y, Biran D, **Sura T**, Otto A, Gophna U, Becher D, Hecker M, Ron EZ.  
The *Escherichia coli* type III secretion system 2 has a global effect on cell surface  
Published in *mBio* 2018  
10.1128/mBio.01070-18
  - Hoyer J, Bartel J, Gómez-Mejía A, Rohde M, Hirschfeld C, Heß N, **Sura T**, Maaß S, Hammerschmidt S, Becher D.  
Proteomic response of *Streptococcus pneumoniae* to iron limitation  
Published in *International Journal of Medical Microbiology* 2018  
10.1016/j.ijmm.2018.02.001
  - Otto A, Biran D, **Sura T**, Becher D, Ron EZ.  
Proteomics of septicemic *Escherichia coli*  
Published in *Proteomics - Clinical Applications* 2016  
10.1002/prca.201600049

### Conference contributions

- **Sura T**, Gering V, Cammann C, Maaß S, Seifert U, Becher D.  
Proteomic analysis of E3 ligase expression and ubiquitination in epithelial cells infected with human respiratory pathogens.  
EMBO Conference “The ubiquitin system: Biology, mechanisms and roles in disease”, 13 – 17 September 2019 | Cavtat, Croatia (Poster presentation)
- **Sura T**, Gering V, Cammann C, Maaß S, Seifert U, Becher D.  
Ubiquitin signaling in bacterial infection.  
14<sup>th</sup> European Meeting on the Molecular Biology of the Pneumococcus (Europneumo), 11 – 14 Juni2019 | Greifswald, Germany (Poster presentation)
- **Sura T**, Gering V, Ritter U, Cammann C, Maaß S, Seifert U, Becher D.  
Proteomic analysis of changes in E3 ligase expression in epithelial cells driven by *Streptococcus pneumoniae* infection.  
12th European Summer School “Advanced Proteomics”, 29. July- 4. August 2018 | Brixen/Bressanone, Italy (Poster presentation)
- **Sura T**, Mücke P, Ritter U, Koch A, Slevogt H, Cammann C, Maaß S, Seifert U, Becher D.  
Proteomic analysis of changes in E3 ligase expression in epithelial cells driven by *S. pneumoniae* and IAV Infection.  
EMBO Conference “Ubiquitin and SUMO: From molecular mechanisms to system-wide responses”, 15 – 19 September 2017 | Cavtat-Dubrovnik, Croatia (Poster presentation)